Aus der

Medizinischen Klinik und Poliklinik III

Klinikum der Ludwig-Maximilians-Universität München

Irradiation of the microenvironment affects epigenetic therapy by LSD1 inhibition in murine AML model

Dissertation
zum Erwerb des Doktorgrades der Medizin
an der Medizinischen Fakultät
der Ludwig-Maximilians-Universität München

vorgelegt von
Maria Despoina Mariggi

aus
München

Jahr
2025

Mit Genehmigung der Medizinischen Fakultät der
Ludwig-Maximilians-Universität München

Erstes Gutachten:	Prof. Dr. Philipp Greif
Zweites Gutachten:	Prof. Dr. Stefan Eber
Drittes Gutachten:	Priv. Doz. Dr. Christian Wichmann

Dekan: Prof. Dr. med. Thomas Gudermann

Tag der mündlichen Prüfung: 25.03.2025

Table of content

Table of content ... **3**

Zusammenfassung (Deutsch) ... **5**

Abstract (English) ... **6**

List of figures ... **7**

List of tables ... **9**

Abbreviations ... **10**

Objectives of the study ... **14**

1. Introduction ... **15**

1.1 AML ... 15
1.2 Role of mesenchymal cells in AML development ... 22
1.3 Irradiation and LSD1 inhibition ... 24

2. Materials and Methods ... **26**

2.1 Materials ... 26
2.1.1 Technical Equipment and materials ... 26
2.1.2 Buffers, chemicals, and reagents ... 28
2.1.3 Antibodies ... 30
2.1.4 Culture media ... 31
2.1.5 Kits ... 33
2.1.6 Mouse cells ... 33
2.2 Methods ... 35
2.2.1 Cell culture ... 35
2.2.2 Colony Forming Unit (CFU) Assay ... 36
2.2.3 Co-culture of GMP-AML with feeder cells ... 37
2.2.4 May-Giemsa-Grünwald staining ... 37
2.2.5 Immunofluorescence ... 39
2.2.6 Fluorescence Activated Cell Sorting (FACS) ... 39
2.2.7 Western blot ... 42
2.2.8 Cytokine Release Assay ... 44
2.2.9 RNA sequencing ... 46

3. Results ... **49**

3.1 Effects of irradiation and LDS1i on MSCs ... 49
3.1.1 Proliferation and viability of stromal cells ... 49
3.1.2 Morphology, immunophenotype and differentiation of stromal cells under the influence of different conditions ... 51
3.1.3 Cytokine release of stromal cells under different conditions ... 59
3.2 Effects of LSD1i and MSC presence on MLL-AF9 ... 62
3.2.1 OP9 supernatant reduces growth of AML cells, but also reduces response to LSD1i treatment of AML cells ... 62
3.2.2 Colony forming unit assay, proliferation, and differentiation ability of AML cells under the influence of stromal supernatant. ... 64

3.2.3 Immunophenotypic and morphological changes of the *MLL-AF9+* AML cells upon different conditions 67
3.2.4 Cytokine release of MLL-AF9+ AML cells in different culture systems 74
3.3 MSC Transcriptomics 81
3.3.1 Irradiation of MSC depletes inflammation-related genes 82
3.3.2 LSD1 inhibition of MSC alters the metabolic pathways. 84
3.3.3 Combination of irradiation and LSD1i 87
3.3.4 Uniquely differentially expressed genes in the combination[116] 92

4. Discussion 95

References 100

Acknowledgements 106

Affidavit 107

Zusammenfassung (Deutsch)

Die Bestrahlung des Knochenmarks ist ein wichtiger Bestandteil der Therapie einer Akuten Myeloischen Leukämie (AML). Eine Chemotherapie (ggf. in Kombination mit anderen Substanzen) reicht oft nicht aus um eine längerfristig anhaltende Komplette Remission (CR) zu erreichen. Dabei kommt eine allogene Stammzelltransplantation oft ins Spiel, deren Protokolle eine Ganzkörperbestrahlung voraussetzen können. Auch in der experimentellen Leukämie-Forschung wird häufig eine Ganzkörperbestrahlung der Versuchstiere (u.a. Mäuse) eingesetzt, damit das Leukämie-Transplantat besser anwachsen kann. Aktuell sind noch viele Aspekte einer bestrahlten Knochenmark-Mikroumgebung ungeklärt. Daher widmet sich diese Dissertation einer genaueren Erforschung des Einflusses einer bestrahlten Mikroumgebung gegenüber der Wirksamkeit der epigenetischen AML Therapie mit einem Inhibitor der Lysin-spezifischen Demethylase 1 (LSD1i). Insbesondere wurde die Untergruppe der AML untersucht, die durch die MLL-AF9 Fusion hervorgerufen wird.

In vorausgehenden Versuchen wurden syngene Mäuse mit MLL-AF9 positiven AML Zellen transplantiert. Dabei wurde eine Untergruppe der Mäuse zuvor subletal bestrahlt, während die andere nicht bestrahlt wurde. Die nicht bestrahlte Mausgruppe sprach auf die Therapie an und wies eine längere Überlebenszeit auf. Dem gegenüber zeigte die bestrahlte Gruppe kein gutes Ansprechen auf und die durchschnittliche Überlebenszeit war signifikant kürzer. Um das besser untersuchen zu können, wurden vereinfachte in-vitro Versuche mit Mesenchymalen Stroma Zellen (MSC), sowie Ko-Kulturen mit AML Zellen durchgeführt.

Zusammengefasst konnte gezeigt werden, dass in vitro bestrahlte und LSD1i-behandelte MSC Zellen ihr Transkriptom verändern. In einer RNA-Sequenzierung der MSC konnten 606 unter der Kombination von Bestrahlung und Behandlung differenziell exprimierten Gene im Vergleich zur unbehandelten und nicht bestrahlten MSC-Kontrollgruppe nachgewiesen werden. Dabei verloren MSC Zellen ihre Stammzelleigenschaften und machten eine gewisse Differenzierung durch. Eine Bestrahlung des Stromas führte am ehesten zur Adipogenese.

Zudem ergab sich der Hinweis, dass die bestrahlungsabhängige Resistenz gegenüber LSD1i durch das Zytokin CCL5 vermittelt sein könnte. Schließlich konnte der protektive Effekt der Stromazellen, unabhängig von deren Bestrahlung, in-vitro dargestellt werden.

Abstract (English)

Irradiation of bone marrow is an important aspect in treating Acute myeloid leukemia (AML). Chemotherapy (in combination with additional substances) is often not enough to achieve a long-lasting complete remission. Because of that an allogenic stem cell transplantation is required, which is often done after a total body irradiation. Moreover, in experimental leukemia research, total body irradiation of lab animals (e.g. mice) is often implemented to achieve better cell engraftment.

Currently, many aspects of the irradiated bone marrow microenvironment are still unknown. Therefore, the focus of this thesis encompasses the mechanisms of how an irradiated microenvironment influences epigenetic therapy with the inhibitor of the lysine specific demethylase 1 (LSD1i). The AML subgroup emerging from the MLL-AF9 fusion was specifically examined.

Syngeneic mice were transplanted in previous experiments with MLL-AF9 positive AML cells. Prior to transplantation, some of the mice were sublethally irradiated and some were not irradiated. The irradiated group responded to LSD1i therapy and showed a longer overall survival. In contrast, the not irradiated group did not respond to the therapy and had a shorter overall survival. Simplified in-vitro experiments with mesenchymal stem cells (MSC) were carried out to further investigate this bone marrow phenomenon, as well as co-culture experiments with AML cells.

The results suggest that in-vitro irradiated and with LSD1i treated MSCs have an altered transcriptome in comparison to normal MSCs. RNA-Sequencing results show that after irradiation and treatment of MSC with LSD1i there are 606 differentially deregulated genes in relation to untreated and not irradiated MSC. This altered transcriptome led to loss of stem cell features in the stromal cells and induced differentiation. Irradiation of MSCs leads most likely to adipogenesis.

Furthermore, there was supporting evidence that the irradiation-dependent LSD1i resistance could be mediated by the cytokine CCL5. Lastly, the protective effect of stromal cells, independent of irradiation, could be demonstrated in-vitro.

List of figures

Figure 1 MLL-AF9 rearranged AML 19
Figure 2 Production of MLL-AF9 leukemic cells 33
Figure 3 Harvesting Mesenchymal Stem Cells 34
Figure 4 Preparation of a fourfold dilution series of cytokine standards 46
Figure 5 Proliferation of OP9 feeder cells after different radiations doses. 49
Figure 6 Effect of irradiation on proliferation of BM-MSC. 50
Figure 7 Cell count of MSC monoculture. 50
Figure 8 Annexin staining of MSC. 51
Figure 9 Immunophenotype of OP9 51
Figure 10 CD29 Expression und CB and BM-MSC 52
Figure 11 Immunophenotype of OP9 53
Figure 12 Morphological changes of OP9 upon LSD1i treatment. 54
Figure 13 MSC Cell Morphology after LDS1i and Irradiation 55
Figure 14 RNA sequencing - FABP4 Gene Expression. 56
Figure 15 Immunophenotypical characterization of differentiation potential of MSC. 56
Figure 16 FABP4 MSC immunofluorescent Staining 57
Figure 17 Western blot analysis of FABP4 in MSC, ... 58
Figure 18 RNAseq - differential gene expression of SPP1 In MSC 59
Figure 19 Cytokine release of BM-MSC: 60
Figure 20 Cytokine release of BM-MSC: CXCL1 and IL6. 60
Figure 21 RNA Expression of CB-MSC after 15 days at 37°C: CXCL1 and IL6 61
Figure 22 RNA Expression of CB-MSC after 15 days at 37°C: CCL2 and CCL5 61
Figure 23 Proliferation of AML cells in the presence of supernatant from OP9 and treated with LSD1i. 62
Figure 24 Proliferation of AML cells with transmembrane system with coculture of OP9, 64
Figure 25 Images of murine Colony forming units. 65
Figure 26 CFU Assay from coculture from transmembrane system 66
Figure 27 Proportion of c-kit/Mac-1 double positive AML cells upon treatment 68
Figure 28 Immunophenotype of AML cells treated in a trans-membrane system with continuous supply of fresh medium from feeder cells. 69
Figure 29 Immunophenotype of cells from 1° methylcellulose /CFC assay. 70
Figure 30 Proportion of CD86 positive AML cells upon co-culture (cell-to-cell contact) with primary bone marrow derived mesenchymal stromal cells (MSC). 71
Figure 31 Cytospin preparations from cultures of GMP-AML cells upon treatment. 72
Figure 32 Images of the culture morphology of primary bone marrow MSC 73
Figure 33 Cytokine release assay 74
Figure 34 CCL2 and CCL5 cytokine release of AML monocultures 75
Figure 35 CCL4 and CXCL1 cytokine release of AML monocultures. 76
Figure 36 TNFa and CSF2 cytokine release of AML monocultures. 77
Figure 37 IL3 and IL6 cytokine release of AML monocultures 78
Figure 38 Culture conditions of AML/MSC co-culture 79
Figure 39 TNF-a and CSF2 cytokine release of BM-MSC and *MLL-AF9*+ AML co-culture: 80
Figure 40 Cytokine release of BM-MSC and *MLL-AF9*+ AML co-culture: 80
Figure 41 Principal component analysis. 81
Figure 42 Transcriptional changes of CB-MSC upon irradiation. 82
Figure 43 Gene Set Enrichment Analysis of Differentially Expressed Genes upon irradiation on MSC. 83
Figure 44 Transcriptional changes of CB-MSC upon LSD1i treatment. 84

Figure 45 Gene set enrichment analysis plots enriched in MSC upon LSD1i 85
Figure 46 Gene set enrichment analysis plots depleted in MSC upon LSD1i..... 86
Figure 47 Transcriptional changes of CB-MSC upon combination treatment. 88
Figure 48 Gene set enrichment analysis plots depleted in MSC upon Irradiation and LSD1i 89
Figure 49 Gene Set Enrichment Analysis plots..... 90
Figure 50 FACS staining analysis of the CB-MSC 91
Figure 51 Transcriptional changes on MSC under the different conditions. 92
Figure 52 Gene Set Enrichment Analysis of Differentially Expressed Genes. 93

List of tables

Table 1 Abbreviations - General 10
Table 2 Abbreviations - Genes 12
Table 3 WHO-classification of AML 2022[5] 15
Table 4 Technical Equipment and materials 26
Table 5 Buffers, chemicals, and reagents 28
Table 6 FACS Antibodies 30
Table 7 Primary antibodies 31
Table 8 Secondary antibodies 31
Table 9 Culture media 31
Table 10 Kits 33
Table 11 Murine cell lines 34

Abbreviations

Table 1 Abbreviations - General

adj.p	adjusted p-value
AML	Acute myeloid leukemia
APL	Acute promyelocytic leukemia
ATO	arsenic trioxide
ATP	Adenosine triphosphate
ATPase	ATP phosphatase
ATRA	all-trans retinoic acid
BCA	bicinchonicic acid
BM	Bone marrow
BM-MSC	Bone marrow mesenchymal stem cells
BSA	bovine serum albumin
C57BL/6	C57 black 6 (inbred strain of laboratory mouse)
CB-MSC	Compact bone mesenchymal stem cells
CCL	C-C Motif Chemokine Ligand
CCR2	Chemokine receptor type 2
CD	Cluster of differentiation
CFU	Colony forming unit
c-Kit	Proto-Oncogene KIT
COMB	Combination (LSD1i+IRR)
CR	Complete remission
CTRL	Control
DAPI	4',6-Diamidino-2-phenylindol
ddH2O	double distilled water
DE	Differentially expressed
DEG	Differentially expressed genes
dH2O	distilled water
DMEM	Dulbecco Modified Eagle Medium
DMSO	Dimethylsulfoxid
DNA	Desoxyribonucleic acid
DPBS	Dulbecco's phosphate buffered saline
ECM	Extracellular matrix
EDTA	Ethylenediaminetetraacetic acid
EV	Extracellular vesicles
FAB	French-American-British cooperative group
FACS	Fluorescence Activated Cell Sorting
FBS	Fetal bovine serum
FCS	Fetal calf serum
FDR	False discovery rate
FSC	forward scatter
GF	Growth factor
GFP	green fluorescent protein
GM-CSF	Granulocyte monocyte - Colony Stimulating Factor, CSF2
GMP	Granulocyte monocyte progenitor
(number) x g	gravitational force

GO	Gene Ontology
GS	gene set
G-SCF	Granulocyte-colony stimulating factor
GSEA	gene set enrchment analysis
GSK-LSD1	GlaxoSmithKline - Lysine specific demethylase 1 (inhibitor)
Gy	Gray
H3K4	Histone 3 lysine 4
HSPCs	Hematopoietic Stem and Progenitor cells
HLA	Human leukocyte antigen
HRP	Horseradish peroxidase
HSC	Hematopoietic stem cells
IgG	Immunglobulin G
IL	Interleukin
IMDM	Iscove's Modified Dulbecco's Medium
inv	Inversion
IRR	Irradiation
logFC	log. fold change
LSD1	Lysine-specific histone demethylase 1A
LSD1i	Lysine-specific histone demethylase 1A inhibitor
Mac-1	Macrophage-1 antigen
MDS	Myelodysplastic syndrome
MEM alpha	Minimal Essantial Medium alpha
MGG	May-Grünwald-Giemsa
MLL	Mixed lineage leukemia
MLL-AF9	Mixed lineage leukemia AF9 fusion
MSC	Mesenchymal stem cells
NES	normalized enrichment score
NFkB	nuclear factor k-light-chain-enhancer of activated B cells
nom.p	nominal p-value
NT	Not treated
OP9	stem cell line, mouse, stroma
PBS	Phosphate buffered saline
PBST	Phosphate buffered saline, 0.1% Tween 20
PCR	Polymerase chain reaction
PI	Propidium iodide
PVDF	polivinylidene difluoride
r.p.m.	revolutions per minute
RIPA	Radioimmunoprecipitation assay puffer
RNA	Ribonucleic acid
RNAseq	RNA sequencing
RT	room temperature
RT-PCR	Real time - polymerase chain reaction
S17	stem cell line, mouse, stroma
SA-PE	streptavidin-phycoerythin
Sca-1	Stem cells antigen 1
SCF	Stem cell factor
SDS	sodium dodecylsulfate polyacrylamide

SN	supernatant
S-phase	synthesis-phase
SSC	side scatter
t	Translocation
TBI	Total body irradiation
TBS	Tris-buffered saline
TBST	Tris-buffered saline with 0.1% Tween 20
TC	Tissue Culture Dish
TKI	tyrosinekinase inhibitor
TNF	Tumor necrosis factor
TNFa	Tumor necrosis factor alpha
WB	Western blot
WHO	World health organization

Table 2 Abbreviations - Genes

ACTG2	Actin Gamma 2, Smooth Muscle
ALDOC	Aldolase, Fructose-Bisphosphate C
ANKRD1	Ankyrin Repeat Domain
AQP5	Aquaporin 5
ASS1	Argininosuccinate Synthase 1
ASXL1	Additional Sex Combs Like 1
ATP6v0e2	ATPase H+ Transporting V0 Subunit E2
ATP9a	ATPas Class II Type 9A
BGLAP	Bone gamma-carboxyglutamate protein
BGLAP	Bone Gamma-Carboxyglutamate Protein
CAR3	Carbonic Anhydrase
CCDC152	Coiled-Coil Domain Containing 152
CCNA2	Cyclin A2
CEBPA	CCAAT enhancer binding protein alpha
CHCHD10	Coiled-Coil-Helix-Coiled-Coil-Helix Domain Containing
CHRNB1	Cholinergic Receptor Nicotinic Beta 1 Subunit
CLEC3B	C-Type Lectin Domain 3 Member B
CSF2	GM-SCF, Colony Stimulating Factor 2
CXCL1	C-X-C Motif Chemokine Ligand 1
DNMT3A	DNA Methyltransferase 3 Alpha
EGFL6	EGF Like Domain Multiple 6
FABP4	Fatty acid binding protein 4
FAIM2	Fas Apoptotic Inhibitory Molecule 2
FLT3	Fms related receptor tyrosine kinase 3
IBSP	Integrin binding sialoprotein
IDH1	Isocitrate Dehydrogenase (NADP(+)) 1
IDH2	Isocitrate Dehydrogenase (NADP(+)) 2
KMD1A	Lysine (K)-specific demethylase 1A
KMT2A	Lysine methyltransferase 2A
KRAS	KRAS Proto-Oncogene, GTPase
MLLT3	Mixed-Lineage Leukemia Translocated To Chromosome 3

MSMP	Microseminoprotein, Prostate Associated
MyoD	Myogenic Differentiation 1
OTOR	Otoraplin
PCBD1	Pterin-4 Alpha-Carbinolamine Dehydratase 1
PENK	Proenkephalin
PI15	Peptidase Inhibitor 15
PML	PML Nuclear Body Scaffold
PPARγ	Peroxisome proliferator activated receptor gamma
RARRES2	Retinoic Acid Receptor Responder 2
RUNX1	Runt related transcription factor 1
RUNX2	Runt related transcription factor 2
Sox9	SRY-Box transcription factor 9
SPINT2	Serine Peptidase Inhibitor Kunitz Type 2
SPP1	Secreted phosphoprotein 1
SPP1	Secreted Phosphoprotein 1, Osteopontin
STMN2	Stathmin 2
SVIP	Small VCP Interacting Protein
TET2	Tet methylcytosine dioxygenase 2
TP53	Tumor protein P53
TPH2	Tryptophan Hydroxylase 2
WIF1	WNT Inhibitory Factor 1

Objectives of the study

Acute myeloid leukemia is the most common adult form of acute leukemia with the median age of diagnosis being about 70 years of age. The majority of AML patients experience a relapse after the standard 7 + 3 AML therapy. There is emerging evidence that targeted therapies could ameliorate standard therapy. The epigenetic therapy with the Lysine specific demethylase 1 inhibitor (LSD1i) has shown to have a potent antileukemic effect in preclinical models. The interaction of leukemic cells with the stroma could increase the growth of leukemic blasts. Various studies have tried to analyze the response of tumor cells to therapy influenced by released cytokines and cell interactions. MSC have often been speculated to be involved in resistance mechanisms against anti-tumor therapies and to play an important role in the interaction of the tumor and hematopoietic cells with their microenvironment.

Irradiation therapy is a common part of the cytotoxic treatment of solid tumors, and it is also used to prepare leukemia patients for a stem cell transplantation. In vivo experiments with irradiated recipient mice have shown better engraftment of transplanted leukemia cells in comparison to non-irradiated mice.

In previous in vivo experiments carried out by our research group, mice were treated with LSD1 inhibitor (0.5 µM) as soon as engraftment was measurable (1-2 weeks after transplantation). Non-irradiated treated mice showed longer survival in contrast to irradiated treated mice, which developed AML. It was hypothesized that irradiation alters the bone marrow in such a way, that a therapy resistance is built up and LSD1 inhibition cannot exert its antileukemic potential anymore.

The goal of this study is to assess the mechanisms responsible for this resistance phenotype and to better understand how LSD1 works, and how the microenvironment could be influenced to achieve a better therapy response in AML.

In this thesis following points are to be adressed:

- To analyze the changes of MSC cells under LSD1i treatment and irradiation:
    - Proliferation, immunophenotype, cell morphology,
    - Cytokine release, differentiation, transcriptome
- To assess how MSC supernatant (humoral substances) influences the survival of AML cells under treatment and changes their properties.
- To evaluate the role of direct cell-to-cell contact between AML and MSC and the blast persistence.

1. Introduction

1.1 AML

1.1.1 Epidemiology, risk factors and prevention

Acute leukemia is defined by the excessive proliferation of immature hematopoietic progenitor cells inside the bone marrow (BM) microenvironment, which are often morphologically non-distinguishable from normal blast cells. These immature cells suppress normal hematopoiesis in the BM and are often released into the blood stream, causing severe health issues such as anemia, neutropenia, and leukostasis. Acute myeloid leukemia is the most common form of acute leukemia in adults. Between 2017 and 2018, 27 % of the newly diagnosed female leukemia patients in Germany had AML and 23% of the male leukemia patients, whereas 7 % of each gender were diagnosed with ALL. Out of 100.000 children under 18 years of age, 0,7 children per gender were newly diagnosed with AML between 2010 and 2019, whereas 3.5 girls and 4.3 boys were diagnosed with lymphatic leukemias[1]. AML involves the cells of the myeloid lineage (Basophiles, Neutrophiles, Eosinophiles, Monocytes, Macrophages, Erythrocytes and Platelets). This type of leukemia is mostly predominant in the older population. AML is the result of clonal expansion of myeloid hematopoietic precursors and consists of various origins and mutations[2].

Acute myeloid leukemia is a biologically heterogenous disease, due to the various possibilities of combinations of genetic abnormalities. Historically AML was classified with the help of the FAB Classification, first established in 1976 by the French-American-British cooperative group. This classification was based on cellular morphological and cytochemical methods[3]. In 2002 The WHO classification, based on cytogenetic and molecular characteristics, began to replace the FAB classification[4]. The 5th edition of the WHO classification 2022 divides the illness into subtypes: AML with defining genetic abnormalities and AML defined by differentiation (see Table 3).

Table 3 WHO-classification of AML 2022[5]

AML with defining genetic abnormalities	
	Acute promyelocytic leukemia with *PML::PARA* fusion
	AML with *RUNX1::RUNX1T1* fusion
	AML with *CBFB::MYH11* fusion,
	AML with *DEK::NUP214* fusion
	AML with *BCR::ABL1* fusion

	AML with *KMT2A* rearrangement
	AML with *MECOM* rearrangement
	AML with *NUP98* rearrangement
	AML with *NPM1* mutation
	AML with *CEBPA* mutation
	AML myelodysplasia related
	AML with other defined genetic alterations
AML defined by differentiation	
	AML with minimal differentiation
	AML without maturation
	AML with maturation
	Acute basophilic leukemia
	Acute myelomonocytic leukemia
	Acute monocytic leukemia
	Acute erythroid leukemia
	Acute megakaryoblastic leukemia

The average age of AML occurrence is about 70 years[6]. According to the Centre for Cancer Registry Data, one out of 99 women and one out of 75 men are likely to fall ill to a form of leukemia over the course of their life. With about 25% of all forms of leukemia, AML is the most common type of acute leukemia in adults. Approximately 12.000 patients were newly diagnosed with leukemia in Germany in 2018, out of which about 3000 with AML[1]. The patient age at the time of diagnosis plays an important role in the overall survival rate. While children have the best chances of a longer overall survival, the elderly are more likely to have a poorer survival expectancy, due to comorbidities limiting the intensity of the therapy. Although significant improvements in AML treatment have been observed over the past decades, people aged 75 and older have no apparent increase in overall survival rate when compared to the previously available therapies[7].

Several risk factors can be associated with the development of acute myeloid leukemia. Therapy-related forms of leukemic malignancies have been proved to be caused by ionizing radiation used for treatment of solid tumors. Ionizing radiation also occurs from environmental exposure. The incidence of leukemia is directly correlated with the degree of exposure (duration and dose)[8]. However, the effect is usually seen years after exposure. One example would be the increased incidence of leukemia, as described by Japanese Data after the atomic explosions in Hiroshima and Nagasaki, where they measured a peak of blood neoplasms 6 years after the explosion[9]. Another

form of therapy-related neoplasms can be attributed to cytotoxic chemotherapy. Some of the agents responsible are alkylating agents, such as chlorambucil or melphalan, and topoisomerase II inhibitors such as etoposide and anthracyclines[10]. Further substances that increase the risk of leukemia development are cigarette smoke, benzene, trichlorethylene and pesticides[11].

Genetic background also plays a significant role in the development of AML. Myelodysplastic syndromes (MDS) and AML share various common genetic mutations. About 30% of MDS patients develop AML in the course of the disease (known as “secondary AML”). It has been shown that DNA splicing and methylation alterations are likely to provoke the development of MDS into a more severe form[12]. Additionally, elderly patients with increased clonal hematopoietic proliferation are known to often have mutations in genes like *DNMT3A, ASXL1, TET2, IDH2*[13]. These mutations increase the risk of developing AML. There are also several reports of familial accumulation of MDS and AML cases, with known inherited mutations such as *RUNX1* and *CEBPA*. It is therefore fundamental for future disease prevention to offer unaffected family members access to early diagnostic and treatment options[2,13,14].

Apart from the inherited risk factors and the known environmental risk factors, from which the latter can be avoided (such as smoking), there is a third factor to be considered: the number of stem cell divisions within the tissue. The more often a cell divides, the more likely it is to succumb to genetic aberrations, ultimately triggering cancer development[15].

1.1.2 Pathophysiology of AML

AML can arise from the pathological clonal proliferation of myeloic progenitor cells and can exhibit immunophenotypic characteristics more often similar to progenitor cells (CD34+/CD38+) and sometimes similar to stem cells (CD34+/CD38-)[2]. These cells repress the healthy bone marrow impeding its function due to their clonal expansion. This process leads to the depletion of mature and healthy granulocytes, thrombocytes, and erythrocytes and can cause infection, bleeding, and anemia, while defective malignant cells rapidly increase in number. The symptoms develop very rapidly and can be severe. The pathogenesis of AML has been historically explained by the 2-hits theory: block of differentiation and increased proliferation[16].

In general, when AML is suspected, a stepwise diagnostic is performed. Morphological changes (e.g. pathognomonic Auerrods) or other immunohistochemical features can

help to identify, which AML subtype occurs, such as esterase and myeloperoxidase, as well as iron-staining (ring sideroblasts e.g. when AML develops on a basis of certain MDS subtypes). Cytogenetic analysis(chromosome banding) and fluorescence-in-situ-hybridization (FISH) can also be performed, as well as routine diagnostic panels for small alterations and certain mutation[2,17].

The cytogenetic changes that lead to AML include chromosomal translocations such as t(8;21) and t(15;17), inversions (inv(16)), deletions and numeric aberrations (trisomy 8, monosomy 7). Nine groups of genetic changes in AML have been identified, categorized by their function: Signaling pathway changes (e.g., *FLT3*, *KRAS*), DNA methylation (e.g., *IDH1* and *IDH2*), Chromatin modifications (e.g., *MLL* fusions, *ASXL1*), Nucleophosmin, Myeloid transcription factors (e.g., *RUNX1*, *CEBPA*), Transcription factors, Tumor suppressors (e.g., *TP53*), Spliceosome complex, Cohesin complex. Mutations of these factors are included in the routine diagnostic panels. In refractory situations a Next-Generation-Sequencing (NGS) is performed to detect unusual mutations, which could be used for off-label treatment alternatives[2,18].

1.1.3 MLL rearranged AML

A chromatin modification investigated in this thesis is the *MLL-AF9* chromosomal translocation. This alteration is found in 5-10% of all leukemias, myeloid and lymphoid[19,20]. There are numerous characterized MLL gene fusions that have been found in AML, with 80 fusion partners so far reported[19]. The not-mutated gene is known as “Mixed Lineage Leukemia 1” or as *KMT2A*, coding for Lysine Methyltransferase 2A and plays an essential role in early hematopoiesis. This enzyme methylates the lysine 4 of histone 3 (H3K4) at the target gene triggering its expression. The *MLL genes*, modified by the fusions and the resulting proteins, is able to dock onto nuclear factors but lacks the methyltransferase domain. This leads to hematopoietic malignancies[21,22]. One of the *MLL* fusions often investigated is the *MLL-AF9*. Here *MLL* is fused to the C-terminus of *AF9*, which is encoded by the *MLLT3* gene (Figure 1). This chimeric protein is part of a multiprotein complex containing chromatin modifiers and members of the superelongation complex leading to aberrant expression of target genes and therefore to transformation[23].

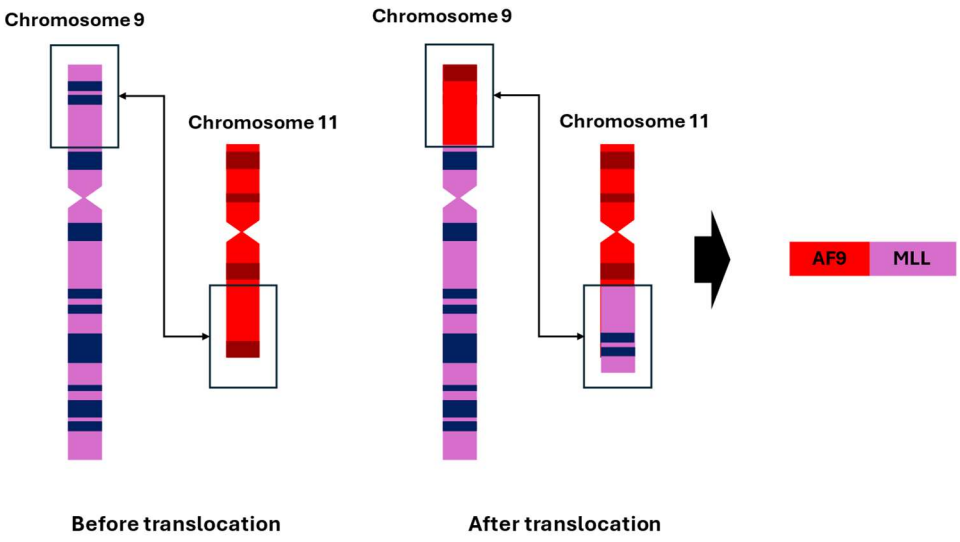

Figure 1 MLL-AF9 rearranged AML
MLL is fused to the C-terminus of AF9, which is encoded by the MLLT3 gene (based on Dave et al [24]).

Retrovirally induced fusion of this gene produces a driver mutation for an aggressive form of AML. It has been shown that this fusion gene can transform different target cells other than hematopoietic stem cells (HSC), including more differentiated progenitor cells such as granulocyte-monocyte progenitor cells (GMP)[25].

1.1.4 Therapy of AML

Within one year after the symptomatic onset AML, without any treatment provided, almost all patients would experience a lethal outcome[26]. Chemotherapy makes complete remission possible and significantly increases the survival rate, depending on the subtype and the prognostic subgroup. According to the ELN classification, AML can be initially diagnosed as favorable, intermediate, or adverse risk[27]. However, relapse is quite common and therefore an intense subject of experimental cancer research. It is possible that after reaching complete remission, some leukemic blasts with residual clonal ability are sheltered by the bone marrow, having escaped chemotherapy. This could be explained by the underlying heterogeneity of the blast's properties. A smaller proportion of resistant cells can thus survive the therapy and expand over time causing a relapse[28-30]. Many efforts have been made to identify the subpopulations of cancer

cells within a patient allowing to define a clonal architecture, with a different sensitivity to therapy.

Standard AML treatment protocols include the 7 + 3 regimen as induction therapy, as well as an additional drug, depending on the leukemia's pathophysiology, in an attempt reach complete remission. The 7 + 3 regimen is comprised of intensive chemotherapy, such as the cytostatic drug cytarabine for 7 days and simultaneously an anthracycline (e.g., daunorubicin) for 3 days. The regimen can be accompanied by a tyrosine kinase inhibitor (e.g. midostaurin) if a mutation of the *FLT3* gene can be detected or by an antibody-based treatment such as gemtuzumab ozogamicin (GO) in case of a CD33+ AML subtype[31]. The bone marrow response, in terms of blasts clearance, is assessed promptly after therapy. If a remission occurs, a consolidation therapy, followed by a maintenance therapy, can be taken into consideration, depending on the genetic subtypes and risk classification. For adverse subgroups (such as complex karyotypes) an allogeneic stem cell transplantation is always performed, even if after induction therapy there is an initial remission; in these cases, the risk of an early fatal relapse is very high[2].

Prior to an allogeneic stem cell transplantation, a total body irradiation (TBI, myeloablative: ≥ 5Gy single-dose or ≥ 8Gy fractionated but total max. 12Gy[32] can additionally be required, as to suppress the host immune system and avert a rejection of the cell graft. Cancer cells that did not respond to the induction therapy could be eliminated by the TBI and the minimal residual disease can further be reduced. TBI is highly toxic with multiple side effects, such as like nausea, diarrhea, swallowing difficulties, an elevated infection risk[33-35]. The toxicity and level of damage done to the bone marrow are dependent on the radiation dosage. For example, a nonmyeloablative conditioning has a smaller radiation dose (≤ 2Gy) compared to the myeloablative regimen[32]. On the other hand, solid tumors that are topographically close to the bone marrow might need a higher therapeutic radiation dose, therefore causing side effects and collateral damage. The remaining bone marrow cells (stem cells, leukemic cells, and normal hematopoietic progenitor cells) do not possess the ability to regenerate after TBI, due to the damage inflicted by the ionizing radiation. This side effect make a stem cell transplantation necessary to repopulate the bone marrow and restore the hematopoiesis again[36]. There is a significant difference between targeted irradiation of the bone marrow and TBI. While the same amount of radiation might have severe consequences in case of a TBI, a targeted radiation of the bone marrow can allow for a partial recovery,

due to the other BM compartments[37]. In the clinical routine however, a low-dose TBI is applied.

Although the percentage of patients reaching complete remission after the 7+3 regimen is very high, over 50 to 70% of the AML patients experience a relapse after a maximum of three years post-remission, depending on the risk subgroup. This chemoresistance of the remaining leukemic cells could be caused due to a mutation of the TP53 gene, responsible for apoptosis induction, resulting in further tumor progression[38-40]. When AML develops anti-apoptotic characteristics, cytotoxic agents are often insufficient and other targeted therapies such as immune-based (e.g. bi-specific antibodies) or epigenetic (e.g. acazitidine) options can be evaluated[39,41]. The microenvironment of AML can express protective factors that allow the tumor cells to escape therapy, as an early form of resistance at the beginning of the disease. In later therapy stages the AML cells can express an altered metabolism and protein expression as a late form of resistance and become non-responsive to antileukemic drugs, such as gilteritinib[42].

1.2 Role of mesenchymal cells in AML development

A popular model for ex vivo experiments focused on the complex bone marrow microenvironment, involves a co-culture of mesenchymal stem cells (MSC) and hematopoietic stem or cancer cells. A limitation of these co-cultures is that many factors, responsible for hematopoietic stem cell maturation, normally present in vivo, are absent in the ex vivo model.

MSCs are a multipotent stem cell type and can be extracted from various parts of the body. Some of the many potential tissues of origin are the umbilical cord, the bone marrow, or adipose tissue[43]. The term “mesenchymal” is misleading in regard of their potential differentiation pathways. While the mesenchyme is originally shaped from the mesoderm during the embryonic process and possesses the ability to produce hematopoietic cells, the MSC lack that potential[44,45]. The term “Mesenchymal Stromal Cells” is additionally used as a synonym to MSC, indicating that they are connective tissue cells. They constitute the niche for other functional cells and support them. Hematopoiesis and immune cell maturity are largely dependent on MSCs via intense cell-to-cell and humoral paracrine interaction[46,47]. According to the International Society for Cellular Therapy, MSCs need to be positive for CD105, CD73, CD90 and negative for CD14 or CD11b, CD79α or CD19 and HLA-DR[48].

MSC are very heterogenous: they vary in their cell shape, surface markers, renewal, mitotic capacity as well as in their overall microscopic morphology. There have been several attempts to categorize them into different groups. One version, based on their adherent cell culture morphology is the distinction between: small rapidly renewing cells, elongated and spindle-shaped cells, slowly replicating and flattened cells[49]. It has been reported that the lower cell-renewing potential of the flattened MSC correlates with increased cell maturity. A smaller subgroup of MSC contains the fast-proliferating cells, which are less mature precursor type of MSC. In vitro, the frequency of passaging as well as the duration of the cell culture can both affect the morphology of the MSC. Over time, fast-proliferating cells decrease in number and after multiple changes of the cell medium flattened MSCs accumulate. The behavior of actin as a structural protein of the cytoskeleton is dependent on the cell culture conditions and dictates the development of the cell as well as their physiological properties through interactions with the extracellular matrix and other cells[50].

MSCs have the potential to differentiate into several cell types including osteocytes, chondrocytes, adipocytes, and myocytes. Different factors take part in the differentiation of the MSCs (transcription factors, cytokines, and microenvironmental elements). The exact role of some transcription factors in the differentiation process of MSCs, such as *RUNX2, SOX9, PPARγ* and *MYOD1* has recently been examined[51]. *RUNX2* has been shown to manage osteoblastic differentiation, *SOX9* - chondrocytic differentiation, *PPARγ* - adipogenic differentiation and *MYOD1* - myogenic differentiation[52]. Cytokines and other soluble factors also play an important role in the differentiation of MSCs. It has been described that the interleukin 6, which is also highly secreted by the MSCs, partly inhibits their differentiation altogether[53]. The MSC's ability to proliferate, and their differentiation potential can influenced by their cell recognition capabilities and thus by cell-to-cell and cell-to-matrix interactions[54].

The interplay of AML cells and the bone-marrow niche is very dynamic, and the influence is bidirectional. Integrins, a group of cell adhesion receptors, are very important for cell recognition and therefore for cell communication. They need to interact with the cytoskeleton prior to binding to the extracellular matrix (ECM). These transmembrane proteins are responsible for the intracellular signaling and homeostasis and are therefore involved in processes such as inflammation, immunity, apoptosis as well as in the development of malignancies. Integrins are heterodimers assembled by an alpha and a beta subunit. One example of an integrin is the Macrophage-1 antigen (Mac-1) which is composed of CD11b (integrin α_M) and CD18 (integrin β_2) and are often expressed on AML cells. Integrins bind cell-surface ligands, such as cytokines, ECM components and other molecules to actualize the transmembrane interaction[55-57].

The close interaction of the different cells in the microenvironment, as well as the communication with the ECM are co-responsible for the secretion of several soluble factors as well as the release of exosome contents. Both can lead to therapy resistance and ineffective tumor elimination[58]. In another study, macrophages isolated from the bone marrow were treated with extracellular vesicles (EV) of MSC. In the control culture, the macrophages expressed significantly elevated quantities of the pro-inflammatory markers CD11b and CD86 (among others) compared to EV-treated macrophage cell cultures. It was therefore concluded that EVs regulate the immune and regenerative potential of macrophages[59].

1.3 Irradiation and LSD1 inhibition

Cancer treatment results vary from patient to patient, based on many factors, such as the tissue of origin, the extent of spreading and the expression of specific markers. The treatment can be a combination of chemotherapy, radiation therapy, surgery, immunotherapy, hormone, or targeted therapy. Until not too long ago, the treatment of tumor cells was almost solely based on the interference with proliferating cells in the S-phase of the cell cycle by classical chemotherapeutic drugs. With research progress, new methods and options have evolved. Cells can nowadays be attacked more selectively and in different phases of cell cycle. Targeted therapies directly aim for cells expressing a protein of choice, which can be essential to the survival of malignant cells or are specifically activated in a certain type of tumor or in a single patient (personalized medicine). These treatments consist of small-molecule drugs or monoclonal antibodies. Small molecules pass easily through the double lipid cell membrane and take effect on an intracellular target[60-64].

One small-molecule drug on which this thesis focuses, is the Lysine-specific histone demethylase 1A inhibitor (LSD1i). This protein coded by the *KDM1A* gene can demethylate histone 3 lysine 4 (H3K4me1/me2) and lysine 9. LSD1 is an important epigenetic regulator and plays a pivotal role in cell development[65,66]. *KMD1A* has been proven to be essential in the clonal expansion of AML[67]. Therefore, an inhibition of *KMD1A* can be an enticing strategy to address the malignant epigenetic aberrations with the drug GSK-LSD1. The differentiation blockage of AML can be lifted by this drug, leading to inhibition of further progress of the tumor. Treatment with GSK-LSD1 leads to a depletion of more immature leukemic cells, which are double positive for CD11b and CD117 in the *MLL-AF9* model. Furthermore, overall survival of mice with the aggressive *MLL-AF9+* AML was significantly increased under LSD1 inhibition[68]. LSD1i has also been tested for other tumors, such as small cell lung cancer and Ewing sarcoma[69].

LSD1 inhibition has been reported to effect MSCs. The treatment triggers a double-stranded RNA stress reaction in C57BL/6 mice according to a recent study. Primary BM-MSC cells were cultured in a non-toxic concentration of Tranylcypromine (a LSD1 inhibitor) and the cells, while converting them into potent antigen presenting cells, they did not change any of the MSC specific surface markers CD44, CD73, CD90.1 and CD105[70]. A second study conducted with the LSD1 inhibitor Pargyline has shown that BM-MSC under treatment have an increased osteogenesis potential[71], suggesting that

LSD1 might be involved in maintaining an immature phenotype of the MSC. In the same study MSC were cultured for two weeks in osteogenic medium with or without LSD1 inhibition. The expression of *Runx2* (as osteogenesis related gene) by RT-PCR was significantly upregulated in the LSD1i-treated group[71]. If MSC enter osteoinduction, they can differentiate into osteoblasts. Additionally, it has been questioned whether osteoblasts are essential to HSC regulation. Osteoblasts produce numerous growth factors, such as G-CSF, necessary for hematopoietic maturation. A decrease of osteoblast number and elimination of important cytokines, such as SCF in experiments did not cause significant changes of HSC numbers[72].

Apart from soluble agents, ionizing radiation can play a major role in cancer treatment. Irradiation usually has the biggest impact on cells that have a high rate of proliferation by causing irreparable DNA damage. When the DNA damage reaches a critical point, a permanent cell cycle arrest is induced and cancer cells, which tend to proliferate rapidly can be eliminated. Additionally, irradiation has not only an immunosuppressive effect but also immunomodulatory effects[73,74]. The cell injury created by the radiation can also lead to imbalance in the differentiation process of MSCs, in favor of adipogenesis according to a study on rat-derived BM-MSC (Dose: 6Gy). The study's aim was to take a closer look at BM-MSC derived exosomes and their part in functional recovery of MSC from DNA and oxidative stress damage after irradiation[75]. MSC exosomes can strengthen cell proliferation, reduce cell death, mediate the communication with other cells, and have immunomodulatory effects[76].

2. Materials and Methods

2.1 Materials

2.1.1 Technical Equipment and materials

Table 4 Technical Equipment and materials

Autoclavable bags	Ratiolab, 7001005
Automated cell counting	Vi-Cell XR cell viability analyzer Beckman Coulter
Blunt-End Needles	STEMCELL #28110
Bio-Plex Cytokine release assay reader	Bio-Rad Luminex Bio-Plex 100 systems
Cell Culture Dishes	TC dishes, suspension/standard Diameter 100 mm Sarstedt
Cell Culture Flasks	TC flasks, suspension/standard T25, T75, T125 Sarstedt
Cell Culture Incubator	BINDER INCUBATOR
Cell Culture Plates with insert	12 Wells 12mm Transwell 0.4µm Pore membrane insert Corning, 3401
Cell culture well plates	TC plates, suspension/standard 6- 12- 24- 48- 96- Wells Sarstedt
Cell Scraper	Cell Or Scraper neoLab, C-8123
Cell Sorter	MoFlo Astrios EQ Beckman Coulter
Centrifuges	Centrifuge 5417R Centrifuge 5415D Eppendorf MEGAFUGE 40R TX-750 Thermo Scientific
Centrifuge tubes	Conical bottom tubes Sarstedt 15 ml, 62554502 50 ml, 62547254
CFU assay plates	6-wells SmartDish STEMCELL, #27370
12-channel pipettes	Eppendorf Research Plus 300µl
Cheminulescence imaging system	Vilber Lourmat Peqlab FUSION SL

Coverslips	Deckgläser Stärke 1, 18 x 18 mm ROTH Karlsruhe, 0657.2 Deckgläser 10mm #1, rund Thermo Scientific, 631-1340
CryoTube vials	Thermo Scientific 368632
Cytopin 2 SHANDON	Thermo Scientific
Digital pH meter	Lab pH meter inoLab pH 7110 inoLab wtw
Digital Scales	Kern PCP 6000-0 Präzisionswaage Analysenwaage KERN ABS-N/ABJ-NM
Electrophoresis Cell	Xcell SureLock Electrophoresis Cell Thermo Scientific, EI0001
FACS tubes	5ml Polystyrenen Round-Bottom Tube FALCON, Corning, 352052, 352235
Flow Cytometer	FACSCanto II, BD Bioscience
Freezing container	NALGENE Cryo 1°C Freezing Container Mr. Frosty Thermo Scientific, 5100-0001
Hemocytometer cell counting	Neugebauer improved cell counting chamber, Brand GmbH & Co. KG
Laminar Flow Hood	BERNER FlowSafe, B-[MaxPro]²-130
Magnetic stirrer	IKA big squid IKAMAG IKA Labortechnik
Microplate reader	GloMax Discover Promega
Microscope	Leica Microsystems DMi8 AE2000 Series Motic Microscope
Microscope Slides	Superfrost Thermo Scientific 12134682
Mini Protein gel	Novex Wedge Well 12% Tris-Glycine Gel Invitrogen XP00122BOX
Orbital shaker	IKA KS250 basic IKA Labortechnik
Parafilm M	PM-996
Pipette Controller	Accu-jet Pro Pipette Controller BRAND; Z637688
Pipettes	5 ml, 10 ml Stripettes Corning Incorporated, Costar, 4487, 4488 25 ml Serological Pipette Greiner bio-one, 760107
Pipette tips	Graduated Tips Starlab 10 µl, S1111-3700 200 µl, S1111-0700 1000 µl, S1111-6700

Protein denaturation	ThermoMixer F1.5 Eppendorf
Roller Shaker	IKA Roller 6 digital IKA Labortechnik
Round-Bottom Tube	14 mL Polystyrene Round-Bottom Tube FALCON, Corning, 352051
Safe lock tubes	1.5 ml, Sarstedt, 72706400 2.0 ml, Eppendorf, 0030 120.094
Shandon filter cards	Thermo Scientific 5991022
Single-channel pipettes	Eppendorf Research Plus 2.5 µl, 10 µl, 100 µl, 200 µl, 1000 µl
Syringe filter	Millex-HV Filter Unit PVDF 0.45µm Merck Millipore SLHV033RS
Vortex	Vortex-Genie 2 Scientific Industries
Water bath	LAUDA Hydro Wasserbäder GFL Technology
WB protein transfer	Trans-Blot Turbo Transfer System BIO-RAD
X-ray irradiator	XSTRAHL Cabinet Irradiator RS225

2.1.2 Buffers, chemicals, and reagents

Table 5 Buffers, chemicals, and reagents

Albumin, Bovine	Sigma-Aldrich A-7906
Annexin V Staining	10X Annexin V Apoptosis Detection Kit I BD Bioscience 559763
Blotting substrate	Pierce ECL Plus Western Blotting Substrate Thermo Scientific 32132
Bromophenol Blue	Sigma-Aldrich B-5525
Buffer RLT Plus, Rneasy Plus lysis buffer	Qiagen 1053393
Buffer tablets pH 6.8	Sigma-Aldrich 111374
Cell counting reagents	Vi-Cell Reagent Pak Beckman Coulter 383260
Collagenase Type I 0.25%	STEMCELL #07902
DAPI	Sigma-Aldrich D9542
DMSO	AppliChem A3672,0250

DPBS	Dulbecco's PBS w/o Ca and Mg Gibco, P04-36500
Ethanol	ROTH Karlsruhe 5054.3
Electrophoresis buffer	Electrophorese-Puffer (10x) Apotheke, KUM Campus Großhadern T0018
16% Formaldehyde Solution, Methanol-free	Thermo Scientific 28906
Glycerol	ROTH Karlsruhe 3783.1
Giemsa's Azur Eosin Methylene Blue Solution	Sigma-Aldrich 109204
Immersion oil	Type N Immersion Liquid Leica Microsystems, 11513860
Liquid Blocker	Science Services N71310-N
May-Grünwals's Eosine-Methylene Blue Solution	Sigma-Aldrich 101424
2-Mercaptoethanol	Sigma-Aldrich M3148
Methanol	ROTH Karlsruhe 8388.5
Mounting Medium	Ibidi 50001
Neo-Mount	Sigma-Aldrich 109016
Paraformaldehyde	ROTH Karlsruhe 0335.1
Powdered milk	ROTH Karlsruhe T145.2
ProLong Gold antifade reagent with DAPI	Invitrogen P36941
Propidium Iodide	Sigma-Aldrich P4170
Protease Inhibitor Cocktail	cOmplete Roche CO-RO, 11697498001
Protein Assay	Bio-Rad Protein Assay Dye Reagent Concentrate BIO-RAD # 500-0006
Reducing Agent	Bolt Sample Reducing Agent (10X) Invitrogen, Novex, Life Technologies B0009
Sample buffer	Bolt LDS Sample Buffer (4X) Invitrogen, Novex, Life Technologies B0007
µ-Slide 8 Well ibiTreat	Ibidi 80826

Sodium Dodecyl Sulfate	ICN Biomedicals 811030
Sodium hydroxide - Pellets	AppliChem A6829,0500
Stripping buffer	Restore PLUS Western Blot Stripping Buffer Thermo Scientific 46430
TBS buffer pH 8.0	TBS-Puffer pH 8,0 (10x) Apotheke, KUM Campus Großhadern T03290
TRIS - (hydroxymethyl) - aminomethane	ROTH Karlsruhe 5429.3
Tween20	ROTH Karlsruhe 9127.2
Trypsin	Detaching of adherent cells 0.05 % Trypsin-EDTA (1X) Gibco, 25300-054
WB weight marker	Page Ruler Plus Prestained Thermo Scientific #26619

2.1.3 Antibodies

2.1.3.1 FACS Antibodies

Table 6 FACS Antibodies

Reactivity	**Conjugated fluorochrome**	**Catalogue number**	**Manufacturer**
Anti-mouse CD11b	APC	553312	BD Bioscience
Anti-mouse/human CD11b	Brilliant Violet 510	101245	BioLegend
Anti-mouse CD45	FITC	103107	BioLegend
Anti-mouse CD105	PE/Cy7	120409	BioLegend
Anti-mouse/human CD44	PerCP/Cy5.5	103031	BioLegend
Anti-mouse/human CD44	FITC	103021	BioLegend
Anti-mouse/rat CD29	APC/Cy7	102225	BioLegend
Anti-mouse/rat CD29	PE/Cy7	102221	BioLegend
Anti-mouse CD117	APC	553356	BD Bioscience
Anti-mouse CD90.2	Brilliant Violet 510	140319	BioLegend
Anti-mouse Ly-6A/E	PE	553108	BD Bioscience
Anti-mouse Ly-6A/E	APC	108111	BioLegend
Anti-mouse CD11b	PE	553311	BD Bioscience
Anti-mouse CD86	APC/Cyanine7	105029	BioLegend
Anti-mouse CD106	FITC	105705	BioLegend
Anti-mouse CD106	APC	105717	BioLegend
Anti-mouse CD45	APC	147707	BioLegend
Anti-mouse CD31	PE	102407	BioLegend
Anti-mouse podoplanin	PE/Cy7	127411	BioLegend

2.1.3.2 Primary antibodies used in Immunofluorescence and Western Blot

Table 7 Primary antibodies

Host	Reactivity	Catalogue number	Manufacturer
Rabbit	Actin (I-19)-R	sc-1616	Santa Cruz Biotechnology
Rabbit	Anti-Aggrecan Antibody (mouse)	AB1031	Sigma-Aldrich
Goat	Mouse/Rat FABP4/A-FABP4 Antibody	AF1443	R&D Systems
Rabbit	Anti-Osteocalcin Antibody	ab93876	Abcam
Rabbit	beta-Tubulin (9F3)	2128S	Cell Signaling

2.1.3.3 Secondary antibodies used in Immunofluorescence and Western Blot

Table 8 Secondary antibodies

Host	Reactivity	Catalogue number	Manufacturer	Used for
Donkey	Anti-Goat IgG Alexa Fluor 555	A-21432	Invitrogen	IF
Goat	Anti-Rabbit Alexa Fluor 594	8889S	Cell Signaling	IF
Rabbit	Anti-Goat IgG-HRP	sc-2768	Santa Cruz Biotechnology	WB
Mouse	Anti-Rabbit IgG-HRP	sc-2357	Santa Cruz Biotechnology	WB
Donkey	Anti-Rabbit IgG-HRP	sc-2313	Santa Cruz Biotechnology	WB
Donkey	anti-goat IgG-HRP	sc-2020	Santa Cruz Biotechnology	WB

2.1.4 Culture media

Table 9 Culture media

Adipogenesis	StemPro Adipogenesis Differentiation Kit Gibco A10070-01
CFU assay medium	Methylcellulose based medium 10X IMDM (2% FBS) MethoCult GF M3434, STEMCELL, #03434
Chrondrogenesis	StemPro Chondrogenesis Differentiation Kit Gibco A10071-01
Cytokine Cocktail	Cytokine Cocktail 100X, add final concentration in the stock of cytokines Preparation of 5ml stock DMEM (15% FBS) 5000 µl rm IL3 5 µg rm SCF 50 µg rm IL6 5 µg

	DMEM, Gibco rm SCF, Immunotools, 12343325 rm IL-3, Immunotools, 12340033 rm IL-6, Immunotools, 12340063
Freezing Medium	FBS 1ml 10% DMSO FBS supreme, PAN Biotech, P30-3031 DMSO AppliChem, A3672,0250
Murine AML cell culture medium	IMDM medium (500 ml) 15% FBS 1% Penicillin-Streptomycin 1 ml Plasmocin Prophylactic (Mycoplasma elimination reagent) IMDM, Gibco, 12440-053 Penicillin-Streptomycin, PAN Biotech, P06-07050 FBS supreme, PAN Biotech, P30-3031 Plasmocin Prophylactic InvivoGen, ant-mpp
OP9 cell line medium	MEM alpha medium (500 ml) 20% FBS 1% Penicillin-Streptomycin 1 ml Plasmocin Prophylactic MEM alpha medium, Gibco, 12561-056
Osteogenesis	StemPro Osteogenesis Differentiation Kit, Gibco, A10072-01
Primary murine MSC cell culture medium	MesenCult Expansion Kit (Mouse, 500ml) 5ml Penicillin-Streptomycin 1ml Plasmocin Prophylactic Preparation in 50ml falcon: Shelf life at 4°C max. 2 weeks Basal Medium 44,5 ml 10X Supplement 5 ml 100X GlutaMax 0,5 ml Optional: 100X MesenPure MesenCult Expansion Kit, STEMCELL, #05513 GlutaMAX, Gibco, 35050-038

2.1.5 Kits

Table 10 Kits

Cytokine Release Assay Kit	Bio-Plex Pro Mouse Cytokine Grp I Panel 23-Plex BIO-RAD, M60009RDPD
Protein Assay	Pierce BCA Protein Assay Kit Thermo Scientific 23227
WB-Transferring	Trans-Blot Turbo RTA Transfer Kit, LF PVDF BIO-RAD #1704274

2.1.6 Mouse cells

2.1.6.1 AML cells

Murine AML cells were generated as per a protocol previously described[68]. Hematopoietic progenitors were isolated from healthy donor mice by established FACS protocols. These cells were cultured for two days to induce proliferation in the presence of cytokines (SCF, IL-3 and IL-6). After this “cycling”, the cells were transduced with retroviral particles containing the reporter gene for GFP, which allows for tracking the leukemic cells using FACS. After a short culture time, the cells were sorted based on their GFP expression and used for in vitro assay as well as for further transplantation into syngeneic mice to generate 1°AML. At AML onset the mice were sacrificed, and cells were harvested from the BM to perform further analysis (Figure 2).

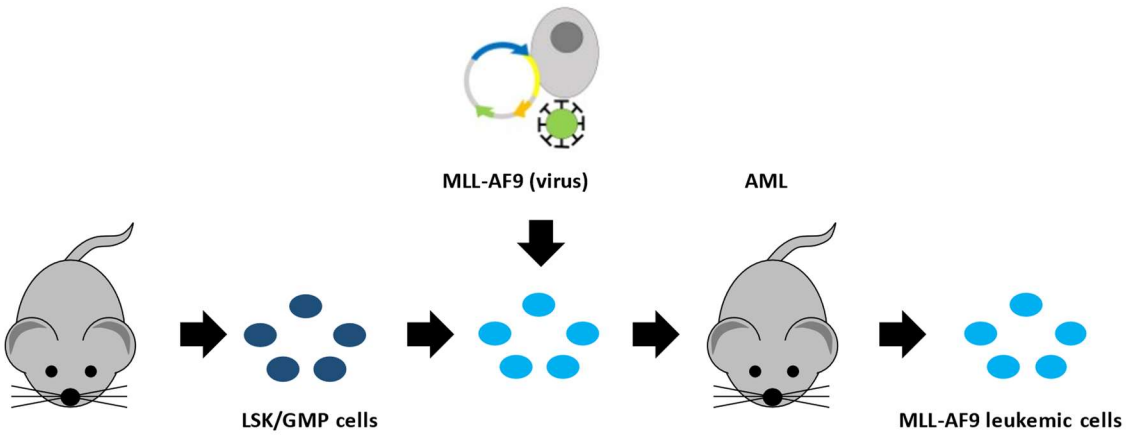

Figure 2 Production of MLL-AF9 leukemic cells

Murine hematopoietic progenitor cells (dark blue) are retrovirally transduced (light blue) and transplanted into syngeneic mice, which are later sacrificed to harvest the cells.

2.1.6.2 MSC

2.1.6.2.1 MSC Harvesting

The Compact bone (CB) MSC were isolated according to the manufacturer's instructions (MesenCult Expansion Kit, ID: #05513, Stemcell) from C57BL/6 mice (Figure 3).

The BM-MSC used, were purchased, expanded with the MesenCult Expansion Kit and aliquoted: OriCell Strain C57BL/6 Mouse Mesenchymal Stem Cells was used (ID: MUBMX-01001, Cyagen).

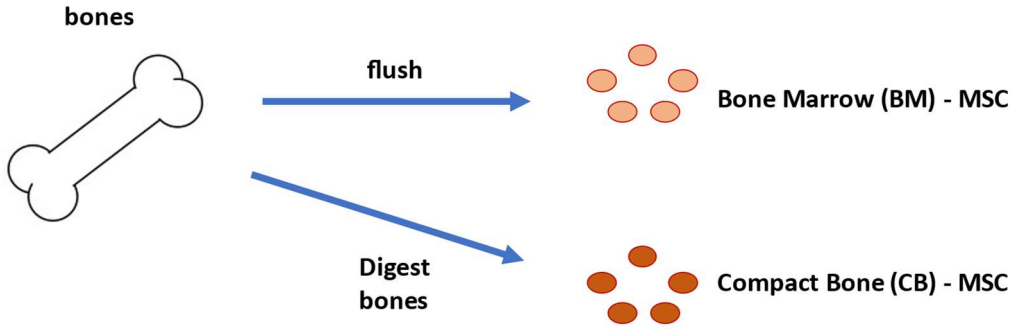

Figure 3 Harvesting Mesenchymal Stem Cells
The bone can be cut and flushed and thus obtaining bone marrow MSC or digested and therefore gaining compact bone MSC.

2.1.6.2.2 Cell lines (murine) used

Table 11 Murine cell lines

OP9 [77]	ATCC Strain: (C57BL/6 x C3H) F3 -op/op Stromal cells
S17 [78]	Strain: BALB/cAn Stromal cells

2.2 Methods

2.2.1 Cell culture

All cell culture experiments were performed under a laminar flow hood. This ensured the sterile environment needed for the appropriate cell growth and reproducibility of the results. After every change of the cell environment, e.g., medium change, splitting or treatment application, the cells were kept in a 37°C incubator under normoxic standard conditions.

2.2.1.1 Cell pelleting

Cultures with suspended cells were carefully transferred into a sterile Eppendorf (1-2 ml) or a sterile conic tube (15/50 ml) depending on the suspension volume. The tube was then centrifuged at 300-400 x g for 5-10 min. The supernatant was discarded, and fresh medium was added to the tube to resuspend the cell pellet.

Cultures with adherent cells were washed 2-3 times with D-PBS after discarding the old medium. The cells were then detached from the plastic surface by Trypsin-EDTA (0.25%) and incubated at 37°C for a few minutes. The Trypsin was subsequently deactivated using cell medium with a ratio of 1:1 to 1:2, Trypsin to cell medium respectively. The following steps are the same as the suspended cells cultures.

2.2.1.2 Counting and subculturing of cells

To find out the growth capability of the cultures under different conditions, it is necessary to count the cells regularly. This was achieved either by using a hemocytometer or a cell counter (ViCell). The resuspended cells were in both cases stained by bromophenol blue. 10 µL of the stain-suspension mixture (ratio 1:1) were added to the hemocytometer between the chamber and a coverslip. The cell number was then counted using a microscope. For the counting using the cell counter (ViCell), a cell type of “default” was used.

After determining the cell number of all cultures, the desired seeding density or splitting ratio was calculated for optimal continuation as per the different experiment protocols.

2.2.1.3 Cryopreservation and thawing of cells

To cryopreserve a cell-pellet, a solution containing 90% FBS and 10% DMSO was used. After following the steps under 2.2.1.1 the pellet was washed 2-3 times with D-PBS and centrifuged at 300 x g for 5-10 min. The cell pellet was then resuspended in the cryopreservative and stored at -80°C in a cryovial.

For cell thawing, the cryovial, previously stored at -80°C, was quicky thawed by gently swirling the vial in a 37°C water bath. The thawed cell suspension was then transferred into a sterile 15 mL conic tube and washed 2-3 times with D-PBS. The tube was centrifuged at 300 x g for 5-10 min and the cell pellet resuspended in culture medium and placed in a cell incubator at 37°C for a minimum of one day prior to the planned experiment.

2.2.2 Colony Forming Unit (CFU) Assay

The CFU assay is a commonly used to test the differentiation potential of individual hematopoietic stem and progenitor cells (HSPCs) by analyzing the colonies (consisting of more differentiated cells) originating from each progenitor cell[79]. As hematopoietic progenitor cells, the GMP have the ability to differentiate into Granulocytes and/or Monocytes. In a semi-solid matrix individual progenitor cells called colony-forming units proliferate and after seven to fourteen days of culture reveal their properties. It can distinguished between Macrophage (M), Granulocyte-Macrophage (GM), Granulocyte (G) or Blast colonies.

The assay was performed according to manufacturer's instructions and under sterile conditions (laminar flow hood)[80]. The methylcellulose medium was aliquoted and stored at -20°C for duplicate and/or triplicate cultures. The required number of pre-aliquoted tubes of medium (MethoCult GF M3434) were thawed prior to the experiment. The cells of the different conditions were prepared as a cell suspension in round bottom tubes with fresh IMDM (+ 2% FBS) medium and their cell number counted as to adjust for the required plating volume of 500 cells per well. That volume was then added to 3 mL (for doublets) or 4 mL (for triplets) of MethoCult and vortexed thoroughly. The cell-methylcellulose mixture was then dispensed into the culture dishes (SmartDish) were according to manufacturer's instructions, with each well of a 6-well-plate containing 1.1 mL medium. The cultures were incubated at 37°C in 5% CO2 and analyzed when the colonies had reached an appropriate size. The counting of the

colonies was performed manually with STEMgrid™-6 for 6 well plates, placed under the culture dishes, with the help of a Leica microscope and a counter clicker.

In case of a replating or FACS analysis, the cell-methylcellulose mixture was washed three times with D-PBS and the cells centrifuged. The subsequent steps were performed according to the CFU or FACS protocol.

2.2.3 Co-culture of GMP-AML with feeder cells

To evaluate the influence feeder cells have on GMP-AML cells, co-culture experiments were set up. Either direct or indirect cell-to-cell contact was allowed and analyzed.

Direct cell-contact was ensured by first plating feeder cells and after irradiation (or no irradiation) AML cells were added to the culture. To separate the two different cell types from each other, a FACS sorting machine was used (see 2.2.6.4).

To evaluate only indirect cell-contact via soluble factors, a chamber culture system with a membrane with a 0.4 µm pore size (ID 3401, Corning) was used, allowing cytokines and mediators to pass freely but preventing cell to cell contact. First the feeder cells were plated in the lower chamber and after irradiation (or no irradiation) the upper chamber was installed, and AML cells added into the upper chamber.

2.2.4 May-Giemsa-Grünwald staining

May-Giemsa-Grünwald staining (MGG) was used to evaluate cell morphology.

First, the cells were placed on microscopy slides for Cytospin. The cells were suspended in D-PBS with ideally 10-15% FBS. The Cytoslide was then inserted into a Cytoclip, and It had to be ensured that the absorbent surface was positioned correctly. A filter paper was used as next layer and a Cytofunnel placed into the clip. The clip was gently fastened. A filled Cytoclip was placed in each recess and balanced. Based on the desired cell density, 100-500 µl of cell suspension were pipetted into the Cytofunnel (ideally 200 µl). The slides were centrifuged for 10 minutes at 500 RPM, preferably using medium acceleration (the suggested settings apply for hematological slides and Shandon Cytospin 2). Each Cytoclip was unloaded horizontally to avoid spilling of residual liquid. The slides were finally air-dried for a minimum of 30 minutes[81].

Prior to staining, the slides were fixed with either methanol for 5 minutes or paraformaldehyde (PFA) for 10 minutes at RT, depending on cell type. The slides were then rinsed with PBS.

For the preparation of one liter of 4% PFA solution, 800 ml of PBS were added to an appropriate vessel. The vessel was then placed on a magnetic stirrer under a ventilated hood. The vessel was the heated to approximately 60°C while stirring and 40 g of PFA powder were added. 1 N NaOH was carefully added dropwise, until the solution cleared. The stirring continued until the powder was dissolved and afterwards the solution was left to cool down. The volume was adjusted to 1 l with PBS and the pH to 6.9 – 7.4. The solution was aliquoted in 50 ml conic tubes and stored at -20°C.

For the MGG staining a buffer solution (buffer tablets, ID: 111374, Sigma-Aldrich) was prepared and used. For this step, a vessel was filled up with 1000 ml of distilled water and placed on a magnetic stirrer, then a buffer tablet was added. The buffer's pH was 6.8.

The working solutions for the staining had to be prepared ahead of time under a ventilated hood. The May-Grünwald stock solution (ID: 101424, Sigma-Aldrich) was mixed with PBS or Weise buffer 1:1 in a sufficient volume (e.g., 50 ml stain with 50 ml PBS). Next, the Giemsa stock solution (ID: 109204, Sigma-Aldrich) was mixed with PBS or Weise buffer 1:20 in a sufficient volume (e.g., 2.5 ml stain with 50 ml PBS). The previously air-dried slides were placed inside a suitable container (e.g., a staining tray). The container was then filled with working May-Grünwald solution for 5-7 minutes, while agitating the slides occasionally. The slides were rinsed with PBS or Weise buffer until the solution was clear of stain. The container was then filled up with working Giemsa solution for 10-15 minutes with occasional agitation. The slides were then rinsed with PBS or Weise buffer until no stain was detectable and left for 3 minutes in fresh buffer (ideally with pH 6.8). The slides were left to dry overnight.

The slides could be either examined directly or first mounted and stored. For the mounting a hydrophobic mounting medium was used.

2.2.4.1 Microscopy

Brightfield, phase, as well as fluorescent cell and culture images were taken on an Inverted Leica DMi8 microscope. Magnifications used were 10x, 20x, 40x and 63x (with immersion oil). The images were acquired by the LAS X software package. Some images have been enhanced (channel intensities) using the native LAS X software. Brightfield and phase images were additionally taken on the AE2000 Series Motic Microscope.

2.2.5 Immunofluorescence

The first step was to prepare the coverslips. Square or round coverslips were stored in a box and autoclaved prior to a cell culture. Under a laminar flow hood, they were placed on the bottom of a culture vessel before it was filled up with cells and medium. After 2-4 days of cell culture the coverslips were removed and fixed using 4% formaldehyde solution (28906, Thermo Scientific) diluted in PBS for 10 minutes at RT. The cells were washed three times with ice-cold PBS. From this point on, drying of the coverslips had to be prevented.

For intracellular target proteins, the cell membrane was made permeable by incubation of the coverslips in PBS with 0.25% Triton X-100 for 10 minutes. They were washed three times with PBS for 5 minutes each. A blocking step was performed to avoid untargeted antibody binding. The blocking buffer consisted of PBST (PBS + 0.1% Tween 20), 1% BSA, 22.52 mg/ml glycine and was applied for 30 minutes to the coverslips. The coverslips were afterwards incubated in a primary antibody solution (10 µg/ml antibody, 1% BSA in PBST) in a humidified chamber overnight at 4°C protected from light. The following day, the solution was discarded, and the coverslips were washed three times with PBS for 5 minutes each. The cells were then incubated with secondary antibody solution (2 µg/ml antibody, 1% BSA in PBS) in the dark for 1 h at RT. The solution was then discarded, and the coverslips were again washed three times with PBS for 5 minutes each in the dark[82].

The cell nuclei were stained using a DAPI enriched mounting medium (ID: P36941, Invitrogen). One drop of mounting medium was administered to the coverslip, which was then sealed on top of a microscope slide with nail polish to prevent drying. The slides were left for incubation of the mounting medium overnight in the dark at RT.

The visualization was performed with the Leica fluorescence microscope. The slides were stored in the dark either at -20°C (for longer term preservation) or at 4°C.

2.2.6 Fluorescence Activated Cell Sorting (FACS)

2.2.6.1 FACS Device preparation and spectrum overlap assessment

Before performing FACS it is important to set up the Sorting machine in accordance with the cell parameters and the fluorochromes of choice. The overlap of the colors should be as small as possible. This was assessed by using the Spectra Analyzer of BioLegend (https://www.biolegend.com/en-us/spectra-analyzer). Furthermore, in case

of a critical combination of overlapping fluorochromes, a compensation should be performed prior to the sorting (according to manufacturer's instructions). As a help to choose the appropriate fluorochromes, I used the Spectra Analyzer.

2.2.6.2 Viability staining

A viability staining is required in every FACS experiment to be able to differentiate between live cells and cell debris or damaged nonfunctional cells. There are two methods of viability staining using DAPI, depending on the duration between the DAPI staining and sample analysis at the FACS machine.

For the first method, the cell suspension was transferred into a round bottom 5 ml tube and a 1 µl of a DAPI stock solution (250 µg/ml) was added for every 250 µl cell suspension. The sample was incubated for 1-5 minutes in a dark room and run through the cytometer. If the sample is not examined at most 5 min after staining, the second method should be preferred.

For the second method, the cell-suspension was also transferred into a round bottom tube. 1 µl of a DAPI stock solution (250 µg/ml) was added to every 250 µl cell suspension. The sample was centrifuged at 4°C at 400 x g for 3 minutes. The supernatant was carefully discarded, and the cell pellet resuspended in 200 µl ice-cold D-PBS (ideally with 10-15% FBS). The sample could then be stored at 4°C in the dark until the acquisition at the FACS, for maximum one hour.

Depending on the FACS machine und and the fluorochromes channel needed, Propidium iodide could be used instead of DAPI, Similar to the first DAPI staining method, Propidium iodide was added to the cell-suspension and not washed again. 10 µl of PI stock solution (10 µg/ml) was added to 100 µl of cell suspension, mixed gently and incubated for 1-3 minutes in the dark before cell analysis.

2.2.6.3 Immunophenotyping of surface molecules[83]

For the staining with primary conjugated antibodies the surface markers were selected as per each experiment protocol. To prevent fading of the fluorochromes, the antibody solutions were prepared in the dark. Ice-cold D-PBS with 10-15% of FBS, was added to a conic 15 mL tube and labeled with the name of the planned antibody-panel ("master mix"). 4-5 µl of each antibody solution were added to the tube.

The cultures were washed, and cells pelleted. Each cell culture specimen was mixed with 200-250 µl of the antibody panel mix in FACS tubes and incubated for 20 minutes at 4°C in the dark. Ice-cold D-PBS was then added to the tubes and centrifuged for 5 minutes at 400 x g to wash out any unbound antibodies. The supernatant was discarded without disturbing the cell pellet and the washing procedure was repeated. Afterwards, DAPI or less frequently PI was added to the FACS tubes.

The FACS analysis was performed within 1 hour to avoid fading of the fluorochromes.

2.2.6.4 Cell sorting

Co-cultures not separated by a membrane needed cell sorting prior to further analysis. The GMP-derived AML cells used in the experiments were carriers of a gene encoding for the GFP fluorochrome. This GFP positivity could further be increased by adding an anti-CD45 antibody conjugated with FITC (ID: 103107, BioLegend). While the GMP cells were positive for GFP and CD45, the MSC (or OP9) cells were negative for both.

First, the supernatant of the co-culture was collected in a tube. Then the adherent cells were washed once with PBS, which also was collected in the same tube. This was containing the GMP-AML cells. The MSC/OP9 cells were detached using trypsin (see 2.2.1.1) and added to the tube. A separate tube was used for each condition and for each replicate. The tubes were centrifuged at 400 x g for 5 minutes and washed with D-PBS. PI buffer (1 µg/ml) was added to the cell suspensions, which were later filtered through cell strainers (35 µm) into the FACS tubes and kept on ice. A positive (only GMP) and a negative (only MSC/OP9) control were prepared, filtered, and stained with PI buffer. Collection tubes were prepared with cell medium for the sorted MSC/OP9 and GMP cells.

The cell sorting was performed by gating out the dead cells (PI positive) and by distinguishing between GFP positive and GFP negative cells, which were then separated.

2.2.6.5 Annexin V staining

The cell suspensions were transferred into round bottom tubes and washed twice with PBS, centrifuged at 400 x g for 5 minutes and after discarding the supernatant, resuspended in 100 µl 1X binding buffer (ID: 559763, BD Biosience). 5 µl of PE Annexin V per 100 µl cell-suspension were added and carefully vortexed. They were incubated for 15 minutes at RT in the dark. 400 µl of 1X binding buffer were added to each suspension [84]. DAPI was used as a dead/alive dye and in case of a MSC and GMP co-

suspension an anti-CD45 antibody. The samples were analyzed with a cytometer within one hour. Annexin V and DAPI double positive cells were dead, whereas only Annexin V positive cells were apoptotic. Double negative cells were alive.

2.2.6.6 FACS software

The flow cytometry results were analyzed using FlowJo v10.6.2 Software (BD Life Sciences) and Flowing Software version 2.5.1 (Terho, P.). Statistics of the FACS data was performed using either FlowJo or Flowing Software.

2.2.7 Western blot

Western blot is the standard procedure to detect specific proteins. The cell lysates are run through a gel and afterwards transferred to a membrane, both applying an electric field. The membrane is incubated with primary and secondary antibodies and can be visualized, for example using x-ray methods [85].

2.2.7.1 Preparation of Laemmli buffer

The Laemmli buffer (2X, for sample running) was prepared under the safety cabinet on a magnetic stirrer. Following ingredients were used: 4% SDS, 10% 2-mercaptoethanol, 25% glycerol, 0.004% bromophenol blue, 0.125 M Tris-HCl and adjusted to a pH of 6.8. The buffer could be aliquoted and stored at 4°C for a few days or at -20°C for a longer period.

2.2.7.2 Preparation of RIPA buffer

The RIPA buffer (for cell lysis) was prepared under the safety cabinet on a magnetic stirrer. Following ingredients were used: 150mM NaCl, 0.1% Triton X-100, 0.5% sodium deoxycholate, 0.1% SDS and 50m Tris-HCl to a pH of 8.0. The buffer was aliquoted and stored at -20°C.

2.2.7.3 Preparation of cell lysates

The cell culture dish was placed on ice and the cells were washed with ice-cold D-PBS. The D-PBS was discarded, and ice-cold RIPA buffer was added to the dish. The adherent MSC cells were collected by using a cell scraper and added to a pre-cooled Eppendorf tube. The cell lysis was executed under constant agitation for 30 min at 4°C. The samples were centrifuged in a microcentrifuge at 4°C for 20 min at 16,000 x g. The tubes were placed on ice and the supernatant was aspirated and placed in fresh

tube on ice. The pellet was discarded. After the addition of Proteinase inhibitor solution (25X) the lysates were stored at -80°C.

2.2.7.4 Bradford protein quantification assay

For a protein quantification assay, first the 5X dye reagent (ID: #5000006, Bio-Rad) was diluted with double distilled water and BSA standards with different concentrations (25 – 2000 µg/mL) were prepared with ddH2O. A small volume of the cell lysate was diluted 1:10 and used as sample for the assay. 10 µL of the standards, diluted sample, and ddH2O (blank) were added in doublets to a 96-well plate. 200 µL of the 1X dye solution were added to each well. An absorbance assay was performed with the Glo-Max device at 600nm. The increase of the absorption was linear to the protein concentration in each sample and therefore a linear regression was calculated by excel software, based on the standards and the blanks. The samples' protein concentration could therefore be estimated by their absorbance.

2.2.7.5 Sample preparation and gel electrophoresis

Prior to SDS-PAGE (Sodium dodecyl-sulfate polyacrylamide gel electrophoresis), a protein quantification assay was conducted, either using the Bradford method or using the BCA protein assay kit (ID: 23227, Thermo Scientific) according to manufacturer's instructions and the GlowMax at 560nm.

First, it was determined how much total protein to load (15-30 µg), depending on the expected protein abundance in the samples, the lysate volume was calculated and the appropriate volume of 2X stock Laemmli buffer or 4X Bolt LDS Sample Buffer (ID: B0007, Invitrogen) with 10X Reducing Agent (ID: B0009, Invitrogen) was added to the samples. The lysates were then denaturized at 95°C for 10 min. Equal amounts of total protein were loaded into the wells of the 12% Tris-Glycine gel (ID: XP00122BOX, Invitrogen), along with a molecular weight marker and if applicable with a positive control. The 10X electrophoresis buffer used, was provided by the pharmacy of the LMU university hospital (T0018) and diluted with distilled water. The gel was run at 70 V until the stocking gel was passed, and the voltage was raised to 120 V for the second part.

2.2.7.6 Transferring to the membrane

The protein transfer was conducted using the Trans-Blot Turbo Transfer Kit (ID: #1704274, Bio-Rad) and Transfer System (ID: #1704150, Bio-Rad). The membrane

used was a PVDF membrane. It was activated with methanol for 1 min and rinsed with transfer buffer. The transfer protocol used was preprogrammed for low molecular weight.

2.2.7.7 Antibody staining

The blocking buffer was prepared from 10X TBS, provided by the LMU university hospital, diluted to an 1X solution with distilled water and with the addition of 0.1% Tween 20. Furthermore, 5% of milk powder was added to the solution.

The membrane was blocked for 1h at room temperature using blocking buffer and incubated overnight with the appropriate dilutions of primary antibody in blocking buffer at 4°C. After washing it three times with TBST for a few minutes the membrane was incubated with the recommended dilution of the HRP-conjugated secondary antibody in blocking buffer at room temperature for 1h. The membrane was again washed three times with TBST for a few minutes. To avoid drying, the membrane was covered in plastic wrap. If necessary, the membrane could be stored in PBS overnight at 4°C.

2.2.7.8 Chemiluminescence imaging

The analysis of the Western blot membrane was performed with the Pierce ECL Plus Western Blotting Substate (ID: 32132, Thermo Fisher) and the Fusion SL imaging system (vilber) according to manufacturer's instructions.

2.2.7.9 Image analysis

The images obtained by western blot were analyzed using the ImageJ software version 1.53f. The area of the bands of the control protein ("first lane") as well as the bands of target protein ("next lane") on the membrane were selected and the lanes plotted. Afterwards, the value (area) of the lanes was measured, and the target protein value corrected by the control protein value (adjusted density).

2.2.8 Cytokine Release Assay

For this assay, the cell culture's supernatant was collected in autoclaved Eppendorf vials and kept on ice. The vials were centrifuged at 1000 x g in the microfuge for 15 minutes at 4°C and the supernatant collected in new Eppendorf. A second

centrifugation took pace at 10.000 x g for 10 minutes at 4°C. The supernatant was transferred into cryovials and stored at -80°C.

This experiment was performed following the manufacturer's instructions[86]. The cytokines analyzed were IL-1α, IL1-β, IL-2, IL-3, IL-4, IL-5, IL-6, IL-9, IL-10, IL-12 (p40), IL-12 (p70), IL-13, IL-17A, CCL11, CSF3, CSF2, IFN-γ, CXCL1, CCL2, CCL3, CCL4, CCL5, TNF-α.

For the assay, first the assay buffer, the wash buffer and sample diluent (MesenCult, ID: #05513, STEMCELL; with GlutaMAX**;** contains serum) were brought to room temperature. The frozen samples were then thawed and kept on ice. The wash buffer (10X) was diluted with distilled water (dH2O). The standard (23 Plex Group I) was dissolved in 500 µl of sample diluent, vortexed for 5 sec and incubated on ice for 30 min. Afterwards a fourfold standard dilution series and a blank were prepared (Figure 4), each dilution was vortexed for 5 sec between liquid transfers. Subsequently, the 10X coupled mouse beats were vortexed for 30 sec and diluted to 1X in Bio-Plex assay buffer, while being protected from light. Before running the assay, 70-100 µl of the undiluted samples were added to a new 96 well-plate according to the layout. The diluted beats were vortexed for 10-20 sec and added to each well of the assay plate, in a volume of 50 µl. The plate was washed twice with 100 µl of diluted wash buffer on the magnetic washer. Standard, blank and samples were added to the assay plate in a volume of 50 µl. Incubation time is according to the manufacturer's instructions minimum 30 minutes at room temperature, in this case the incubation time was 55 minutes. The plate was washed three times with diluted wash buffer. The detection antibodies (10X) were vortexed for a few seconds and diluted with detection antibody solution. A volume of 25 µl of the diluted detection antibodies was added to each well. The plate was again incubated in the dark for 55 min. In the meantime, the Streptavidin-phycoerythrin 100X (SA-PE) conjugate was diluted with assay buffer and the Bio-Plex Manager Software protocol was prepared with the standard S1 values from the assay kit. The assay plate was then again washed three times with diluted wash buffer on the magnet washer. A volume of 50 µl diluted SA-PE was added to each well and the plate was incubated for 20 min at RT at 800 rpm in the dark. Afterwards, the plates were washed three times, and the samples were resuspended with 125 µl assay buffer per well at RT at 800 rpm for a few seconds. The sealing tape was removed, and the plate was read using the Bio-Plex 100 with the BioPlex Manager v6.2.

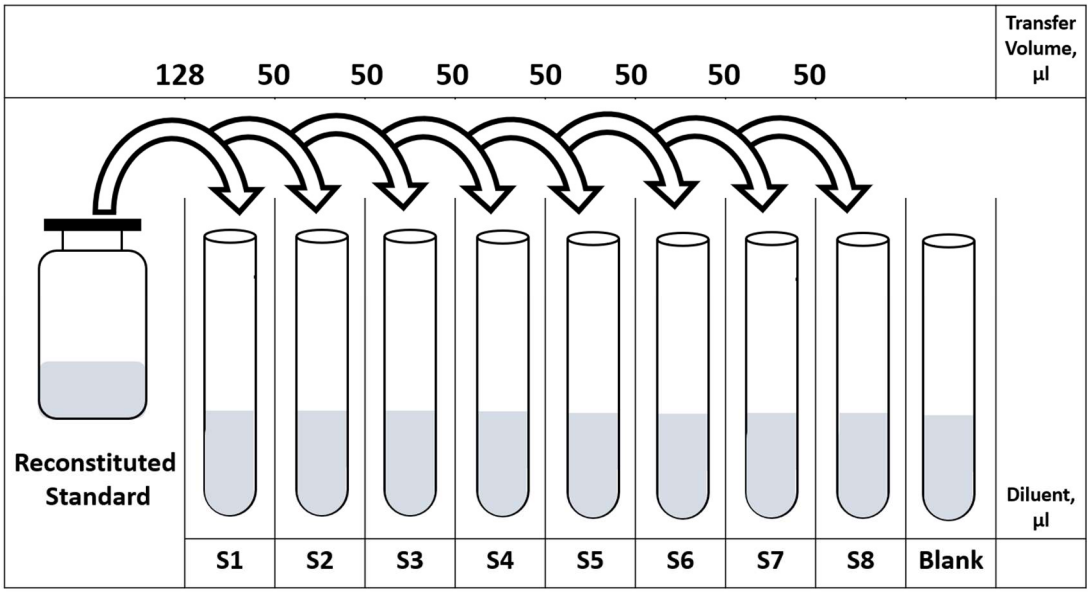

Figure 4 Preparation of a fourfold dilution series of cytokine standards

Schematic representation of the dilution series of cytokine standards (based on [86] p.13 Fig.3).

2.2.9 RNA sequencing

2.2.9.1 Sample preparation

The cells of interest were washed, collected, and counted using a hemocytometer. 10,000 cells were collected for each sample in 1.5 ml Eppendorf tubes. The samples were washed with PBS and centrifuged at RT at 400 x g for 5 min. The supernatant was discarded and the remaining volume of 10 µl was the cell pellet and PBS. The tubes were kept on ice.

The lysis buffer was prepared with Qiagen RLT Plus buffer (#1053393) and 1% 2-mercaptoethanol and kept in a conic tube on ice. A 96-well plate (semi-skirted, Greiner, #652290) was placed on dry ice. 50 µl of the lysis buffer was added to the samples and the mixtures (lysates) were added to an individual well each, while the sample volume was kept under 25% of the total volume. The well-plate was sealed with an aluminum seal and stored at -80°C.

2.2.9.2 Library preparation and sequencing

After the previous step, the samples were transported on dry ice to the department of Anthropology and Human Genomics of the LMU and processed by the Enard Group. The library preparation, including the RNA extraction, and the RNA sequencing (flow

cell) were performed according to the Enard's Lab protocol. To process the data zUMIs was used and a gene expression table (count matrix) was generated. The data was finally analyzed by a bioinformatician to generate differential expression values in comparison to control.

2.2.9.3 Differential gene expression analysis

For further data analysis, outliers of the replicates were excluded. Only genes that consisted of more than ten reads in a minimum of three samples were included in the analysis. The reads were normalized with the Trimmed Mean of M-values (TMM) method using the edgeR package version 3.30.3.[87]. Differential expression analysis was performed with the limma R package version 3.44.3[88].

2.2.9.4 Gene Set Enrichment Analysis (GSEA) and visualization

For the pathway analysis GSEA version 4.0.3 was used. All available Gene Sets at the time of conducting the experiment were used (MSigDB v7.1. 2020)[89]. At the time, MSigDB did not offer Gene Sets (GS) for mouse, therefore the R package msigdbr version 7.2.1. was used. For the GSEA analysis the normalized counts were utilized.

Enrichment maps are a visualization of overlaps amongst enriched pathways. For the generation of such maps, the previously run GSEA results were analyzed with the GSEA software version 4.2.3 and imported into cytoscape version 3.8.1, where the GS of interest could be filtered.

DE gene graphs, top gene graphs and volcano plots were constructed using GraphPad Prism version 8.0.1.

2.2.9.5 Statistical analysis

The statistical analysis (except for the RNAseq) was carried out using the Graphpad Prism Software v8. The data was assumed to have standard gaussian distribution with equal SDs. Depending on the experimental setup different tests for significance were applied. Ordinary one-way ANOVA - for comparing three or more sets of data with one variable. For an ordinary one-way ANOVA either a Dunnet's or Turkey's multiple comparison test was used. Levels of significance: ns $p > 0.05$, * $p \leq 0.05$, ** $p \leq 0.01$, *** $p \leq 0.001$ and **** $p \leq 0.0001$.

3. Results

3.1 Effects of irradiation and LDS1i on MSCs

3.1.1 Proliferation and viability of stromal cells

To assess the effect of the different tested conditions on stroma cells, the stroma cells cultures were passaged multiple times and kept in culture for over two weeks. Each passaging/splitting was completed by the addition of fresh medium and renewal of the treatment. While the treatment seemed to have no apparent effect on the feeder cells' total count, the cell number was inversely proportional to irradiation dose: 2 Gy had no significant impact in comparison to the non-irradiated control (Figure 5), 6 Gy induced a strong decline of proliferation (Figure 7). Upon 20 Gy, a regeneration process 2 weeks after irradiation was observed, before the cells start proliferating again (Figure 5).

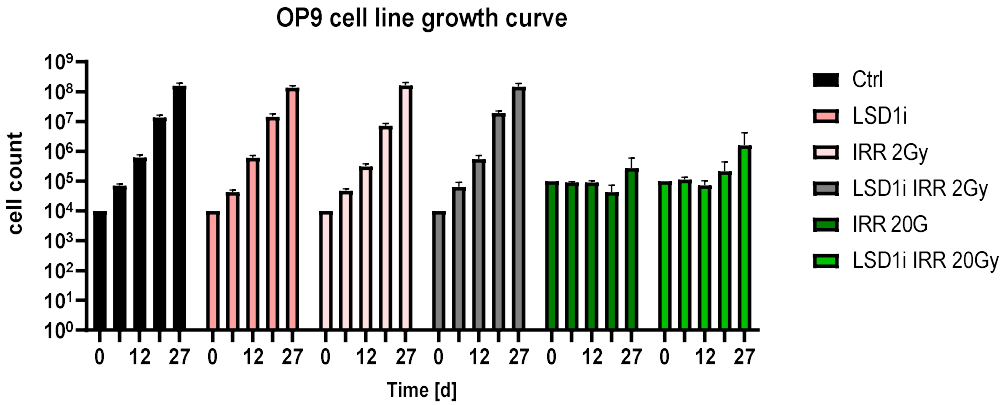

Figure 5 Proliferation of OP9 feeder cells after different radiations doses.
OP9 cells cultured for 27 days at 37°C. CTRL was not treated and non-irradiated. One group was only treated. Irradiated groups were exposed to either 2 Gy or to 20 Gy, and either not treated or treated. n=3

A stronger effect of irradiation (6Gy) on proliferation is shown in Figure 6 and Figure 7, where primary mesenchymal stromal cells from murine bones (bone marrow and compact bone) were irradiated: the CB-MSC were much more sensitive to the radiation with 6Gy (>2fold reduction in comparison to non-irradiated control) (Figure 7), while the effect on BM-MSC was less pronounced. While a higher dose such as 20 Gy is expectedly very toxic to cells, the 6Gy dose seems also to affect in part the growth of stromal cells.

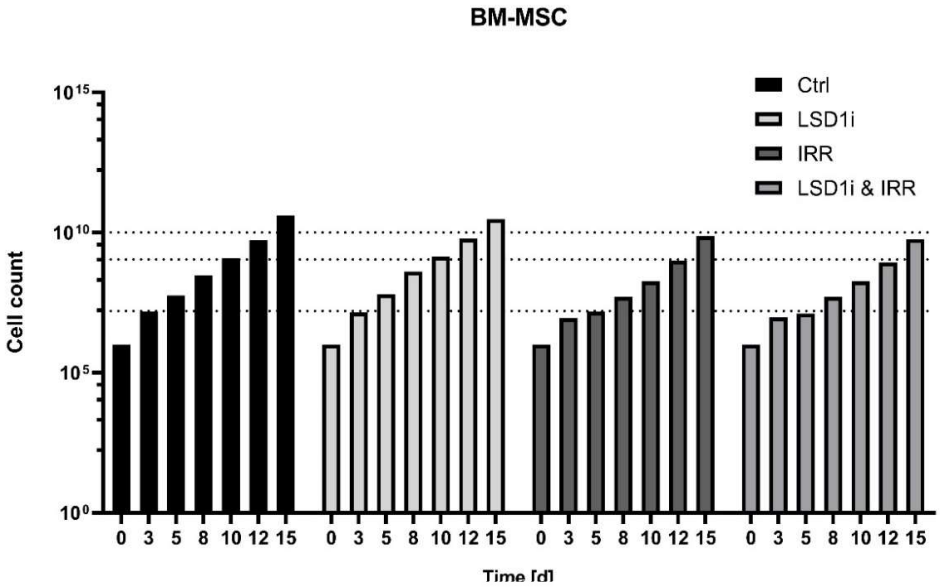

Figure 6 Effect of irradiation on proliferation of BM-MSC.
Primary BM-MSC were cultured for 15 days at 37°C. The cells were either non-irradiated or irradiated at 6Gy and either treated or not treated. n=1

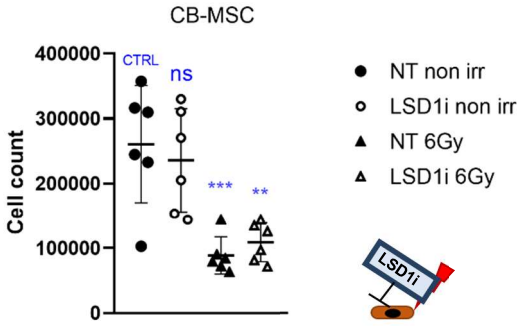

Figure 7 Cell count of MSC monoculture.
Primary CB-MSC were cultured for 15 days at 37°C. The cells were either non-irradiated or irradiated at 6Gy, and either treated or not treated. The groups were compared to “CTRL” (NT non-irr) One-way ANOVA ns > 0.05, * p ≤ 0.05, ** p ≤ 0.01, *** p ≤ 0.001 and **** p ≤ 0.0001.

In order to assess, if the different cell counts were due to a block of the proliferation or cell death / apoptosis, annexin V staining was performed, which in combination with a viable stain (e.g. DAPI) reveals the percentage of alive, apoptotic, and dead cells Figure 8 shows that LSD1 inhibition alone leads to an increased number of dead cells (ca. 20 % vs. 40 %, CTRL vs LSD1i). The irradiation alone and in combination with LSD1i induces almost double number of apoptotic cells.

Taken together, these data show that LSD1i does not affect the growth of MSC and feeder cells, it does increase the apoptotic cell fraction in CB-MSC, and that irradiation with 6 Gy reduces the proliferation of CB-MSC more than BM-MSC and OP9 by apoptosis induction.

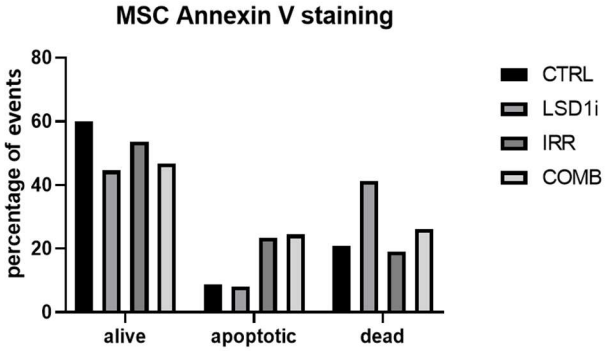

Figure 8 Annexin staining of MSC.
Primary CM-MSC were cultured for 8 days at 37°C. The cells were either non-irradiated or irradiated at 6Gy, and either treated or not treated. n=1

3.1.2 Morphology, immunophenotype and differentiation of stromal cells under the influence of different conditions

The slightest change of the culture conditions can influence the cell metabolism in a significant way. To further investigate the changes induced by the different conditions (irradiation and lSD1i treatment) immunophenotyping was carried out by FACS. CD29 and CD44 are known surface proteins found on MSC from many different origins, such as the bone marrow or the umbilical cord. CD29, also known as Integrin beta-1 is a matrix receptor protein and can therefore be involved in cell migration [90-92]. The proportions of OP9 cells expressing the CD29 marker upon the different conditions is shown in Figure 9. More than 94% of the cells are positive for CD29 in all the conditions.

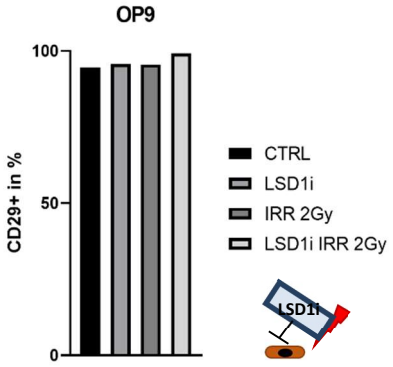

Figure 9 Immunophenotype of OP9
OP9 cells were cultured for 14 days at 37°C. The cells were either non-irradiated or irradiated at 6Gy, and either treated or not treated. n=1

The expression of CD29 is a common feature constantly present in all the MSC considered (Figure 10). Even after multiple passaging and several days in culture, the CD29 expression does not seem to change.

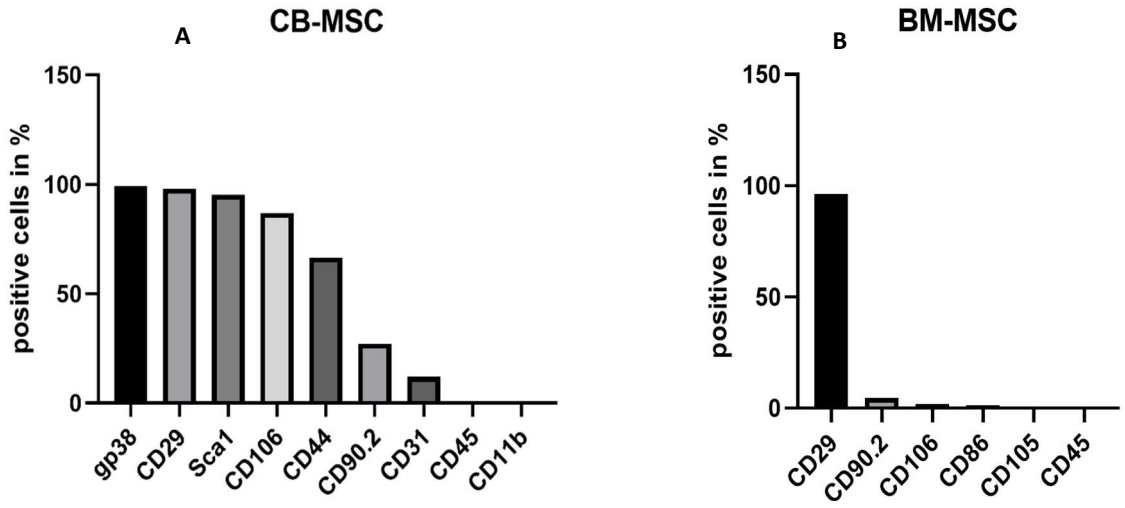

Figure 10 CD29 Expression und CB and BM-MSC

In this figure there are two types of primary MSC (n=1), Compact bone MSC (A), which were kept in culture for a week prior to staining and Bone marrow MSC (B), which were kept in culture for 3 days prior to staining.

Another characteristic marker for MSC is CD44, which can also be found on extracellular vesicles released by MSC[93]. CD44 is a very common surface marker and is important in inflammatory processes[94]. A further typical surface marker is Sca-1 (Stem Cells Antigen 1) coded by the gene *Ly6a*. It can be found on cells of hematopoietic, mesenchymal and endothelial origin[95]. It is known to identify quiescent HSC [96] and its function on other cell types such as MSC is not entirely known. It has been previously described that the number of Sca-1/CD44 double positive MSC increase under hypoxic preexposure[97]. The proportion of OP9 cells positive for both markers in the conditions considered are shown in Figure 11.

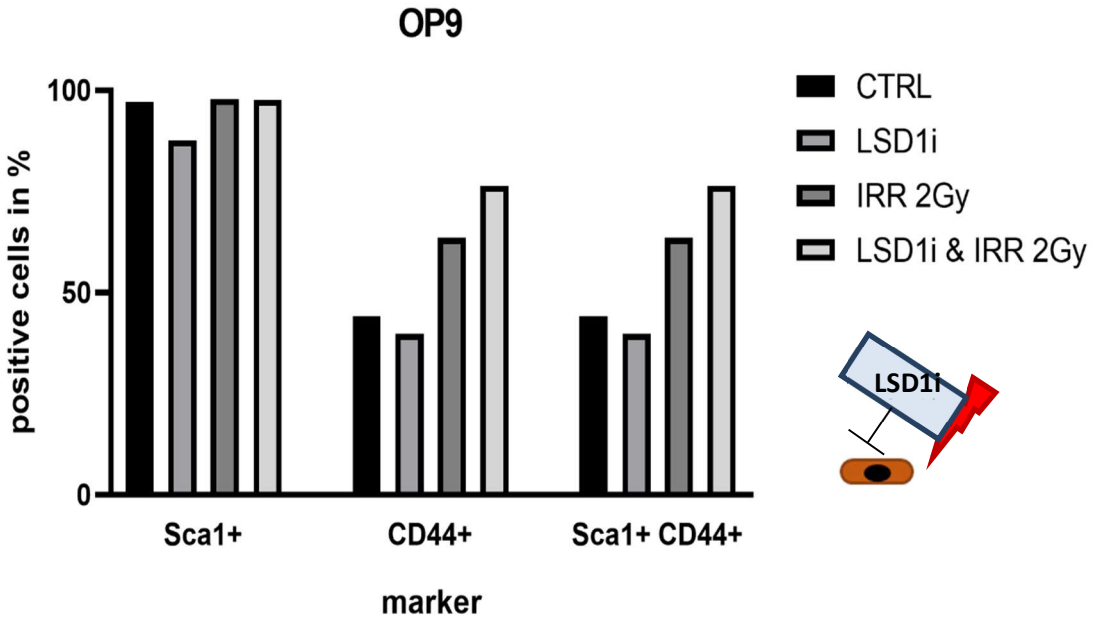

Figure 11 Immunophenotype of OP9
OP9 cells were cultured for 14 days at 37°C. The cells were either non-irradiated or irradiated at 6Gy, and either treated or not treated. Here are the same cultrures as in the experiment of Figure 9, n=1

Sca1 is expressed by more than 85% of live OP9 cells under all conditions (Figure 11). CD44 on the other hand changes from about 40% (non-irradiated cells and upon LSD1i) to over 60% upon irradiation with or without LSD1i. It could be observed that Irradiation increased the CD44 expression on OP9. All CD44+ cells were also Sca-1 positive (see Figure 10 A). According to the International Society for Cellular Therapy, MSCs need to be positive for CD105, CD73, CD90 and negative for CD14 or CD11b, CD79α or CD19 and HLA-DR[48]. Furthermore, according to a study rat derived bone marrow MSC were CD11b-, CD45-, and CD29+, CD73+, CD90+, CD105+[98].

OP9 cells proliferate in vitro with a doubling time of about 26 hours. The morphology of the cells over time was analyzed by May-Grünwald staining: few differences could be observed between the control group (no treatment) and the intervention group (treatment): while the untreated OP9 seem to maintain a smoother cell surface, the LSD1i treated cells are bigger, have bigger nuclei and shows some irregular cell extensions. In the same way, the morphology of CB-MSC in the different conditions was examined (Figure 12).

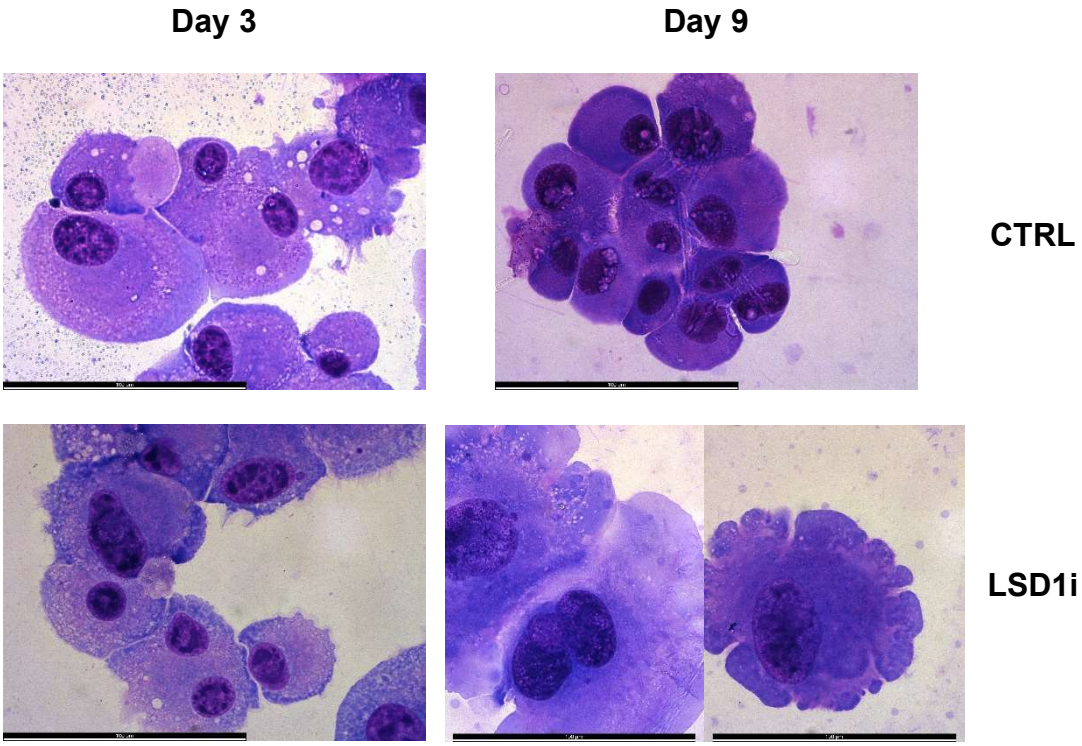

Figure 12 Morphological changes of OP9 upon LSD1i treatment.
A May-Giemsa-Grünwald staining was performed. OP9 cells were cultured at 37°C for up to 9 days and were either treated or not treated. Each black scale bar is 100 µm.

When adherent to the plastic in the culture plate, CB-MSC were spindle shaped, but upon LSD1i (+/- irradiation), cells presented longer and thinner “axonal-like” expansions. In cytospin preparations from the same culture, however, CB-MSC were very similar between the different conditions, with similar size and a constant nuclear-cytoplasmic ratio (Figure 13). Even after irradiation at 6Gy and LSD1 inhibition for about 2 weeks, the MSC do not lose the ability to proliferate, as seen in Figure 6.

MSC are pluripotent cells with many differentiation possibilities, such as adipogenesis and osteogenesis. In the present work, methods of immunofluorescence and western blotting were used to assess the preferred differentiation of the MSC under LSD1 inhibition and/or irradiation. Moreover, the transcriptional program of the MSC has been determined by performing RNAseq. The differentiation into adipocytic cells by positivity for FABP4 and into osteogenic cells by positivity for Osteocalcin was assessed, based on commercially available specific protocols. FABP4 is a fatty acid and osteocalcin is a bone protein secreted by osteoblasts.

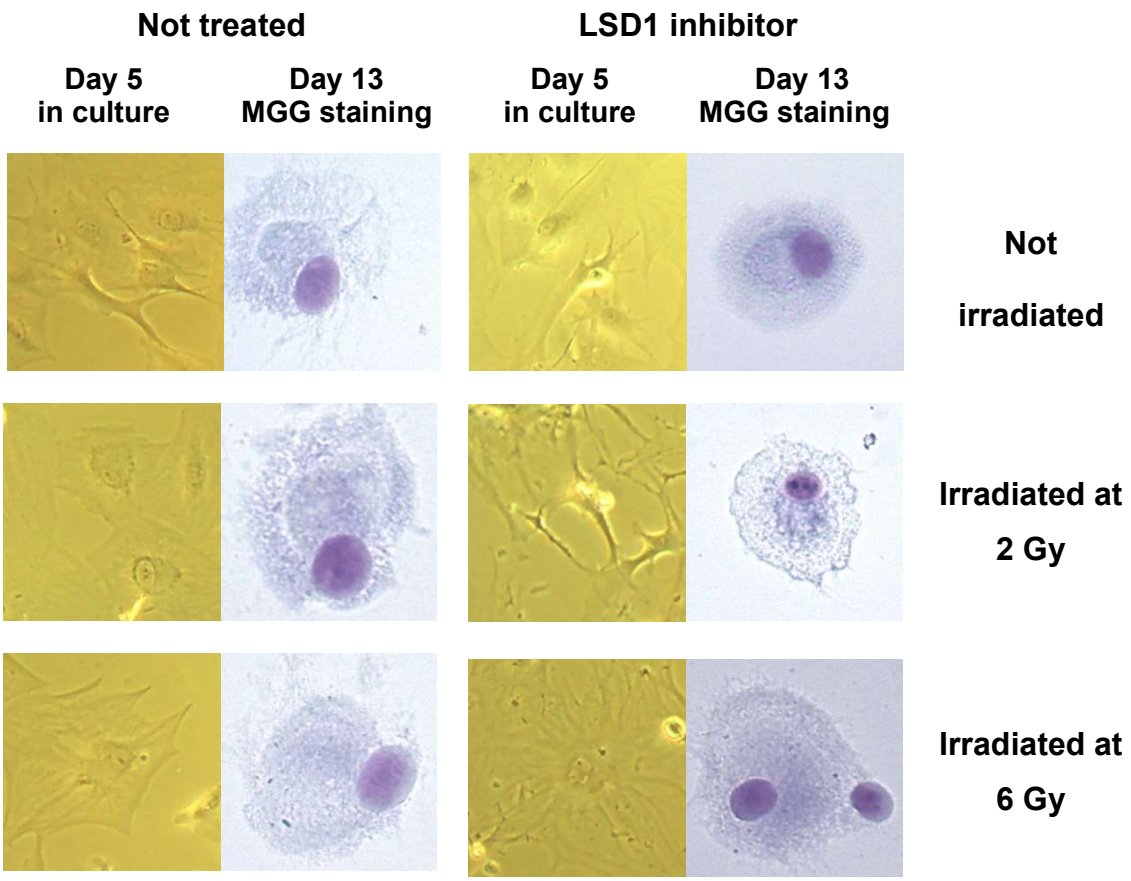

Figure 13 MSC Cell Morphology after LDS1i and Irradiation

Left: images of culture morphology in phase contrast microscopy. Right: May-Giemsa-Grünwald staining after 13 days of culture at 37°C, Cytospin and air-drying of the slides. All pictures were taken in a 400X magnification. The cells of this table were primary CB-MSC, and either not-treated or treated, either non-irradiated or irradiated at 2Gy or 6Gy.

The WB results suggested that the production of FABP4 was increased in the MSC after irradiation. In the presence of irradiation + LSD1i the FABP4 level was lower, but still higher than the controls and LSD1i alone. Figure 15 shows that the MSC after almost two weeks of culture had not yet fully differentiated into more mature cells (in this case adipocytes), which can also be backed by the continuation of proliferation after two weeks in culture (see previous experiments).

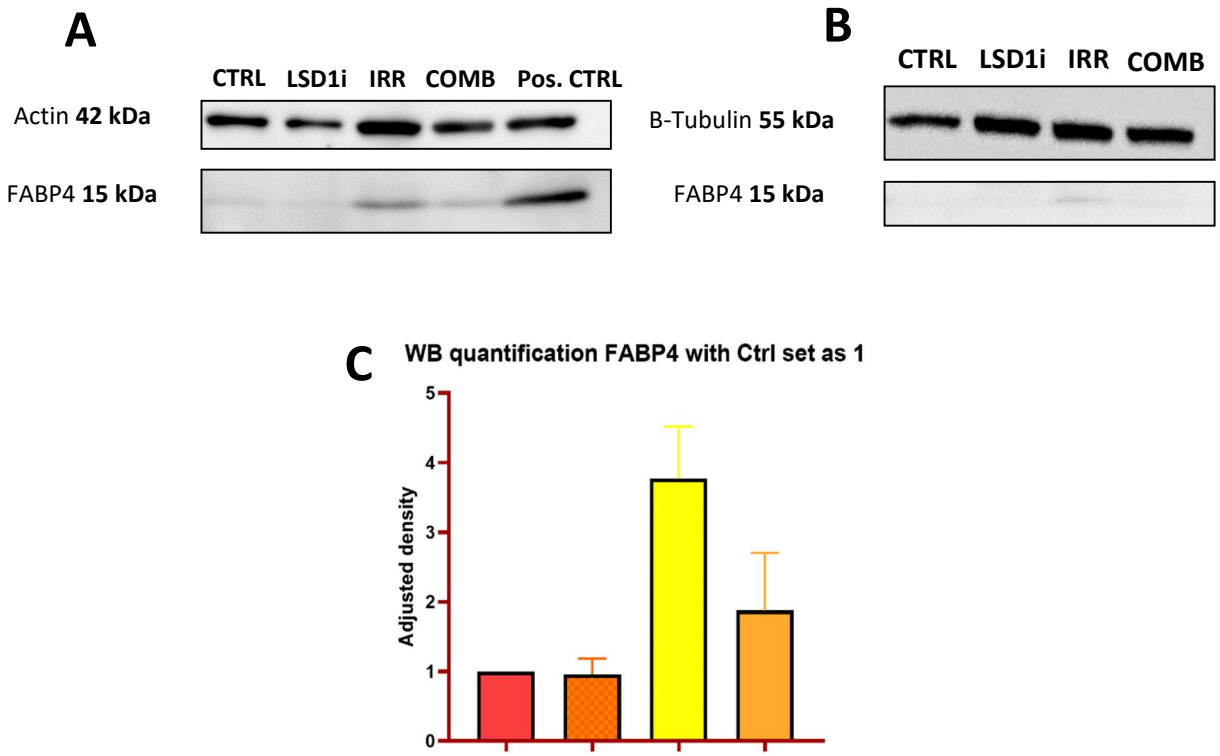

Figure 15 Immunophenotypical characterization of differentiation potential of MSC.
Primary BM-MSC were cultured at 37°C for 12 days. The cells were either not treated or treated, and either non-irradiated or irradiated at 6Gy. On the 12th day the WB lysates were prepared and frozen. The membrane was stained with a primary anti-FABP4 antibody (ID: AF1443, R&D Systems). (A) and (B) show 2 replicates of western blot of whole cell lysate from MSC upon different conditions. (C) Histogram showing the average of band intensities from the replicates of the WB shown above.

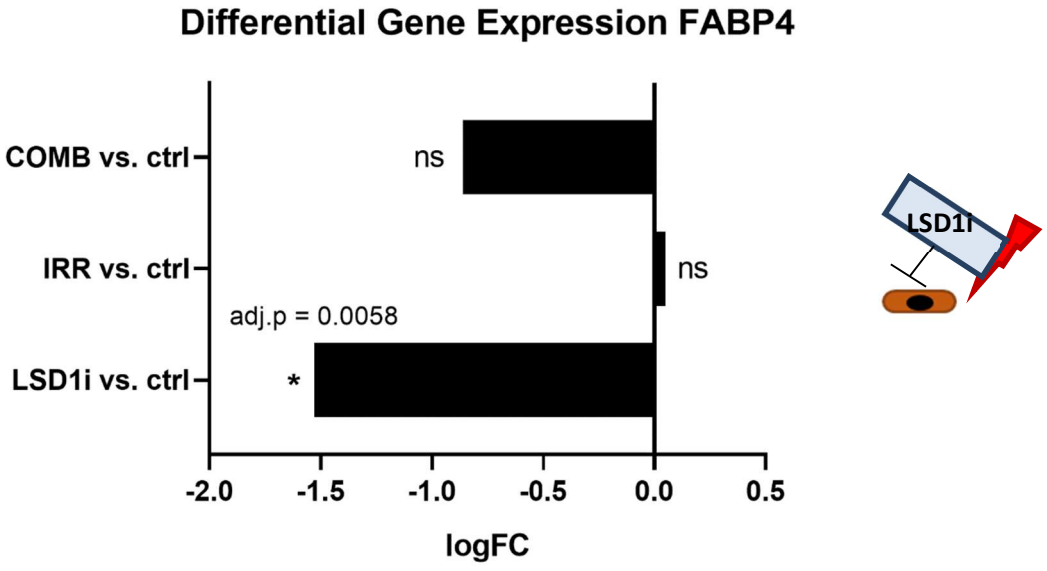

Figure 14 RNA sequencing - FABP4 Gene Expression.
Primary CB-MSC were cultured at 37°C for 15 days. They were either not treated or treated, and either non-irradiated or irradiated at 6Gy. “Combination” is the group of MSC that was irradiated, as well as treated.

Furthermore, expression analysis by RNAseq of FABP4 was performed: the gene expression was significantly decreased in LSD1i in comparison to the control, while the irradiation increased the expression only slightly (ns) (Figure 14). The difference with the WB analysis could be due to different stability of the protein.

Moreover, immunofluorescence staining with FABP4-specific antibody was performed. The condition with the highest signal was the control, followed by the irradiated cells. The LSD1i sample presented less FABP4 signal, while the LSD1i + irradiation had the lowest signal. At this timepoint (14 days) in all conditions, cells were spindle shaped and small (Figure 16).

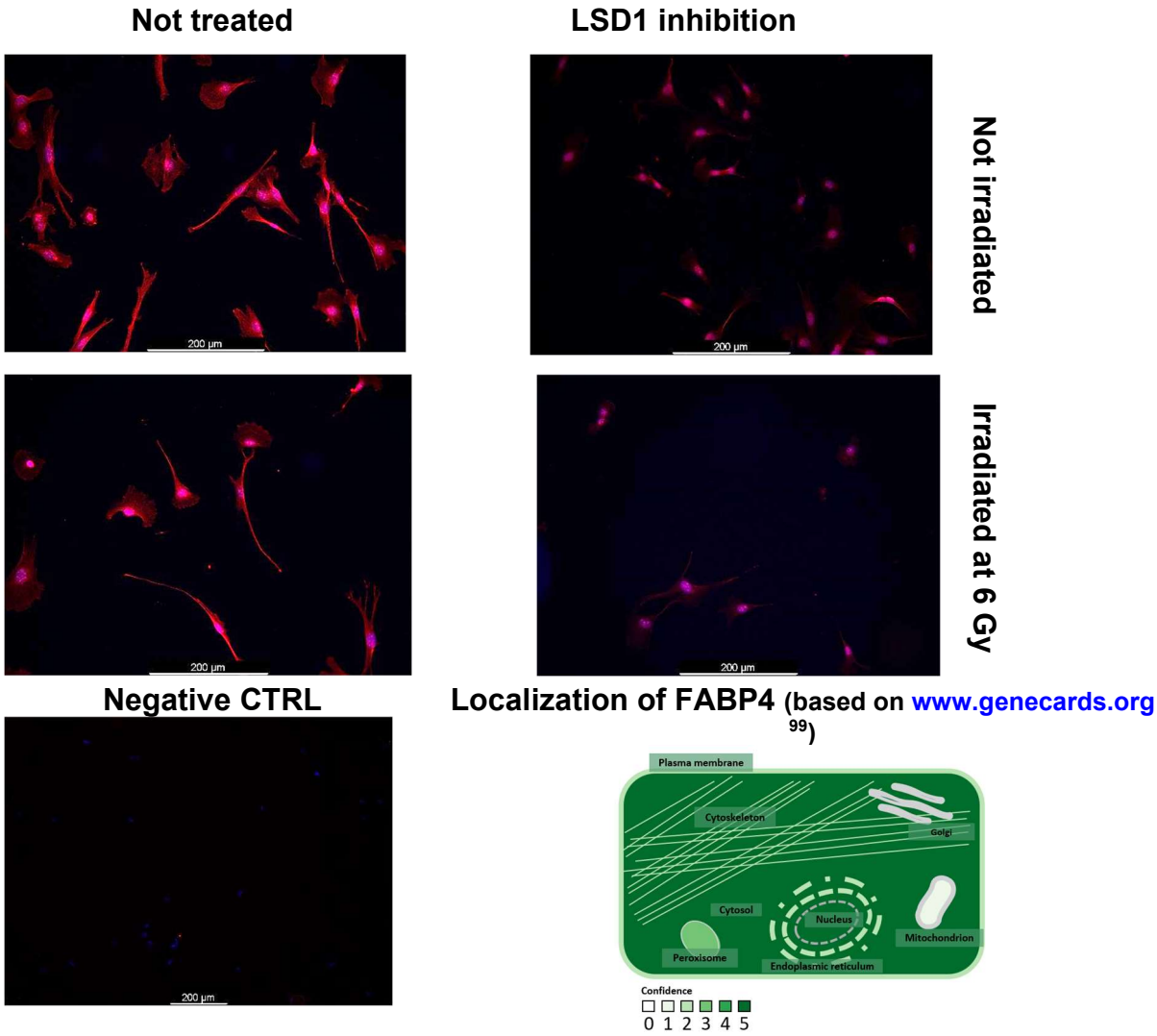

Figure 16 FABP4 MSC immunofluorescent Staining

The cells in this table are from the experiment mentioned in Figure 15. The cells were cultured for 16 days at 37°C. The MSC are stained with the same primary antibody used in the WB. The secondary antibody used was coupled with Alexa Fluor 555 (ID: A-21432, Invitrogen) and the counterstaining was performed with DAPI. The negative control is MSC only stained with secondary antibody and DAPI.

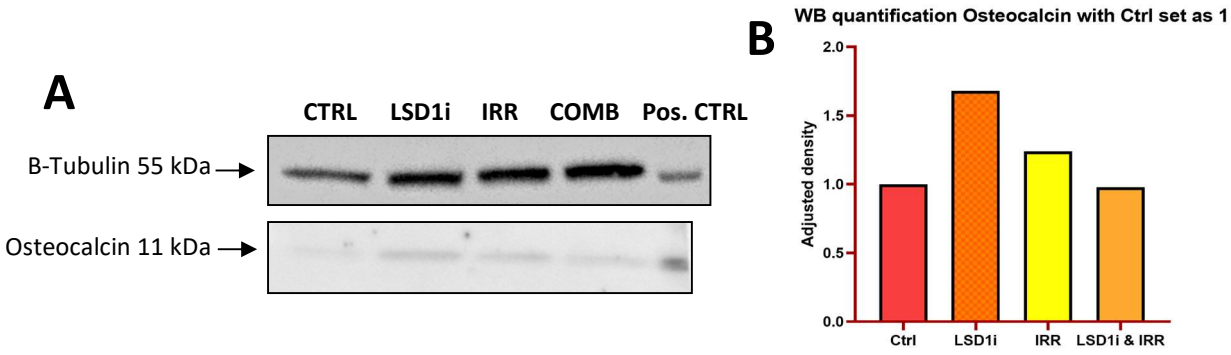

Figure 17 Western blot analysis of FABP4 in MSC,
The lysates for this membrane were prepared from the same cultures as Figure 15. The membrane was stained with a primary anti-Osteocalcin antibody (ID: ab93876, Abcam). The positive CTRL in (A) were MSCs differentiated into osteoblasts, according to manufacturer's instructions of the differentiation kit (ID: A10072-01, Gibco). The WB quantification in (B) was performed with the help of ImageJ.

Beside the potential to differentiate into adipocytes, MSC can also take the path of osteogenesis. In Figure 17, the western blot for osteocalcin is shown. A progressive increase of osteocalcin protein expression in all conditions in comparison to untreated cells was observed. The highest amount was observed in cells treated with LSD1i. It is to be assumed that the main trigger for production of osteocalcin is LSD1 inhibition in this setting. While osteocalcin is a predominantly extracellular protein, the production is intracellular. A further osteogenic protein is osteopontin, a component of the bone, which is coded by the SPP1. In Figure 18 the expression of the gene SPP1 is shown in all conditions compared to the control the expression of SPP1 is significantly upregulated, with the combination of irradiation and treatment being the condition with the biggest change.

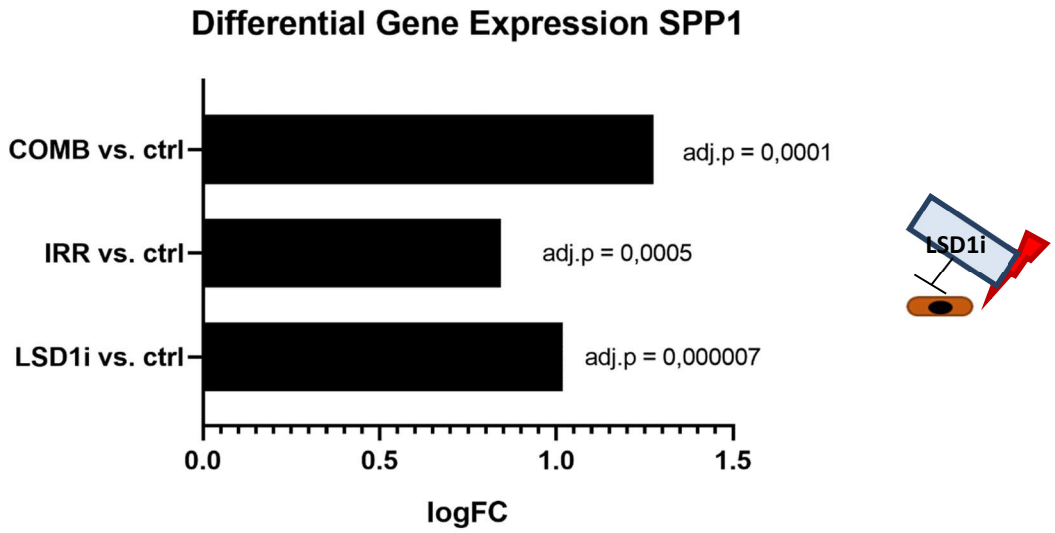

Figure 18 RNAseq - differential gene expression of SPP1 In MSC
Primary CB-MSC were cultured at 37°C for 15 days. They were either treated or not treated, and either irradiated or non-irradiated at 6Gy. “Combination” is the group of MSC that was irradiated, as well as treated.

3.1.3 Cytokine release of stromal cells under different conditions

Cytokines are proteins released in the extracellular space, that manage fundamental cellular processes, such as proliferation and differentiation. They can act as autocrine, paracrine, and endocrine factors. Interleukins, colony stimulating factors, chemokines and tumor necrosis factors are some of the many different cytokine groups important for the hematopoiesis [100].

CCL2 is strongly depleted in cultures of treated and irradiated MSC in comparison to untreated cells (Figure 19); this is similar to what observed in the co-cultures (Figure 39). This also applies to IL6 and CXCL1, while CCL5 did not show significant changes.

CCL2 and CCL5 are released in high concentrations by the MSC (Figure 19). The combination of irradiation and treatment leads to a more than 40 % reduction of the CCL2 concentration compared to not treated and non-irradiated cells. Moreover, the transcription of the genes for both cytokines is reduced by the combination of treatment and irradiation (Figure 22). CCL5 has the highest expression in the control group.

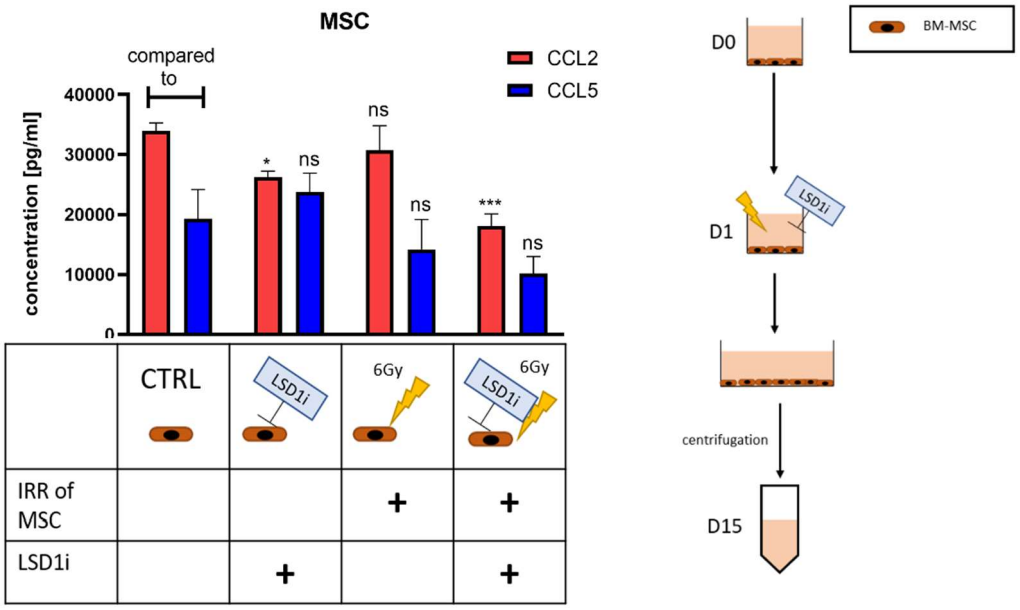

Figure 19 Cytokine release of BM-MSC:
Left: CCL2 and CCL5. n=3 Right: Experimental setup of the cultures for the cytokine release assay. BM-MSC were cultured for 15 days at 37°C. The MSC were either irradiated or non-irradiated. Afterwards, the supernatant was collected and centrifuged. The sample was then stored at -80°C. n=3 (One-way ANOVA). ns > 0.05, * p ≤ 0.05, ** p ≤ 0.01, *** p ≤ 0.001 and **** p ≤ 0.0001.

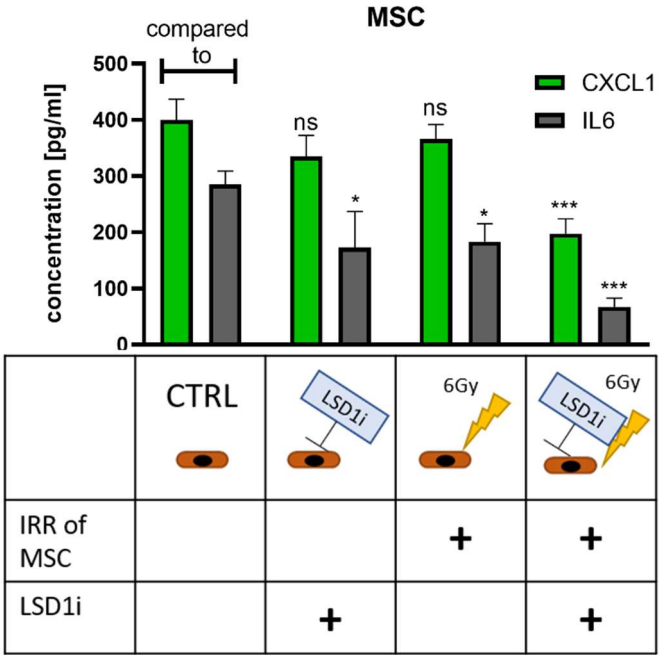

Figure 20 Cytokine release of BM-MSC: CXCL1 and IL6.
n=3 (One-way ANOVA). ns > 0.05, * p ≤ 0.05, ** p ≤ 0.01, *** p ≤ 0.001 and **** p ≤ 0.0001.

CXCL1 and IL6 both have a significantly reduced release when irradiation and treatment are combined in comparison to the untreated control. IL6 levels are also reduced by irradiation and LSD1i alone (Figure 20).

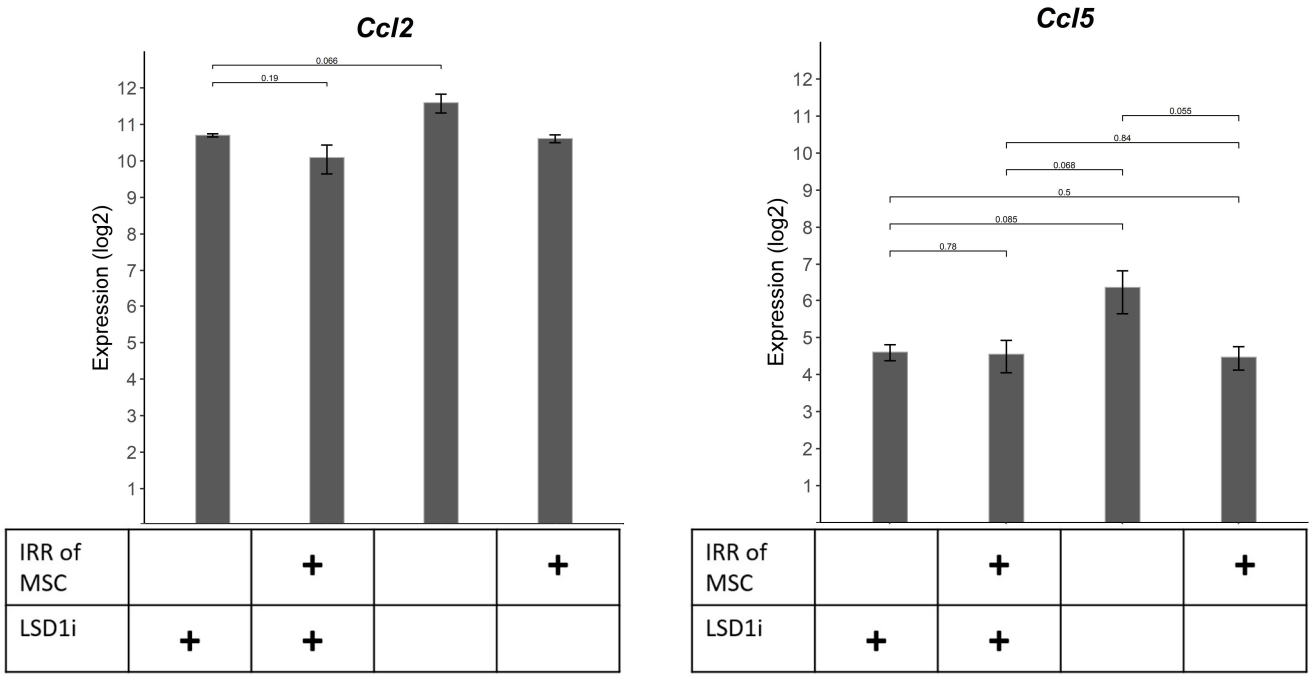

Figure 22 RNA Expression of CB-MSC after 15 days at 37°C: CCL2 and CCL5
Left: the RNA expression of CCL2 in Compact-bone MSC upon irradiation +/- LSD1 inhibition. Right: the RNA expression of CCL5 in CB MSC upon irradiation +/- LSD1i.

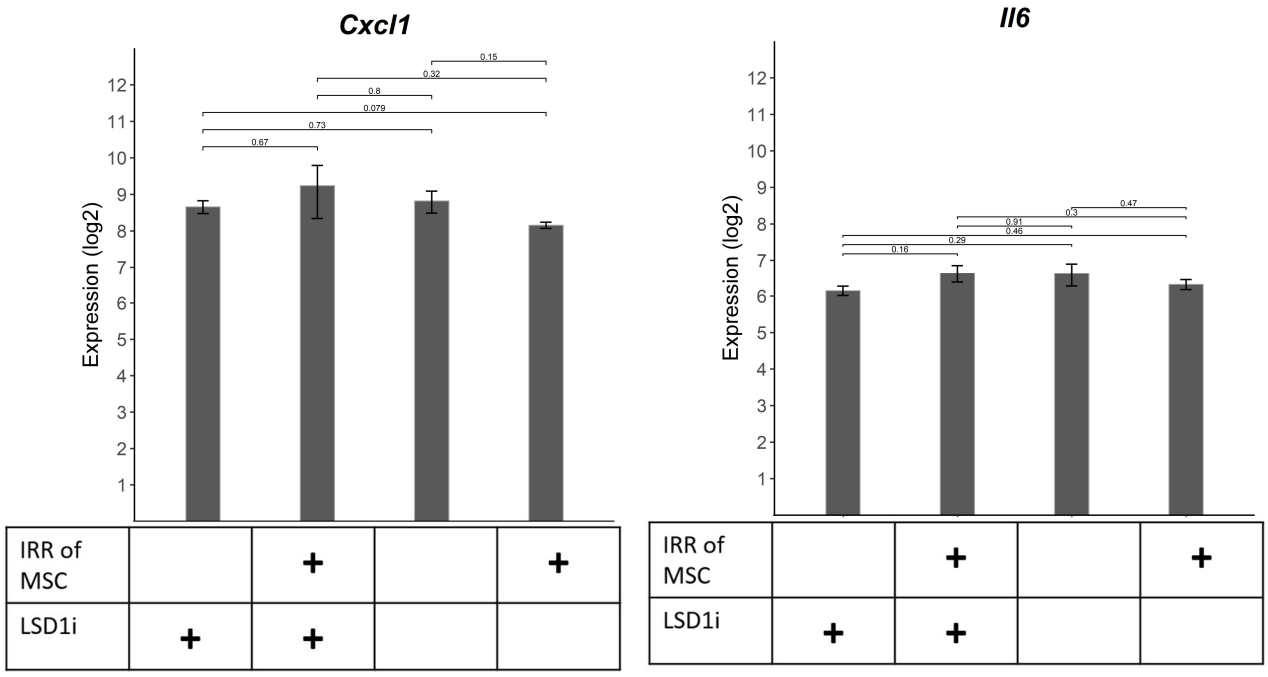

Figure 21 RNA Expression of CB-MSC after 15 days at 37°C: CXCL1 and IL6
Left: the RNA expression of Cxcl1 in Compact-bone MSC upon irradiation +/- LSD1 inhibition. Right: the RNA expression of IL6 in CB MSC upon irradiation +/- LSD1i.

However, the different conditions do not seem to alter the expression of IL6 and CXCL1 RNA significantly (Figure 21). This could mean that the cytokine levels in the culture solely depend on releasing mechanisms instead of transcribing RNA upregulation.

3.2 Effects of LSD1i and MSC presence on MLL-AF9

Hematopoietic progenitor cells (HSC) as well as granulocyte-monocyte progenitor (GMP) cells can be transformed with the MLL-AF9 fusion gene to generate AML in a murine bone marrow transplantation model. The GMP cells used in the following experiments were retrovirally transduced with a vector harboring the leukemic chimeric gene, which was coupled with the gene for the fluorescent protein GFP (emission peak at 509 nm), obtained by the Armstrong Lab (Dana-Farber Cancer Institute, Boston, Massachusetts, https://www.armstronglab.org/) . This way they could be distinguished by FACS analysis and fluorescent microscopy. A culture of GMP-derived AML cells (called GMP-AML) and their treatment with LSD1 inhibitor GSK-LSD1 were performed as previously described[68]. LSD1i is known to display a potent antileukemic effect in preclinical models, leading to apoptosis and differentiation of AML cells[101,102].

3.2.1 OP9 supernatant reduces growth of AML cells, but also reduces response to LSD1i treatment of AML cells

First, the cells proliferation under the influence of LSD1 inhibition was analyzed. After 5 days in culture, cells cultured with LSD1i were significantly less grown than the untreated cells, as expected. In parallel, cells were treated with LSD1i in the presence of supernatant from the feeder cells OP9 cell line or upon direct contact with the feeder cells. AML cells growing in the presence of supernatant from OP9 cells proliferated less than control cells (Figure 23).

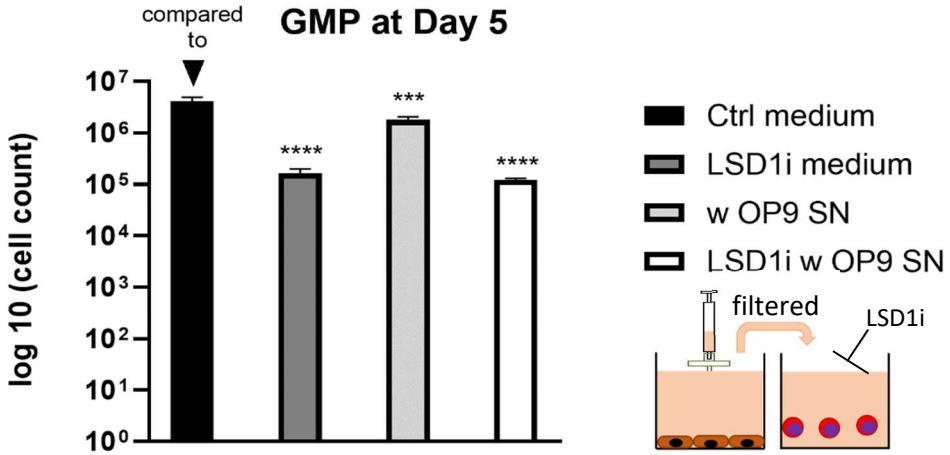

Figure 23 Proliferation of AML cells in the presence of supernatant from OP9 and treated with LSD1i. GMP cells were cultured for 5 days at 37°C. Initially 10^4 cells were plated. There were 4 different conditions, fresh IMDM medium without (Ctrl) and with LSD1i, filtered SN from a OP9 maintenance culture without and with LSD1i. n=3: the cell count of D5 was compared to the cell count of D5 of the Ctrl (One-way ANOVA). The small pictogram right below indicates the experimental settings. Flat brown cells are feeder cells, purple round cells are AML cells. ns > 0.05, * $p \leq 0.05$, ** $p \leq 0.01$, *** $p \leq 0.001$ and **** $p \leq 0.0001$.

Cell medium was collected from feeder cells (OP9) cultures at around 80-90% confluency after 24h or 48h. This medium was then added to AML cell culture. Despite the use of IMDM in the feeder cell culture and the addition of FBS (in total 15%), as well as cytokines addition, this cell medium could be suboptimal for AML, because of the nutrient depletion and presence of other metabolites from the feeder cells.

Treatment with the inhibitor reduced the cell number significantly in comparison to the untreated controls, however the cell numbers in treated cells in the presence of SN from OP9 were similar to the treated cells in the presence of standard cell medium.

This experiment was performed using timepoint-SN. Yet, the bone marrow microenvironment is a dynamic system with constant exchange of factors between the cells in the biological compartment. Therefore, to partially mimic the in vivo conditions, well plates containing an insert (upper chamber) with the AML cells in suspension were used as well as a membrane of a 0.4 µm pore size (ID 3401, Corning), separating them from the OP9 cells, cultured in the lower chamber adherent at the bottom (Figure 24). This system allows the passage of soluble factors but not cells: This experiment is represented in Figure 24: as expected LSD1i treatment lead to a reduction to 2.9% of cell count after 10 days in comparison to the untreated cells: in the presence of the SN from OP9, LSD1i treatment reduced cell count to 19.9% of the corresponding control. The presence of the SN seems to exert a protective effect on the cells to the treatment. Again, it could be seen that the untreated cells grow better in normal medium than in supernatant.

One hypothesis is that the cells in the co-culture are competing for the nutrients of the medium, which influences their proliferation: other inhibitory effects of soluble components cannot be excluded. While LSD1i seems to completely stop AML proliferation in monocultures, the OP9 supernatant appears to manifest a protective effect on GMP-AML cells against the treatment. In this setting the additional irradiation of the feeder did not significantly affect the protective effect in comparison to the non-irradiated feeder.

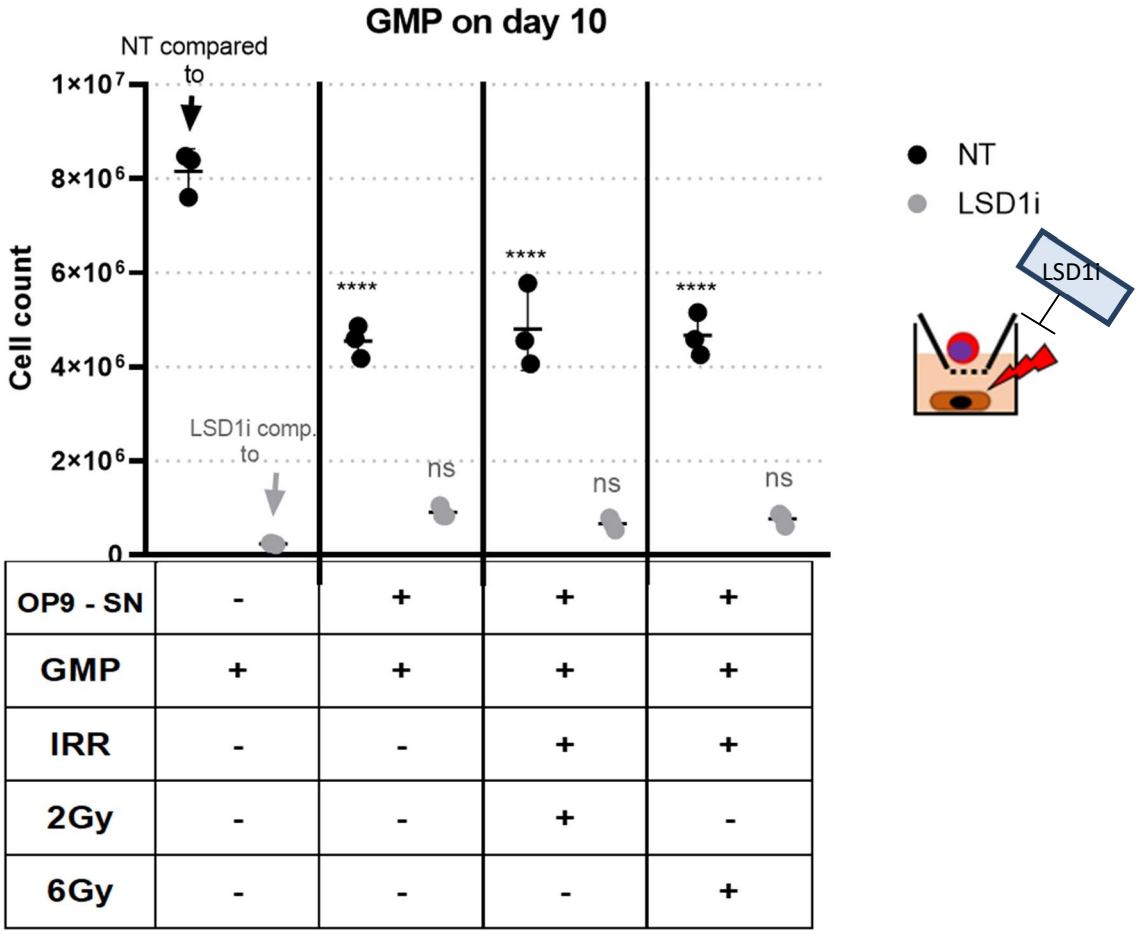

Figure 24 Proliferation of AML cells with transmembrane system with coculture of OP9, Results presented with and without treatment, as well as with and without previous irradiation of OP9. GMP cells were cultured for 10 days at 37°C. There were 8 different conditions. Only-GMP cultures without and with LSD1i. Co-cultures with OP9 non-irradiated, irradiated at 2Gy and irradiated at 6 Gy, each without and with LSD1i. Cell types were separated by a membrane (0.4 µm pore size). n=3: the cell count of the NT groups was compared to the NT GMP monoculture and the cell count of the LSD1i groups to the LSD1i GMP monoculture. (One-way ANOVA). ns > 0.05, * p ≤ 0.05, ** p ≤ 0.01, *** p ≤ 0.001 and **** p ≤ 0.0001.

3.2.2 Colony forming unit assay, proliferation, and differentiation ability of AML cells under the influence of stromal supernatant.

Granulocyte-monocyte-progenitor (GMP) cells can differentiate into unipotent precursors that can take the path of either granulocyte or monocyte production. The GMP-derived AML cells employed here retain a certain differentiation potential, however there is always a subpopulation of cells within the bulk cells, called leukemia-propagating cells or leukemia-initiating cells (LIC), or leukemia stem cells (LSC), which maintain an undifferentiated phenotype and propagate the culture. These cells are immature blast-like cells and do not differentiate even in the presence of dedicated

cytokines. The leukemic transformation induced by the fusion gene therefore changes the characteristic of the initially transformed cells. In different AML subtypes there are different grading of differentiation that can be partially maintained or lost during the disease.

A functional assay to assess the fate of these cells is the colony-forming unit assay (CFU). This allows to assess the growth, self-renewal, and differentiation potential of the cells, especially helping to evaluate, if the cells retain the ability to terminally differentiate.

A predetermined number of AML cells, in this case 500 per well, were cultured in a semi-solid medium (methylcellulose), allowing the formation of colonies from a single progenitor. The colonies form reveals the properties of the progenitor and can be divided into blast colonies (least mature), granulocyte-monocyte (GM), macrophage (M) and granulocyte colonies(Figure 25)[80].

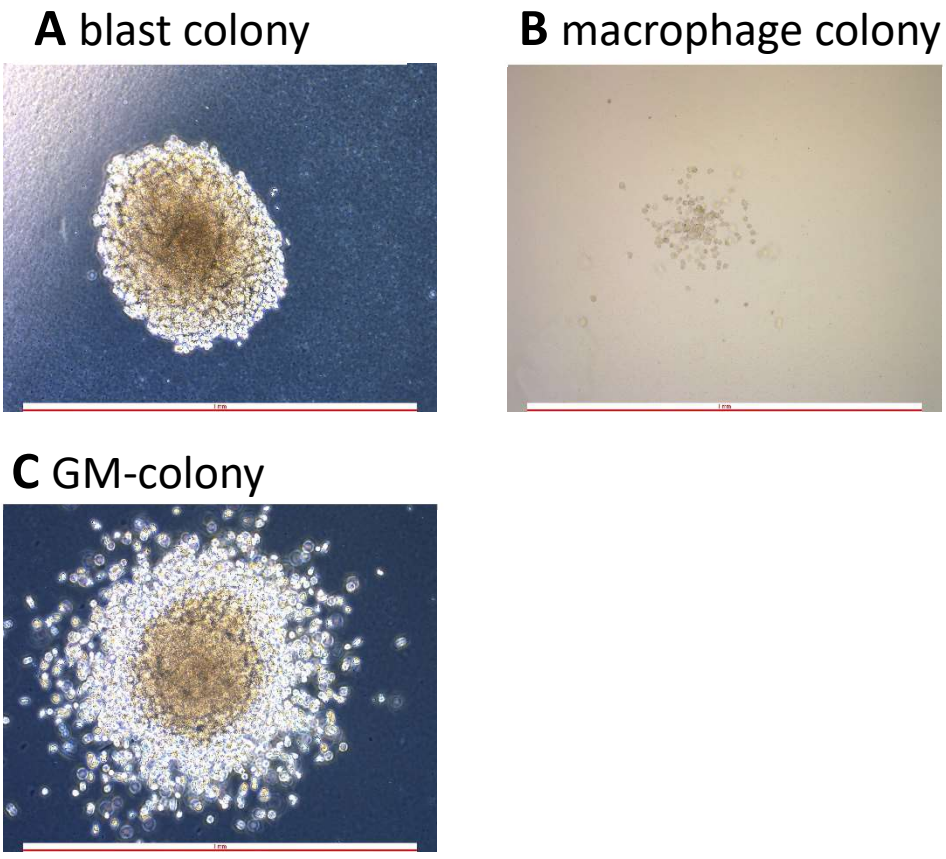

Figure 25 Images of murine Colony forming units.
Scale bar is 1 mm. (A) Blast colony, phase contrast microscopy. (B) Macrophage colony, brightfield microscopy. (C) GM colony, phase contrast microscopy.

The colony forming potential of the AML cells was assessed from the cocultures with feeder cells (OP9 and S17) from the transmembrane system. After 7 days in a co-culture, the GMP-AML from the upper chamber were used for a CFU assay (Figure 26). As shown below, the colony type most present is the blast-like colony, which permanently are built-up in this assay, demonstrating the self-renewal propagating potential of MLL-AF9+ AML cells.

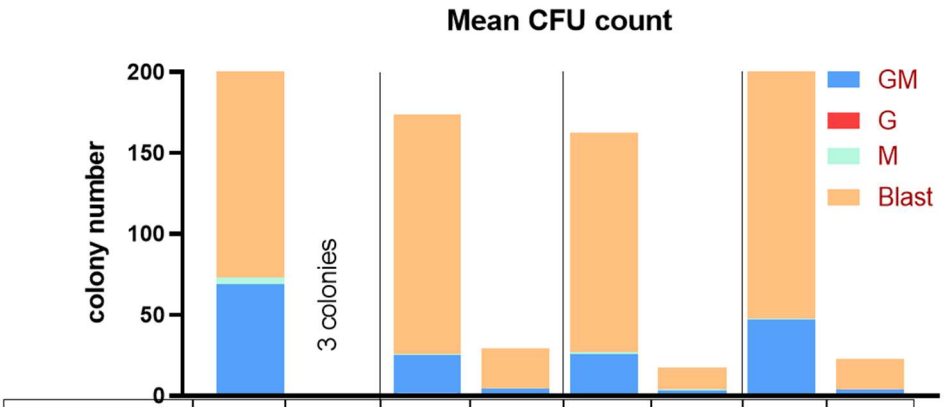

LSD1i	-	+	-	+	-	+	-	+
S17 - SN	-		+		+		+	
GMP	+		+		+		+	
IRR	-		-		+		+	
2Gy	-		-		+		-	
6Gy	-		-		-		+	

Figure 26 CFU Assay from coculture from transmembrane system
GMP cells were kept in culture for 7 days at 37°C. GMP were either not treated or treated. The cells were kept in a monoculture, as well as in a co-culture with S17, separated through a membrane. The S17 were previously non-irradiated, irradiated at 2Gy, and irradiated at 6Gy, all cultures were either not treated or treated. The GMP were used on the 7th day to perform a CFU assay, with 500 cells per culture. The graph represents the mean numbers of formatted colonies. n=3

The highest number of colonies (=colony-forming-cells, CFC) was reported in the control arm where AML cells were cultured with medium only. The GMPs that were co-cultured through the membrane with the S17 cell line irradiated at 6 Gy also demonstrated a higher number of colonies in comparison to the samples where S17 were not irradiated or were irradiated with only 2Gy.

This could indicate that a greater radiation dose drives the S17 to produce substances, which preserve the aggressive potential of MLL-AF9. The LSD1 inhibition almost completely diminishes the proliferation potential of the GMP in the monoculture. When considering the cells treated with LSD1i, in presence of S17-SN the colony formation was less decreased than in the control arm (no feeder in the lower chamber), showing again the protective effect of the stromal cells most probably mediated by humoral factors.

3.2.3 Immunophenotypic and morphological changes of the *MLL-AF9+* AML cells upon different conditions

3.2.3.1 Effect of treatments on the c-Kit+/Mac-1+ leukemic stem cells population (LSC)

AML cells display a characteristic immunophenotype as result of the aberrant expression of molecules on the cell surface. The analysis of immunophenotype is performed in the routine diagnostic and it is based on incubation of cells with surface markers – specific fluorescence-labeled antibodies followed by flow cytometry (FACS = fluorescence activated cell sorting). In the MLL-AF9+ AML model the mature myeloid markers such as Mac-1 and Gr-1 are expressed in more than 80% of the AML cells in this subtype of murine AML model[103]. In normal hematopoiesis c-kit is expressed in more immature cells including stem cells (HSC). The aberrant co-expression of these 2 markers occurs on the small subpopulation of leukemic stem cells (LSC) in this *MLL-AF9+* AML model, which have been functionally characterized by serial transplantation experiments[104] and represent a less differentiated cell subpopulation[68,105]. The FACS antibody used to detect Mac-1 is directed against its alpha subunit CD11b. An analysis on the co-expression of these two markers on the surface of AML cells was performed, to assess the effect of the different conditions on the populations of LSC and to predict their eradication potential in vitro.

After 3 days of treatment with LSD1i, an increased proportion of c-kit+/Mac-1+ in AML cells could be seen, when the feeder cells were irradiated, in comparison to the corresponding untreated cells. Since the number of cells upon treatment was decreased, one could argue that the more differentiated cells (c-kit negative) in the bulk population are indeed more sensitive to the treatment, rather than that the increase observed here is just induction by treatment (Figure 27).

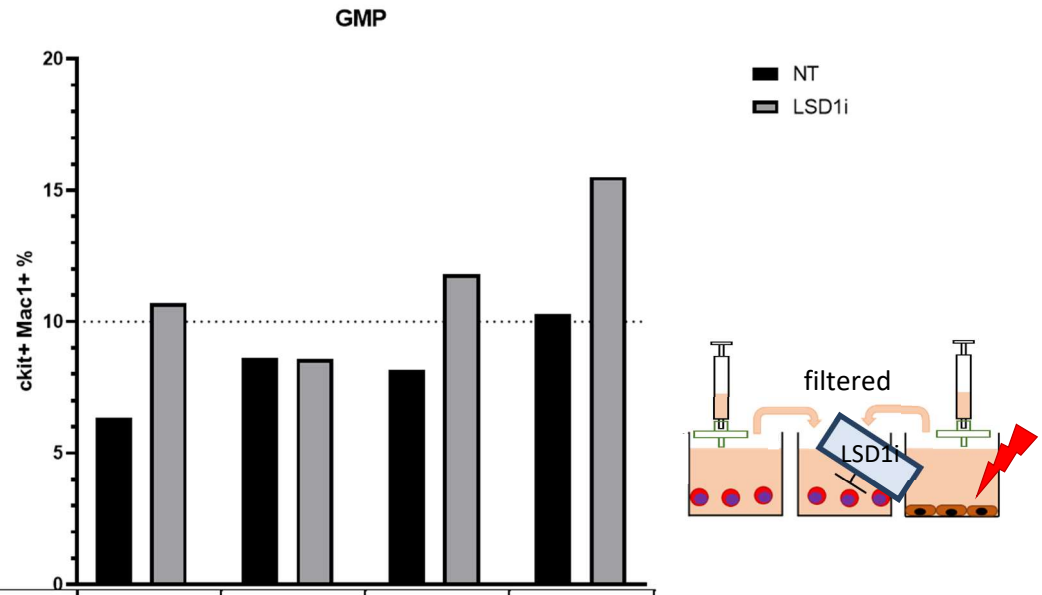

GMP- SN	+	-	-	-
OP9 - SN	-	+	+	+
GMP	+	+	+	+
IRR	-	-	+	+
2Gy	-	-	+	-
20Gy	-	-	-	+

Figure 27 Proportion of c-kit/Mac-1 double positive AML cells upon treatment
GMP cells were cultured in cell-SN for 3 days at 37°C in the presence or absence of LSD1i. Together with the inhibitor as culturing medium, the supernatant from maintenance cultures instead of fresh medium was added: SN from GMP-AML cells, SN from OP9 feeder cells non-irradiated, irradiated at 2Gy, and irradiated at 20Gy, each of which were either not treated or treated. In the carton (right) the experimental procedure is depicted: for the FACS analysis shown in the histogram AML cells from the middle culture were used. n=1

In the previous cultures a decreased proliferation of cell in the presence of any SN from feeder cells was visible (Figure 24). This could be due to the deprivation of molecules from the feeder cells. Therefore, to keep the culture conditions similar to all the arms, for the culture without SN from feeder cells the supernatant from GMP-AML was used.

Furthermore, it is apparent that the more irradiated the OP9 cells were, the higher the percentage of double positive cells was, with the leading group at 15,5 % being the LSD1i treated AML cells cultured in SN from 6 Gy irradiated feeder cells in comparison to the control with 6,3 % (Figure 27).

There is a visible difference between one-timepoint-SN and the co-culture SN, due to the dynamic exchange of soluble factors. Figure 28 shows the FACS staining with the ckit/Mac1 antibodies resulting from the co-culture in the membrane (or 2-chambers) system. Here, the percentage of c-Kit+ Mac-1+ cells in all groups is below 2%. The LSD1i treated groups with S17-SN had a higher proportion of double positive cells in comparison to the corresponding not treated cells. The effect is however not visible at both groups with SN of at 6 Gy irradiated S17; one reason could be that in the feeder cells irradiated with 6 Gy toxic effects could occur. Furthermore, these results also suggest that the presence of feeder cells alone and even more after low irradiation an increased proportion of more immature cells (LSC) is detectable.

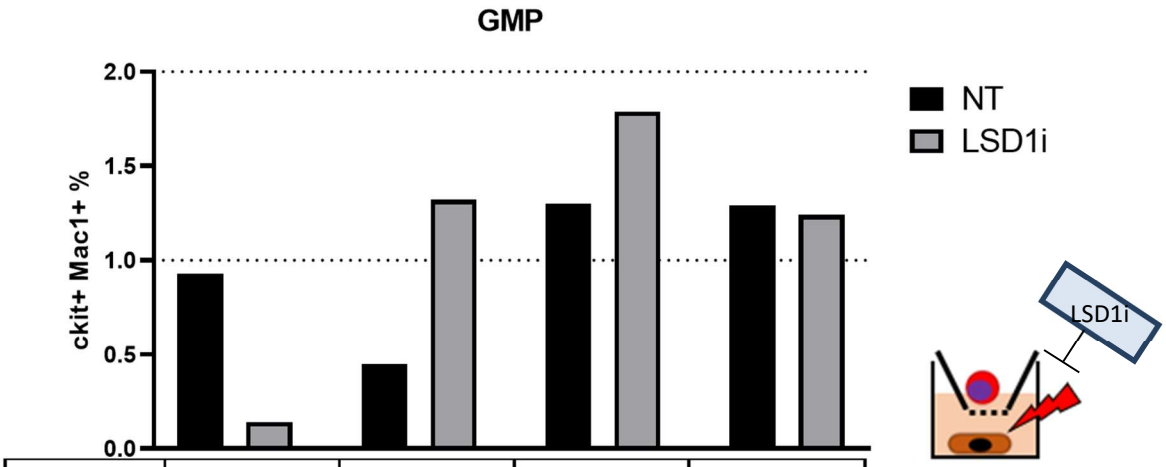

S17 - SN	-	+	+	+
GMP	+	+	+	+
IRR	-	-	+	+
2Gy	-	-	+	-
6Gy	-	-	-	+

Figure 28 Immunophenotype of AML cells treated in a trans-membrane system with continuous supply of fresh medium from feeder cells.

GMP cells were cultured for 5 days at 37°C. There were 8 different conditions. Only-GMP cultures without and with LSD1i. Co-cultures with S17 non-irradiated, irradiated at 2Gy and irradiated at 6 Gy, each without and with LSD1i. Cell types were separated by a membrane (0.4 µm pore size). n=1

Next, the same FACS analysis was performed on the AML cells from the colony forming assay (from Figure 26). As shown in Figure 29 LSD1i treatment led to an increase of c-kit+/Mac-1+ double positive cells proportion in comparison to the not treated cultures. This effect was more pronounced in AML cells treated in the presence of SN from OP9 than the S17-SN. With 6 % of live cells in the colony assay from co-culture with irradiated OP9-SN at 6 Gy, the double positive cells seem to have found better conditions to proliferate.

Taken together these results suggest that the co-culture of GMP-AML with irradiated feeder cells apparently increases the proportion of phenotypically more primitive leukemia cells in vitro (Figure 29).

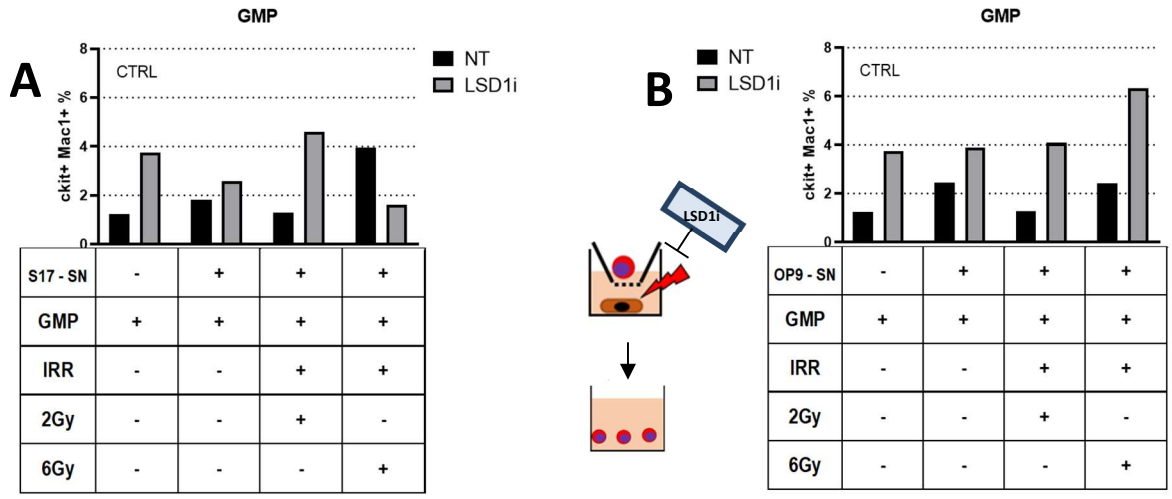

Figure 29 Immunophenotype of cells from 1° methylcellulose /CFC assay.
The schematic in the middle shows the culture conditions (the lower plate is CFC). n=1 Cells were harvested and pooled from the dishes, washed 3 times with D-PBS and stained for a FACS analysis (A). The same culture method was also performed with OP9 cells (B). The CTRL for both is the same GMP monoculture, not treated and treated.

3.2.3.2 Expression of the LSD1 surface target CD86+ on MLL-AF9+ AML cells

Next, the differentiation induction upon the different conditions was assessed by analyzing the expression of CD86 cell surface by FACS. CD86 is known to be upregulated under the influence of LSD1 inhibition and it correlates with myeloid differentiation in AML cells upon LSD1i treatment [68,106]. Figure 30 shows the CD86 expression of GMP cells after a co-culture of over two weeks. The LSD1i treatment was started only three days prior to the FACS analysis. By looking at the graph, it is clear that LSD1 inhibitor is primarily responsible for the upregulation of the gene. The GMP contact to primary

BM-MSC only triggered the upregulation even further, in case of irradiation at 6 Gy prior to the experimental setup.

Taken together, these results indicate that the presence of MSC alone slightly attenuates the differentiation marker expression CD86, induced by LSD1i, in comparison to AML cells cultured without feeder cells.

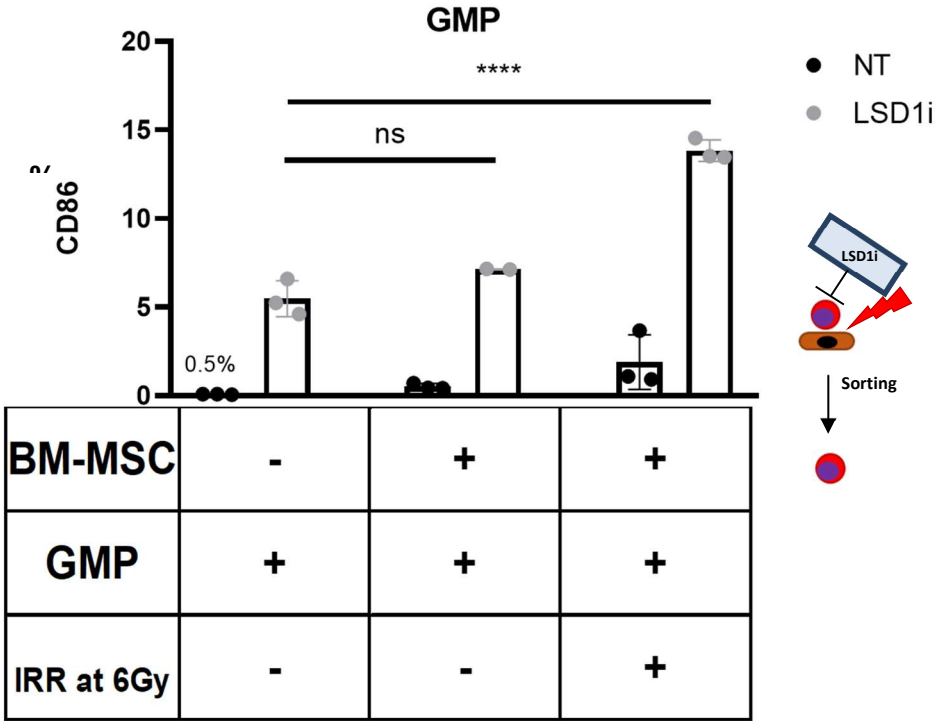

Figure 30 Proportion of CD86 positive AML cells upon co-culture (cell-to-cell contact) with primary bone marrow derived mesenchymal stromal cells (MSC).
GMP cells were monocultured and co-cultured with primary BM-MSC for 18 days at 37°C. LSD1i was added on the 15th day of culture. Monoculture and co-culture with non-irradiated and irradiated MSC (6Gy), both were each either not treated or treated. Prior to FACS analysis, the co-cultures were sorted (GFP+) and the GMP cells stained with antibodies; One-way ANOVA. ns > 0.05, * p ≤ 0.05, ** p ≤ 0.01, *** p ≤ 0.001 and **** p ≤ 0.0001.

3.2.3.3 Morphological changes of GMP-AML cells upon treatment

Morphological analysis of cells under the microscope (cytomorphology) represents the standard method for preliminary diagnosis of a hematological malignancy. Together with the cell culture images from a bright-field microscope, the staining of intracellular components allows for a better evaluation of the cell's changes upon treatment. Cells harvested from liquid cultures, or colony assays, were regularly analyzed with Cytospin and May-Grünwald stain. Figure 31 shows how the morphology of GMP-AML cells under the different conditions changed.

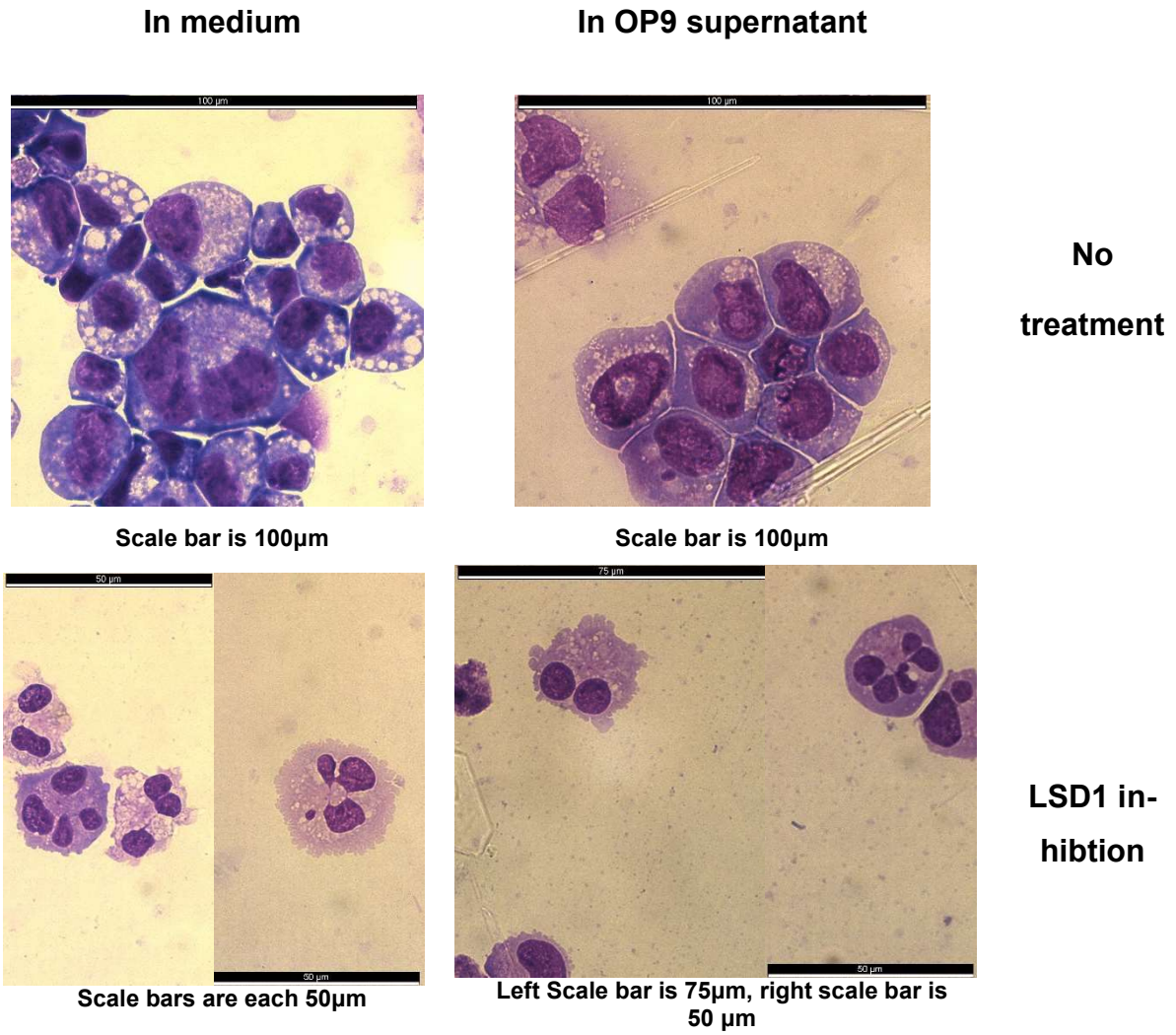

Figure 31 Cytospin preparations from cultures of GMP-AML cells upon treatment.
The cells were taken from the culture **Figure 23**. A May-Giemsa-Grünwald staining was performed.

The not treated cells, regardless of presence or absence of OP9-SN, have bigger round nuclei with visible nucleoli. Furthermore, the nucleus to cytoplasm ratio is in favor of the nucleus. These characteristics indicate an immature state, blast-like, of the GMP-AML cells. In contrast, cells treated with LSD1i, both alone or in the presence of SN from OP9, displayed differentiation features such as segmented, almost picnotic nuclei, and a nucleus-cytoplasm ratio in favor of the cytoplasm. Therefore, the treated cells are more differentiated.

Figure 32 shows images of co-cultures of GMP-AML and BM-MSC, from the different conditions. BM MSC are adherent, and spindle shaped. These cell types proliferate well in culture. Occasionally, some flattened big MSC can be detected on the pictures, most probably reflecting MSC more differentiated. The proportion of these cells in

culture is lower over further culturing, suggesting that they grow less. These cells are more likely to be seen in irradiated cultures. Untreated control GMP-AML cells grow in clumps, as sign of proliferation, while in the LSD1i arm, the cells are dispersed and fewer. In the coculture, GMP-AML cells partially adhere to the MSC cells and are difficult to detach by washing with PBS. Interestingly, in the irradiated + LSD1i arm, the AML cells are visually many.

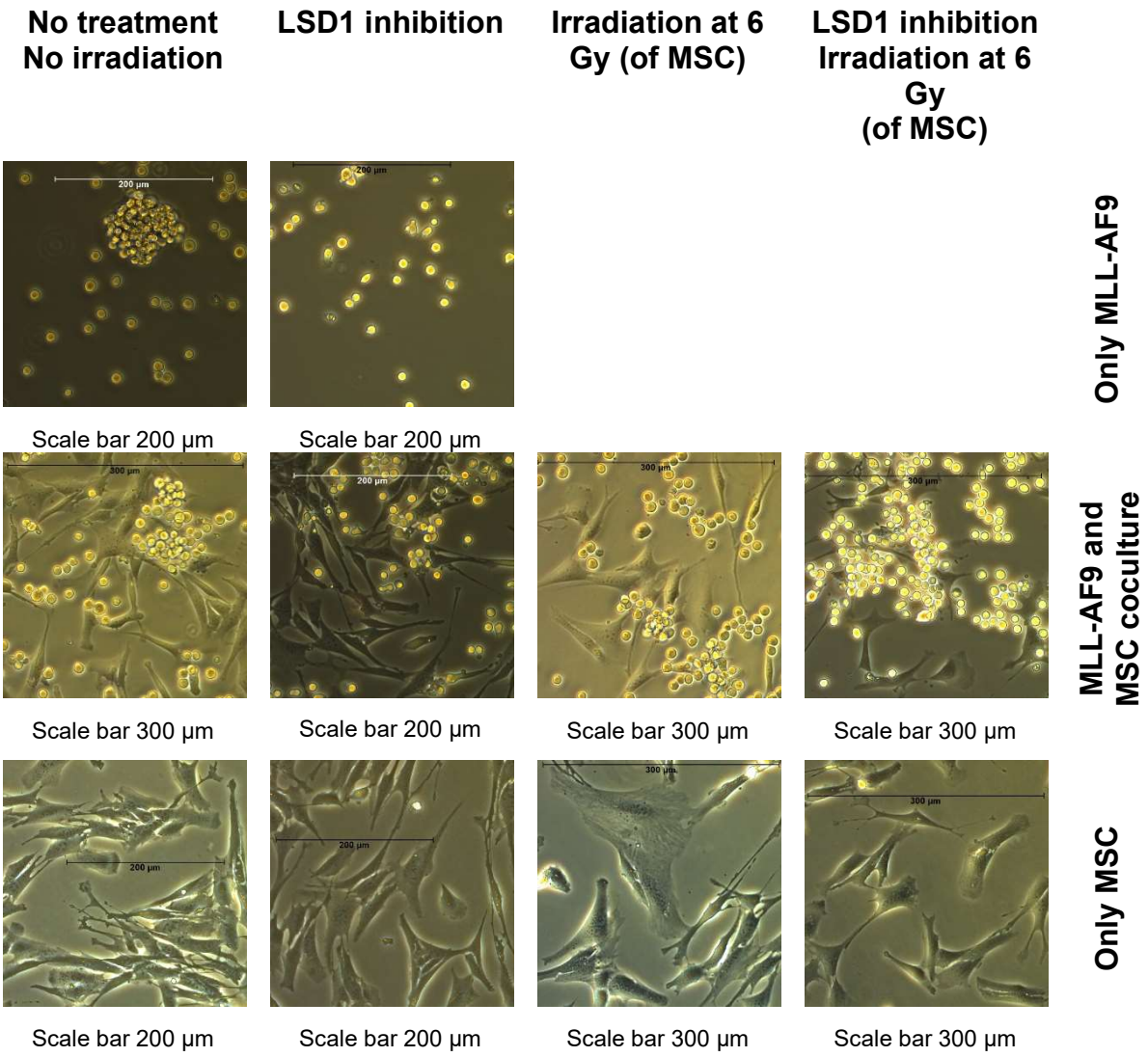

Figure 32 Images of the culture morphology of primary bone marrow MSC
Phase contrast microscopy. The cells were taken from the culture Figure 30 refers to. The pictures were taken on the 17th day of culture. MLL-AF9 change with GMP-AML.

In summary these observations suggest that morphology of AML cells does not finally change upon LSD1i treatment when the supernatant from OP9 cells is added to the culture. Interestingly, when the AML cells were co-cultured with primary MSC, they seem to proliferate macroscopically better in the presence of irradiated feeder.

3.2.4 Cytokine release of MLL-AF9+ AML cells in different culture systems

GMP-AML cells harboring the MLL-AF9 translocation can grow in the culture in the presence of cytokines added to the medium as IL3, IL6, SCF. Moreover, in the medium another source of cytokines is present, the fetal bovine serum (FBS). Therefore, as control for this assay medium and cytokine samples alone were also used, where the IL3 and IL6 concentrations are therefore high (Figure 36, Figure 37). The FBS is produced by centrifugation of blood from donor animals and is used to stabilize the added cytokines in the medium. It also contains small traces of other cytokines and proteins as well. Another aspect to be considered, is that cells (AML as well as MSC) themselves can release cytokines depending on the growth conditions (Figure 33).

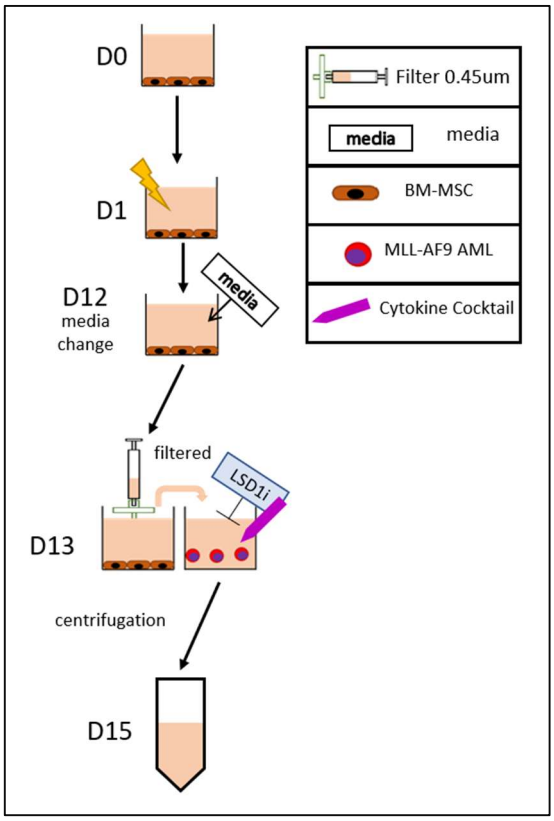

Figure 33 Cytokine release assay

BM-MSC were cultured for 13 days at 37°C. On the 13th day, filtered supernatant of the MSC was added to a new culture dish. Inside the supernatant, cytokine cocktail and AML cells were cultured for another two days. At day 15, the supernatant was collected and centrifuged. The sample was then stored at -80°C until cytokine analysis.

3.2.4.1 One-timepoint MSC supernatant

At first, the supernatants from AML cells cultured in the presence of SN from the MSC, with and without LSD1i were analyzed at day 2. Figure 34 depicts the levels of the cytokines CCL2 and CCL5 measured in the supernatants from AML cells under the different conditions. It could be observed, that in the samples with the SN from feeder cells the level of those chemokines was dramatically higher that in the AML cells alone, suggesting that these were derived from feeder cells. To confirm this, similar levels of the same chemokines were measured in the feeder cultures alone (chapter 3.1.3).

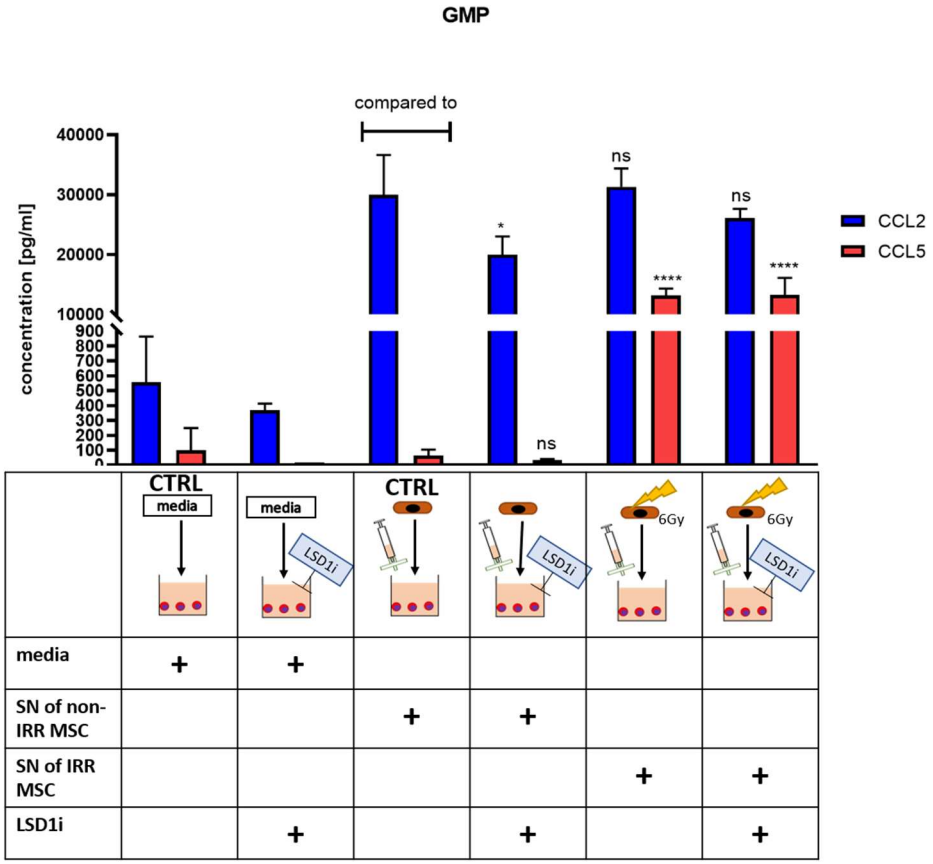

Figure 34 CCL2 and CCL5 cytokine release of AML monocultures

The supernatants of AML monocultures were analysed. The GMP-AML were cultured in either fresh or MSC conditioned medium. n=3 (One-way ANOVA). ns > 0.05, * p ≤ 0.05, ** p ≤ 0.01, *** p ≤ 0.001 and **** p ≤ 0.0001.

AML cells alone show some production of CCL2, and very low level of CCL5 (Figure 34, CTRL media). LSD1i reduced the CCL2/CCL5 levels slightly. In the presence of SN from MSC cells as mentioned, the level of CCL2 was very high, without major differences, when LSD1i was added. Interestingly, in the presence of supernatant from

irradiated MSC a much higher concentration of CCL5 could be seen, which was most probably derived from the MSC themselves, considering the CCL5 level in the MSC culture alone (compare to Figure 19). There was no difference in the concentration of CCL5 upon LSD1i in comparison to the untreated arm. In summary, the major source of these chemokines is the MSC culture, and the level of CCL5 from irradiated MSC was much higher than from non-irradiated feeder cells. More interesting, however, is the observation that CCL5 level does not change dramatically in the MSC culture alone if cells are irradiated as shown in Figure 19, suggesting that the radiation-dependent increase observed in Figure 34 is due to the presence of both AML cells and MSC SN.

CCL4 is another chemoattractant: here it had the highest concentration in the treated AML culture without MSC-SN (Figure 35) in comparison to the culture with SN. In the presence of MSC supernatant the level of CCL4 was much lower, suggesting that the MSC SN inhibited the AML-derived CCL4 production. The production of CCL4 has been shown to be repressed by p38MAPK-mediated IFNγ effect upon infection in macrophages[107]. Similarly to CCL2, the level of CXCL1 was elevated in presence of MSC supernatant and very low in AML cells without any MSC contact. Here treatment with LSD1i and irradiation tended to reduce the level of CXCL1.

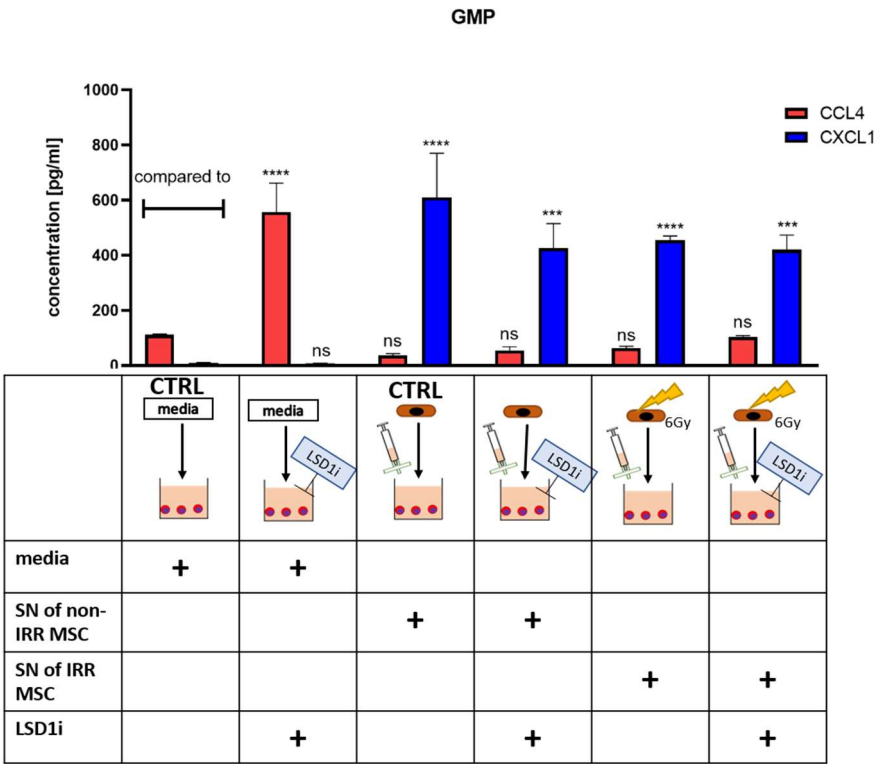

Figure 35 CCL4 and CXCL1 cytokine release of AML monocultures.

The supernatants of AML monocultures were analysed. The GMP-AML were cultured in either fresh or MSC conditioned medium. Cytokine release of AML: CCL4 and CXCL1. n=3 (One-way ANOVA). ns > 0.05, * p ≤ 0.05, ** p ≤ 0.01, *** p ≤ 0.001 and **** p ≤ 0.0001.

TNFα levels were overall similar to the levels in medium only, suggesting that its main source was the FBS. Interestingly, where SN from non-irradiated MSC was added, the level of TNFα was significantly reduced. This could reflect an increased internalization by the AML cells upon SN from irradiated MSC, especially when AML cells were treated; alternatively, the presence of TNFα-neutralizing factors in the MSC-SN cannot be excluded. Interestingly, the irradiation reduced this MSC-derived effect back to control levels. Similarly, the level of another chemokine. CSF2, was constant in all the arms including medium, suggesting that it derives from the FBS in the medium. Interestingly, CSF2 was also reduced when treated AML cells are cultured in non-irradiated supernatant (Figure 36).

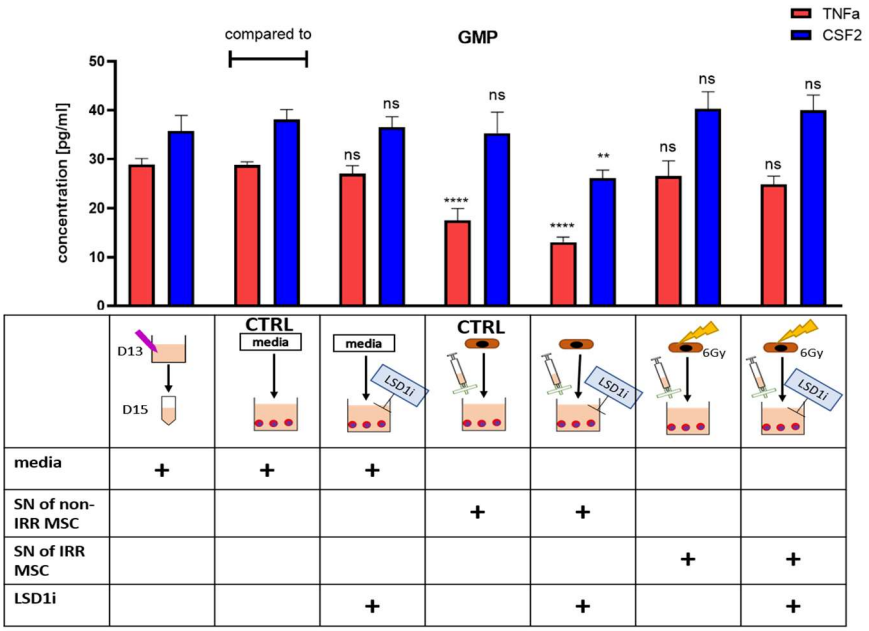

Figure 36 TNFa and CSF2 cytokine release of AML monocultures.
The supernatants of AML monocultures were analysed. The GMP-AML were cultured in either fresh or MSC conditioned medium. Cytokine release of AML: TNFa and CSF2. n=3 (One-way ANOVA). ns > 0.05, * p ≤ 0.05, ** p ≤ 0.01, *** p ≤ 0.001 and **** p ≤ 0.0001.

IL3 and IL6 (Figure 37) are necessary for the growth of immature murine hematopoietic progenitor cells, as well as for many AML cell subtypes. Therefore, these two cytokines are part of the cytokine cocktail used for the growth in vitro of the AML cells, and their level in the cytokine detection assay are similar in all the arms, except for MSC-specific conditions: IL3 was reduced in all MSC arms, and more strongly when they were irradiated, while the treatment in these samples was making no difference; again this could reflect an increased uptake of IL3 by the AML cells, where the SN from MSC was present (Figure 37). Similarly, IL6 was significantly decreased in samples with SN from

non-irradiated MSC, in comparison to the controls (without SN) and also when the SN was from irradiated MSC, irrespectively of the LSD1i treatment.

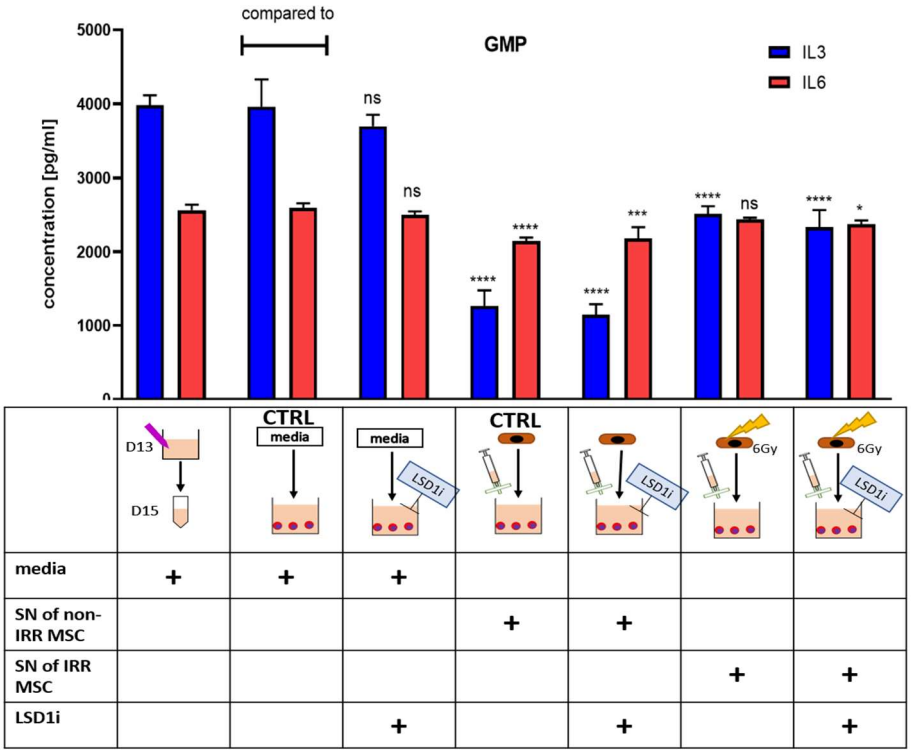

Figure 37 IL3 and IL6 cytokine release of AML monocultures

The supernatants of AML monocultures were analysed. The GMP-AML were cultured in either fresh or MSC conditioned medium. Cytokine release of AML: IL3 and IL6. n=3 (One-way ANOVA). ns > 0.05, * $p \leq 0.05$, ** $p \leq 0.01$, *** $p \leq 0.001$ and **** $p \leq 0.0001$.

Taken together, these results suggest that the presence of SN from MSC significantly changes the amount of cytokines in the medium. On one hand, the MSC cells might themselves release these cytokines, on the other hand, factors released by MSC in the SN could affect the uptake/degradation of the cytokines present in the medium, deriving from FBS or cytokines cocktail.

3.2.4.2 AML and MSC co-culture

In order to investigate cell-to-cell direct interaction, co-culture with the 2 cell types were performed. For this, feeder cells were cultured for 13 days after irradiation, to let the expected changes to establish, and then the AML cells were added (Figure 38). In parallel, treatment with LSD1i was started. After 2 days all the culture was stopped, and the supernatant was collected for detection of cytokines.

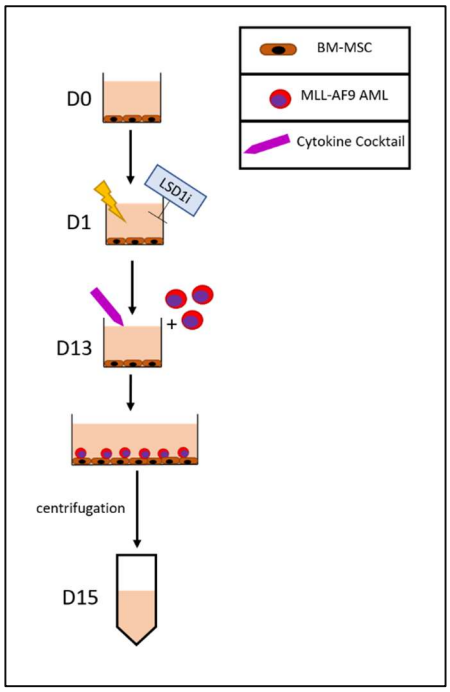

Figure 38 Culture conditions of AML/MSC co-culture
BM-MSC were cultured for 15 days at 37°C. The MSC were either irradiated or non-irradiated. On the 13th day, AML cells and cytokine cocktail were added to the culture. The cultures were kept in the incubator for another two days. Afterwards, the supernatant was collected and centrifuged. The sample was then stored at -80°C. ns > 0.05, * p ≤ 0.05, ** p ≤ 0.01, *** p ≤ 0.001 and **** p ≤ 0.0001.

CCL2 was significantly reduced only in the co-culture where irradiation (6Gy) and LSD1i were combined. CCL5 level was similar in all the conditions. Similarly, to CCL2, CXCL1 level was significantly reduced in the arm with irradiation and LSD1i treatment (Figure 40).

TNFα and CSF2 were also significantly reduced in the co-culture arms combining irradiation of feeder and LSD1i treatment (Figure 39). This could reflect and increased internalization from the cells upon these 2 conditions. This significant effect was indeed not visible when AML cells were cultured with the SN only.

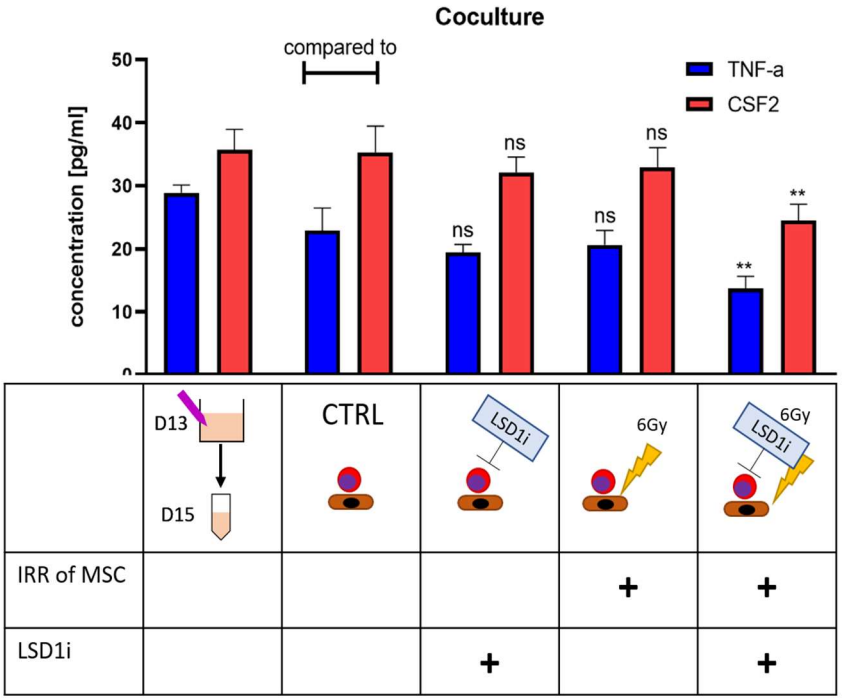

Figure 39 TNF-a and CSF2 cytokine release of BM-MSC and *MLL-AF9*+ AML co-culture:
The supernatants of MSC-AML co-cultures were analysed. The MSC cells were previously either irradiated or not. n=3 (One-way ANOVA). ns > 0.05, * p ≤ 0.05, ** p ≤ 0.01, *** p ≤ 0.001 and **** p ≤ 0.0001.

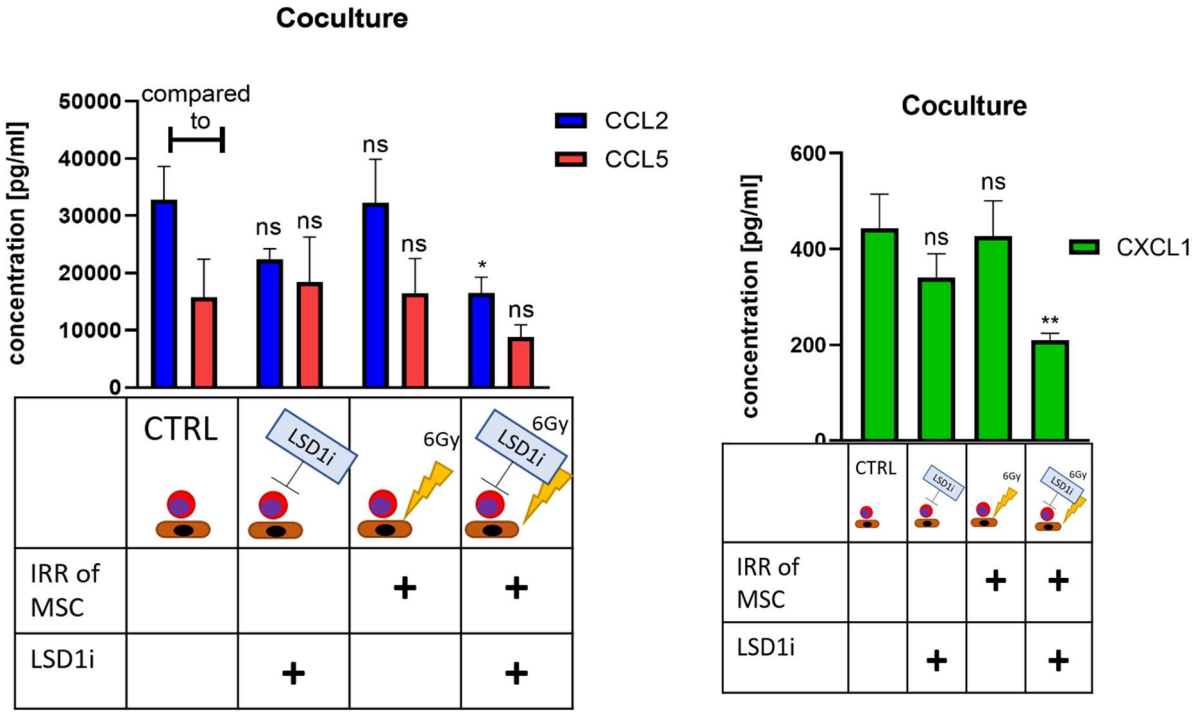

Figure 40 Cytokine release of BM-MSC and *MLL-AF9*+ AML co-culture:
Left CCL2 and CCL5, right CXCL1. The supernatants of MSC-AML co-cultures were analysed. The MSC cells were previously either irradiated or not. n=3 (One-way ANOVA) ns > 0.05, * p ≤ 0.05, ** p ≤ 0.01, *** p ≤ 0.001 and **** p ≤ 0.0001.

3.3 MSC Transcriptomics

To further investigate the cellular changes upon the different conditions, transcriptome analysis by RNAseq was performed. For this compact bone MSC were freshly isolated from healthy donor mice. At day 0 cells alone were plated with MesenCult medium only. At day 1 the irradiation at 6 Gy on the adherent cells was performed, and the treatment was started immediately after this. The cells were kept in culture for 15 days at 37°C; after this they were harvested and lysed to prepare the samples for RNAseq.

After the RNA sequencing outliers were removed from the replicates. The four distinct clusters show the affiliation of each sample to its culture condition group (Figure 41).

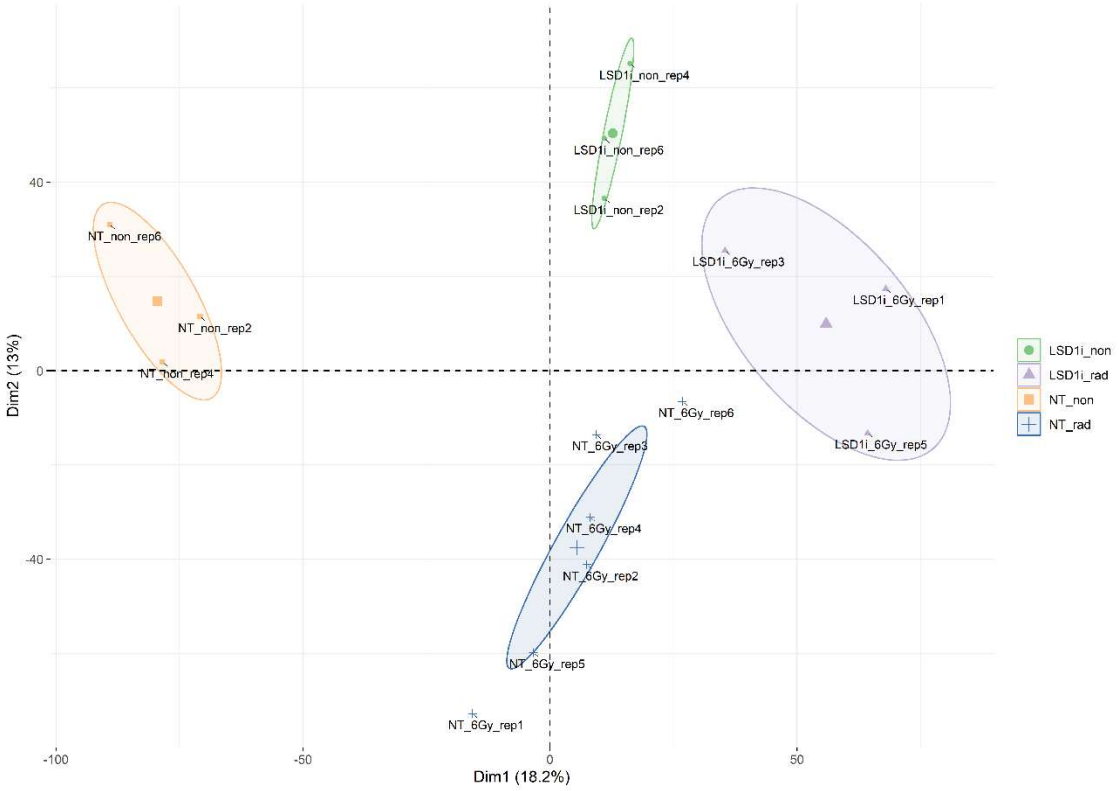

Figure 41 Principal component analysis.
The orange circle is the control group, the green circle the LSD1i treated group, the blue circle the irradiated group, and the pink circle the combination of irradiation and treatment.

3.3.1 Irradiation of MSC depletes inflammation-related genes

Fifteen days after irradiation, a total of 328 genes were significantly differentially expressed in comparison to the control, where 65 were up- and 263 downregulated (adjusted p-value of <0.05) (Figure 42 C). GSEA analysis showed the top signatures with negative correlation were “HALLMARK_TNFA_SIGNALING_VIA_NFKB”[108] (within the Hallmark gene sets), which includes the genes regulated by NF-kB in response to TNF, and the top downregulated GSEA result for Gene Ontology sets collection was “GO_INFLAMMATORY_RESPONSE”[109] (Figure 43). In summary, irradiation seems to inhibit the NF-κB pathway mediated by TNF-alpha and to reduce an inflammation state. NF-κB is well known to be involved in various inflammatory processes and in the production of cytokines[110] .

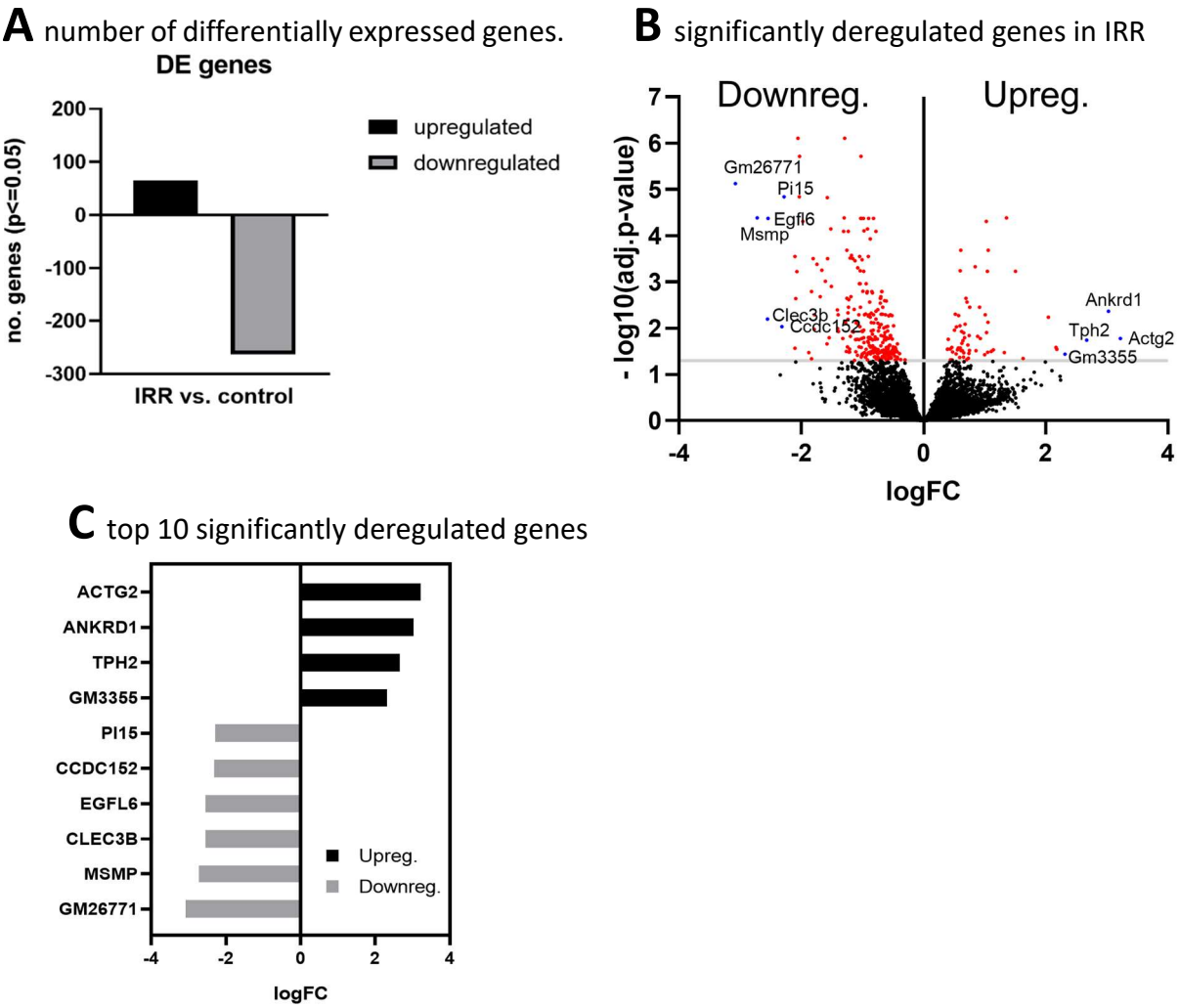

Figure 42 Transcriptional changes of CB-MSC upon irradiation.

(A) The graph depicts the number of differentially expressed genes upon irradiation. (B) The graph shows the corresponding volcano plot, where red dots have an adj. p-value <0.05 and the blue dots are the top 10 significantly deregulated (pseudo-) genes upon irradiation, which can also be found in (C)

Within the top deregulated genes upon irradiation, 4 were up- und 6 were downregulated (Figure 42 B). The downregulated *Msmp* is coding for a cytokine that acts as a ligand for the C-C chemokine receptor CCR2. CCR2 induces a strong chemotactic response for monocytes and lymphocytes. This could reflect a depletion of inflammation state upon irradiation. *Egfl6* (epidermal growth factor like domain multiple 6), which is also downregulated upon irradiation, engages in the regulation of cell cycle, proliferation, and in developmental processes.

The upregulated *Actg2* codes for an actin isoform, which is important for the cytoskeleton and the cell mobility. Therefore, it can be hypothesized, that the cell shape and the cell migration is a reorganization of cytoskeleton occurred by irradiation. The upregulated *Ankdr1* (Ankyrin repeat domain 1) is a nucleic transcription factor induced by IL-1 and TNF-alpha stimulation. In summary, the expression of certain TNF-alpha targets as well as proteins involved in cell proliferation and structure / motility seem to be affected 14 days after irradiation of the MSC[22,111,112].

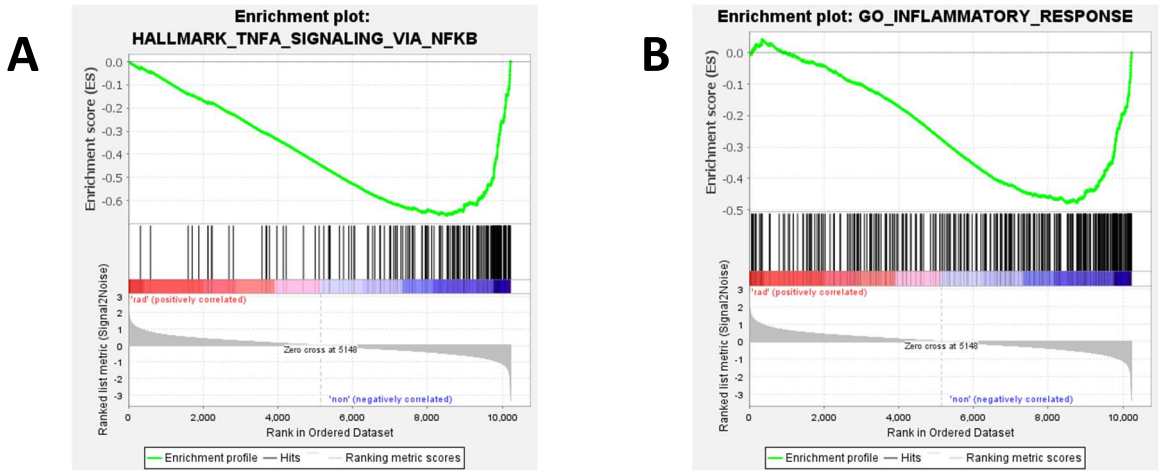

NES= -3.03, nom.p= 0.0, FDR= 0.0

NES= -2.37, nom.p= 0.0, FDR= 0.00003

Figure 43 Gene Set Enrichment Analysis of Differentially Expressed Genes upon irradiation on MSC.

Left: negative enriched gene set “HALLMARK_TNFA_SIGNALING_VIA_NFKB”, Right: negative enriched gene set “GO_INFLAMMATORY_RESPONSE” While the control consisted of 3 samples (n=3), the irradiated samples were 6 in number (n=6).

3.3.2 LSD1 inhibition of MSC alters the metabolic pathways.

The inhibition of LSD1 in MSC induced the upregulation of 191 genes and downregulation of 241 genes in comparison to the control (Figure 44 A). Transcriptional changes were related to metabolism-regulating processes. In particular, in Figure 45 A the top 4 upregulated signatures from "Gene Ontology" dataset are shown: "GO_NAD_METABOLIC_PROCESS", "GO_GLYCOLYTIC_PROCESS_THROUGH_FRUCTOSE_6_PHOSPHATE", "GO_GLUCOSE_CATABOLIC_PROCESS" and "GO_NADH_METABOLIC_PROCESS". Together with these glycolysis-related metabolic signatures, other biological processes, such as protein modification and cell adaptation to environmental changes, were significantly altered.

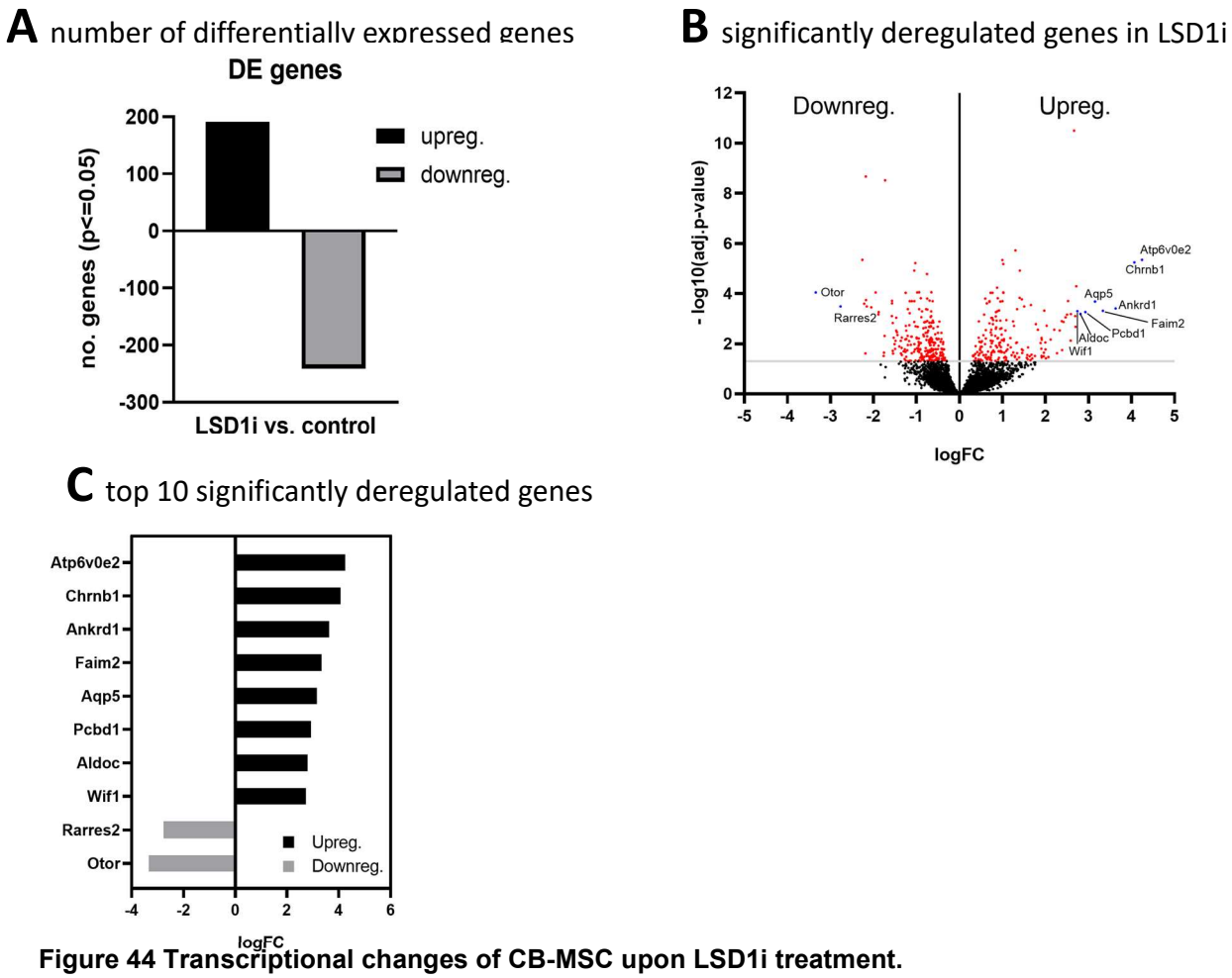

Figure 44 Transcriptional changes of CB-MSC upon LSD1i treatment.

(A) The graph depicts the number of differentially expressed genes upon LSD1i. (B) The graph shows the corresponding volcano plot, where red dots have an adj. p-value <0.05 and the blue dots are the top 10 significantly deregulated (pseudo-) genes upon LSD1i, which can also be found in (C)

The top 4 downregulated signatures within the “Gene Ontology” dataset can be found in Figure 46 A. One possible way to regulate protein synthesis is by influencing the cytosolic ribosomes. Taken together, these data suggest that, upon LSD1i treatment for 15 days MSC cells increase metabolism / glycolysis but reduces protein synthesis.

A Gene Set Enrichment Analysis plots, upregulated in

NES> 2.0, nom.p= 0.0, FDR<

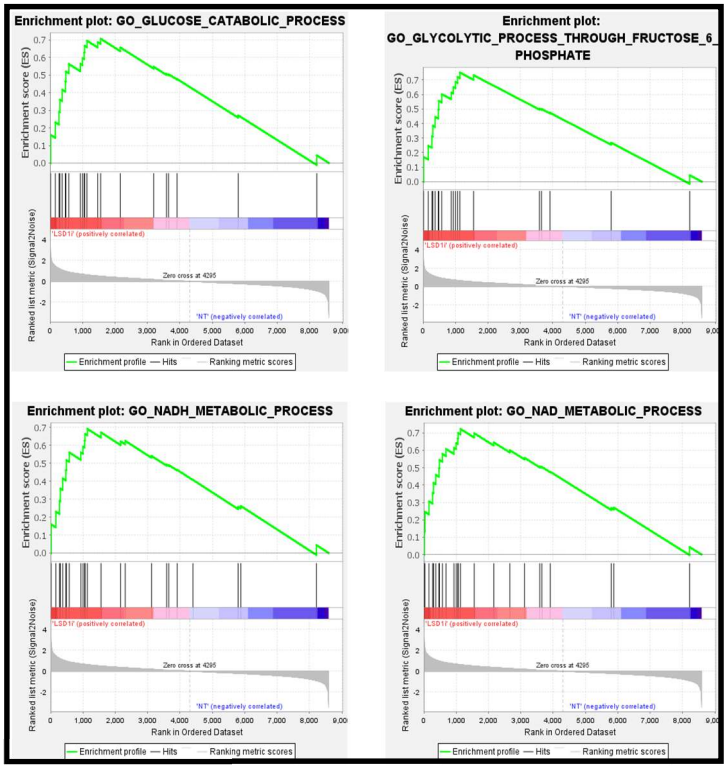

B Enrichment map of GSEA

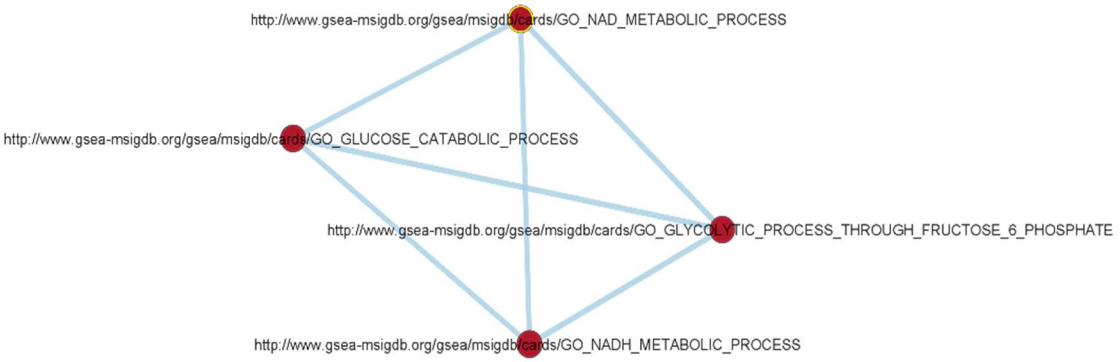

Figure 45 Gene set enrichment analysis plots enriched in MSC upon LSD1i

(A) The graph shows a collection of overlapping GSEA, involved in glucose catabolism. (B) Enrichment map of the GSEA in A. While the nodes represent the size of the Gene Sets, the edges show how many genes are shared.

A total of 432 DEG with an adjusted p-value of <0.05 were identified (control and LSD1i; n= 3 and 3, respectively), including 191 upregulated and 241 downregulated genes (Figure 44 A). Upregulated genes include proteins to regulate the proton and ion gradients across the membrane, as well as water channels to secure the cell structure.

A Gene Set Enrichment Analysis plots, downregulated in LSD1i

NES< -2.1, nom.p= 0.0, FDR< 0.005

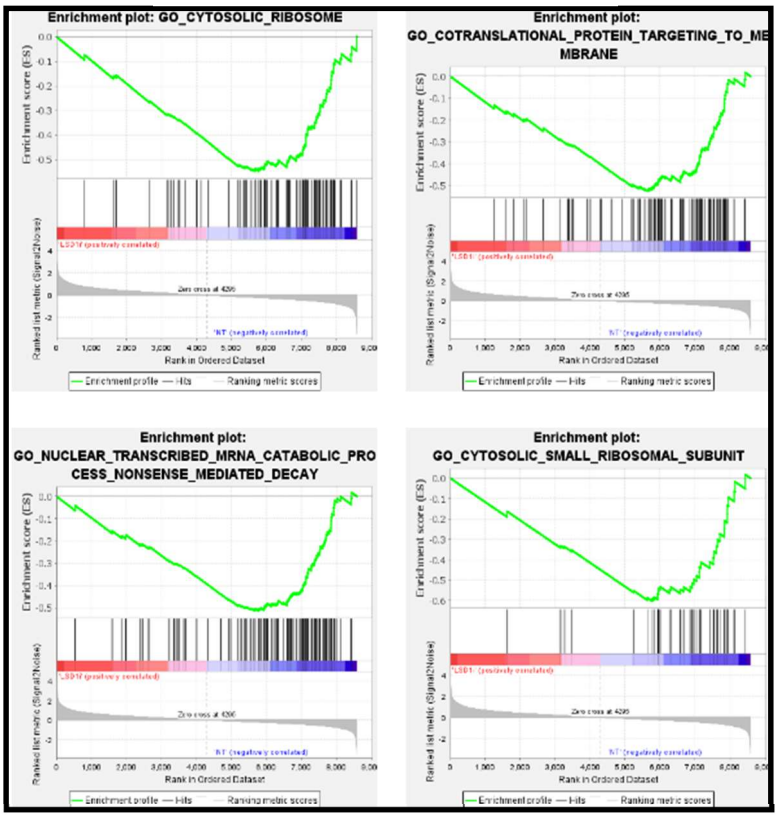

B Enrichment map of GSEA plots

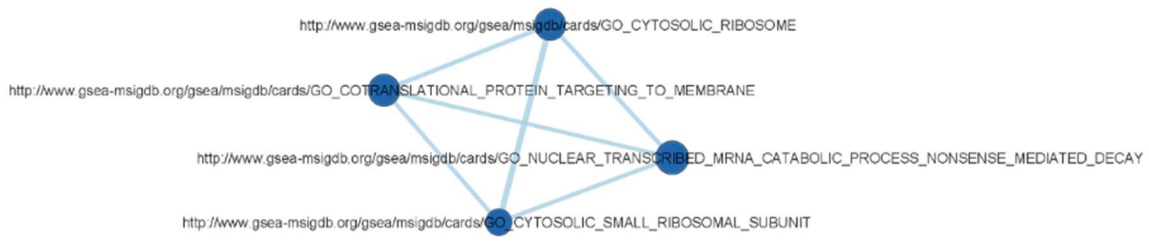

Figure 46 Gene set enrichment analysis plots depleted in MSC upon LSD1i

(A) A collection of overlapping GSEA, involved in normal functioning protein synthesis. (B) Enrichment map of the GSEA in A. While the nodes represent the size of the Gene Sets, the edges show how many genes are shared.

All these mechanisms necessitate a lot of energy, which is provided by the upregulated glycolysis. In this context, the top 2 upregulated genes *Atp6v0e2* and *Chrnb1* code for proteins influencing the membrane potential, *Atp6v0e2* (an ATPase) through hydrogen ion transport and *Chrnb1* (Cholinergic receptor nicotinic beta 1 subunit) through ion transport. *Aqp5* is coding for an aquaporin channel and is also higher expressed. The upregulated *Aldoc* is an aldolase, an enzyme participating in glycolysis. On the other hand, the downregulated *Rarres2* is an adipokine that regulates adipogenesis, metabolism and inflammation through activation of the chemokine-like receptor 1.

3.3.3 Combination of irradiation and LSD1i

A total of 606 genes were significantly expressed in the combination arm (IRR+LSD1i) in comparison to the control (adjusted p-value of <0.05 control and combination; n=3) 158 were up- and 448 downregulated. The top 10 deregulated genes, namely *Ankrd1, Atp6v0e2, Stmn2, Spint2, Aqp5, Penk, Msmp, Egfl6, Rarres2* and *Otor,* are shown in Figure 47.

Out of the 275 uniquely differentially expressed genes in the combination of irradiation and treatment, three are in the top 10 deregulated genes (Figure 47: *Stmn2, Spint2* and *Penk*. *Stmn2* codes for the Stathmin 2 protein, which is a regulator of microtubule stability. *Spint2* is a serine peptidase inhibitor and an inhibitor of HGF activator (Hepatocyte Growth Factor), that acts as tumorsuppressor[113]. The *Penk* gene encodes a neuropeptidase, such as enkephalins, which engage in neurotransmission and apoptotic pathways in synovial fibroblasts[114].

A number of differentially expressed genes **B** significantly deregulated genes in combination

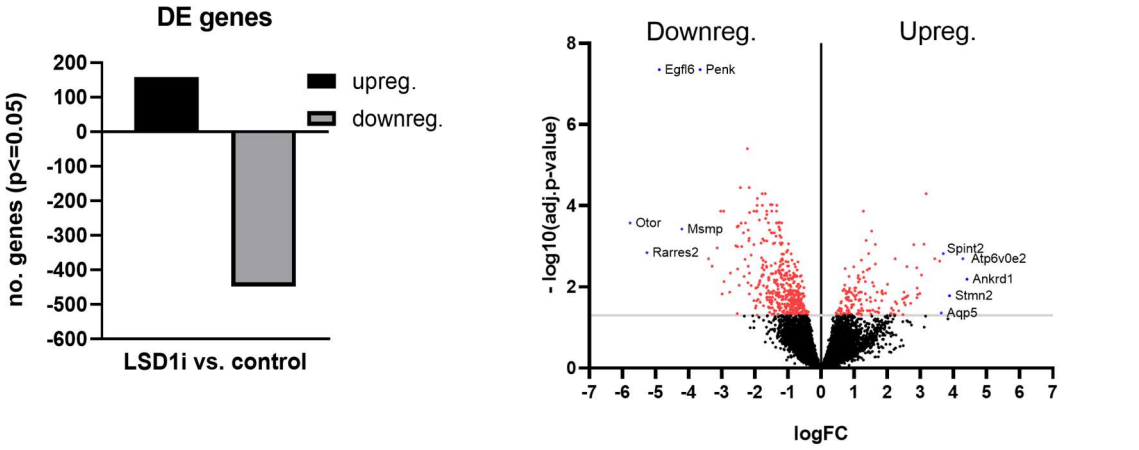

C top 10 significantly deregulated genes

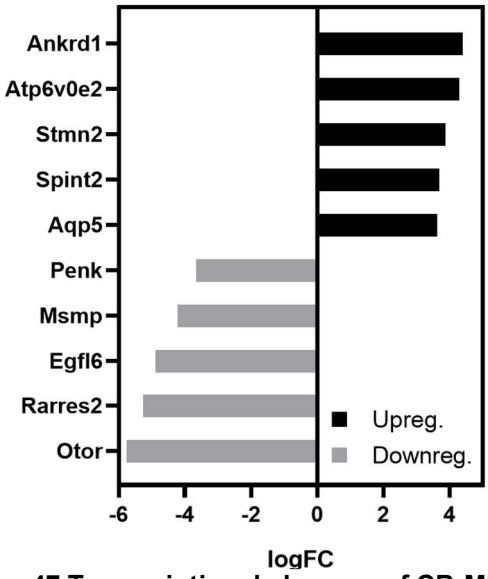

Figure 47 Transcriptional changes of CB-MSC upon combination treatment.
(A) In the DE gene graph are the number of differentially expressed genes upon combination depicted. (B)The graph shows the corresponding volcano plot, where red dots have an adj. p-value <0.05 and the blue dots are the top 10 significantly deregulated (pseudo-) genes upon combination, which can also be found in (C)

By taking a closer look at the enrichment map of Figure 48, it can be seen that four Gene Sets are overlapping: “GO_MICROTUBULE_ASSOCIATED_COMPLEX”, “GO_ATP_DEPENDENT_MICROTUBULE_MOTOR_ACTIVITY_PLUS_END_DIRECTED”, “GO_KINESIN_COMPLEX” and “GO_ATP_DEPENDENT_MICROTUBULE_MOTOR_ACTIVITY”. The enrichment map depicts the top 10 upregulated

results for “Gene Ontology”, with the biggest (in terms of gene number) being the microtubule associated complex. Gene Set Enrichment Analysis plots Gene Set Enrichment Analysis plots

The top upregulated signatures for “Hallmark” dataset, include the E2F targets (Figure 49), which are involved in cell cycle regulation (in positive and negative way). Therefore, in the combination treatment proliferation / cell cycle changes consistently.

A Gene Set Enrichment Analysis plot, upregulated in LSD1i + IRR

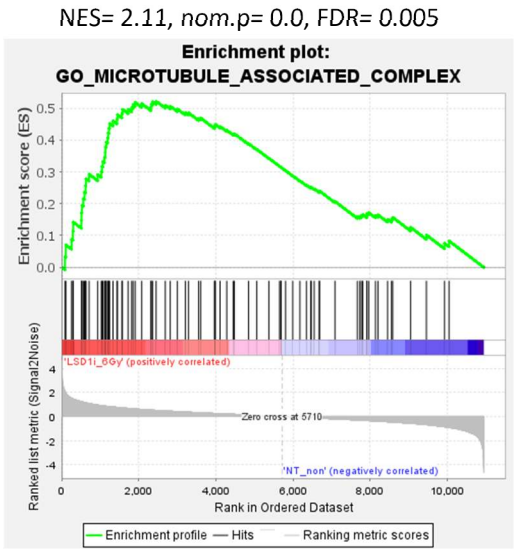

B Enrichment map of GSEA plots

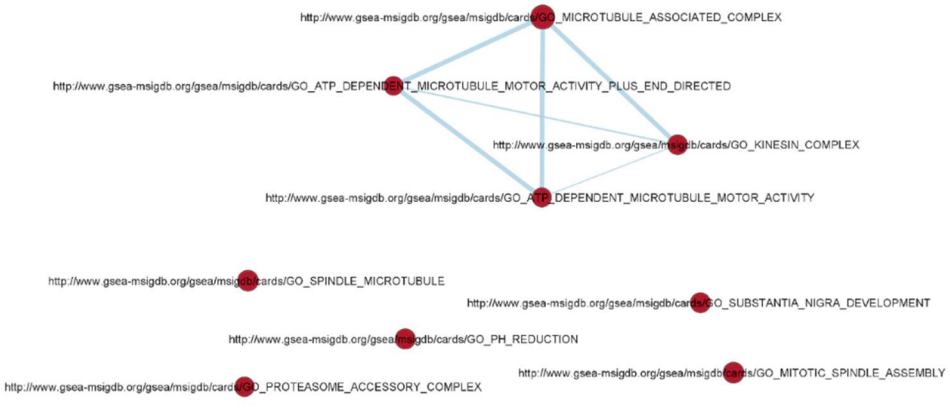

Figure 48 Gene set enrichment analysis plots depleted in MSC upon Irradiation and LSD1i
(A) Gene Set Enrichment Analysis of Differentially Expressed Genes. (B) Enrichment map of the top 10 upregulated “Gene Otology” Gene Sets. While the nodes represent the size of the Gene Sets, the edges show how many genes are shared.

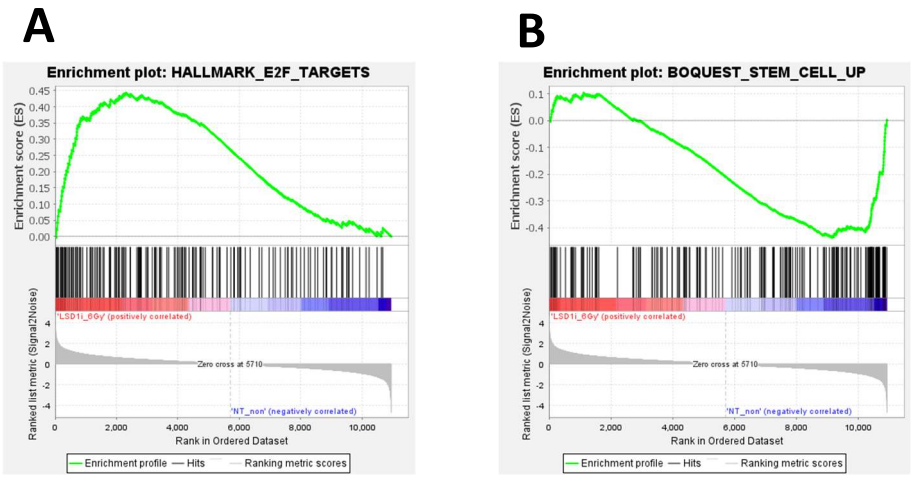

NES= 1.92, nom.p= 0.0, FDR= 0.028

NES= -2.05, nom.p= 0.0, FDR= 0.022

Figure 49 Gene Set Enrichment Analysis plots
Left: GSEA upregulated upon LSD1i and irradiation, "HALLMARK_E2F_TARGETS", Right: GSEA downregulated upon LSD1i and irradiation, "BOQUEST_STEM_CELL_UP"

MSC have stem cell properties when untreated and non-irradiated as can be seen by the FACS staining CD31 (Figure 50). Interestingly they lose their stem cell properties and develop distinct features from the control, according to the in the control enriched GS "BOQUEST_STEM_CELL_UP" (Figure 49), where "Genes up-regulated in freshly isolated CD31- (stromal stem cells from adipose tissue) versus the CD31+ (non-stem) counterparts." are included [115]. Figure 50 shows the results of a FACS staining analysis of MSC, isolated the same way as the cells used for the RNAseq.

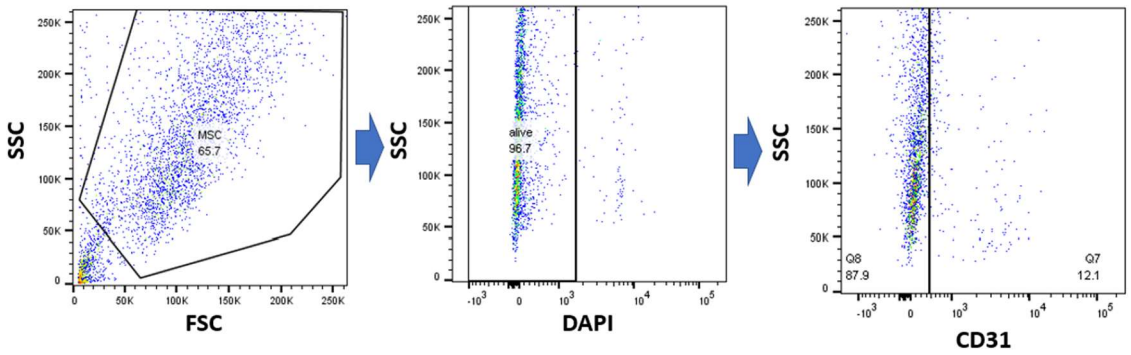

Figure 50 FACS staining analysis of the CB-MSC
Compact bone MSC which were kept in culture for a week prior to staining, MSC, isolated the same way as the cells used for the RNAseq. The debris was gated out and afterwards the DAPI positive events. Ca. 12 % of the live MSC were CD31 positive.

In summary, the combination of irradiation and LSD1 inhibition greatly affects the MSC: proliferation is enhanced, while parallel the cells lose their stem cell features and microtubule- associated features are included. This way, the cells are a distinct group compared to the population they originated from.

3.3.4 Uniquely differentially expressed genes in the combination[116]

In Figure 51 A the numbers of significantly deregulated genes and the overlap between the different conditions are shown ($p<0.05$) The number of differentially expressed genes were 328 upon irradiation (IRR), 432 upon LSD1i, and 606 upon irradiation+LSD1i (Combination), in comparison to the control untreated/non-irradiated MSC. Interestingly the combination of IRR + LSD1i uniquely changed the expression of 276 genes, that were not affected by LSD1i or irradiation alone, the top ten of these are shown in Figure 51 B.

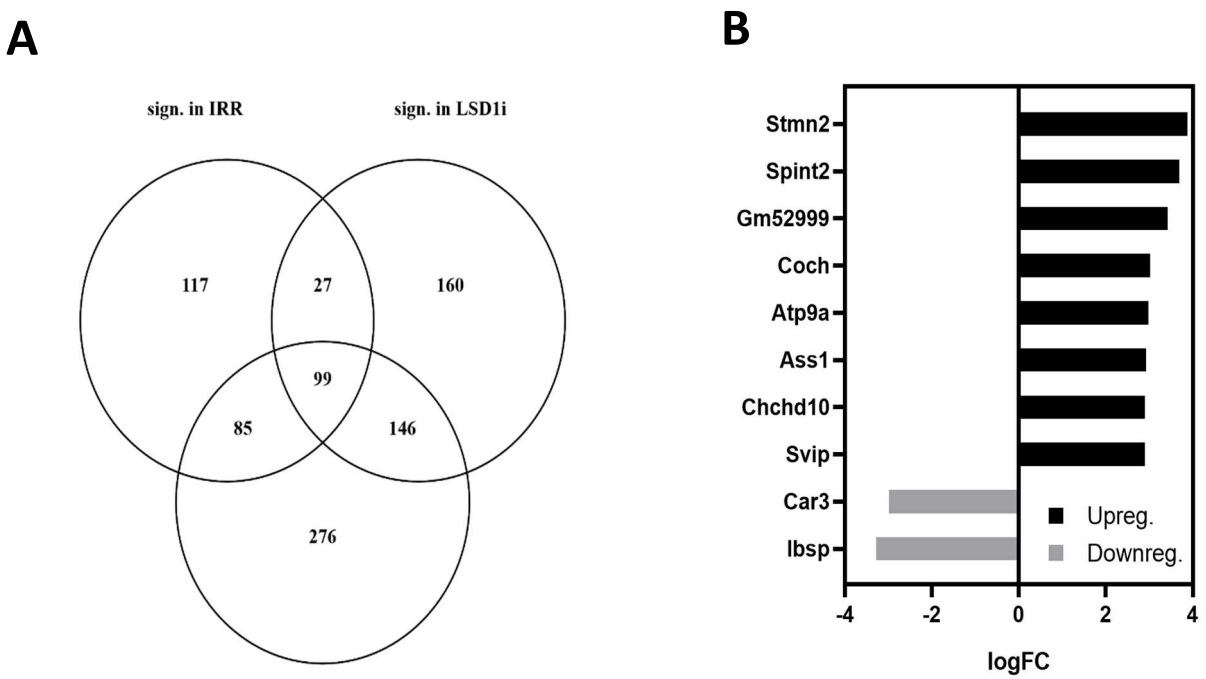

Figure 51 Transcriptional changes on MSC under the different conditions.
(A) Venn diagram (B) top 10 of the 276 (pseudo-) genes and their LogFC value.

As aforementioned, MSC produce proteins for intracellular as well as extracellular purposes. With the use of ECM (extra cellular matrix) proteins, the cells can communicate with each other and build distinct types of tissue such as bone. One example of an ECM molecule within the top downregulated genes is the *Ibsp* (integrin binding sialoprotein), which is a major structural component of the bone matrix and is synthesized by skeletal-associated cell types such as osteoblasts[117]. In one study, periodontal tissue was analyzed from patients to better understand the osteoimmunology of the microenvironment. Patient with a history of periodontitis received initial periodontal therapy, which is carried out to reduce infection and inflammation. It was observed that after this therapy *Ibsp* positive osteoblasts were significantly depleted [118]. Therefore,

downregulation in this work's conditions could also mirror descreased inflammation status.

Within the top 10 genes uniquely upregulated in the combination were *Coch, Chchd10* and *Svip*. *Coch* (Cochlin) plays a role in the control of cell shape. *Chchd10* has been suggested to maintain the mitochondrial cristae structure. The protein encoded by the *Svip* gene is an inhibitor of the endoplasmic reticulum-associated degradation pathway. These three genes allow a glimpse of the altered regulation of metabolic pathways of the MSC, since the cellular respiration as well as the overall cell structure seem to be changed[22].

To further investigate these changes, a GSEA was performed (Gene set enrichment analysis) (Figure 52).

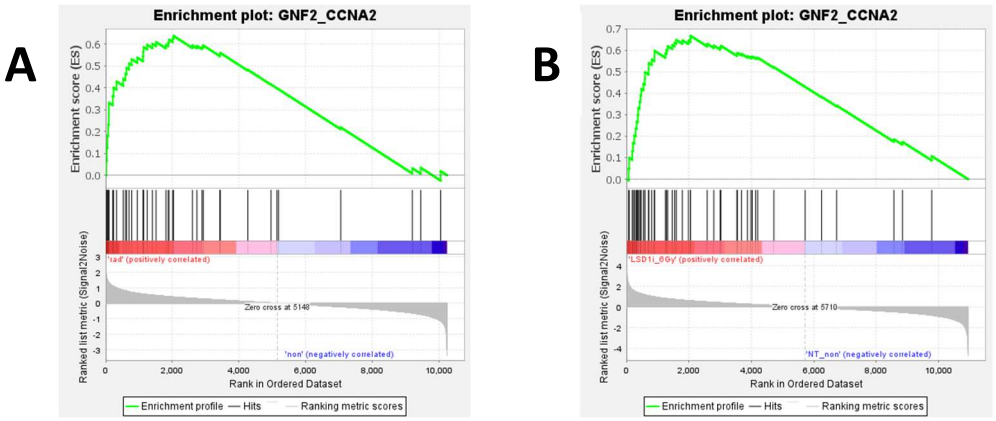

NES= 2.29, nom.p= 0.0, FDR= 0.0003

Irradiation vs. control

NES= 2.36, nom.p= 0.0, FDR= 0.0

Combination vs. control

Figure 52 Gene Set Enrichment Analysis of Differentially Expressed Genes.
This GSEA is upregulated upon irradiation as can be seen on the left side as well as it is upregulated upon the combination of LSD1i treatment and irradiation combined as can be seen on the right.

One of the top enriched gene signatures was "GNF2_CCNA2" both, irradiation and combination arms compared to the control (Figure 52 A-B). This signature represents the: "Neighborhood of CCNA2 cyclin A2 in the GNF2 expression compendium". (GNF2: Novartis normal human tissue gene expression compendium)[119]. Cyclin A2 is expressed in in the phase S of the cell cycle and is involved in the transition G2/M, regulating the cell division. After two weeks in culture, irradiated MSC show regeneration potential and the proliferation increases. Figure 5**Fehler! Verweisquelle konnte nicht gefunden werden.** depicts the cell numbers of MSC of different conditions in-

vitro cultures. While non-irradiated MSC continue to multiply constantly, irradiated MSC go through a “plateau” in the first few days and later, in the second week of cell culture they start to grow again, based on their cell number.

4. Discussion

LSD1 inhibition has been shown to exert a strong antileukemic effect in vitro and in vivo models[68] The treatment of MLL-AF9 mice can induce complete eradication in a proportion of treated animals, while others developed a relapse at a later timepoint. Unfortunately, monotherapy with a LSD1i might not be sufficient to eradicate AML. Therefore, the search of combinatorial therapeutic targets is strongly needed, to ameliorate the treatment and prognosis.

In the well-established mouse model of AML, normal hematopoietic precursors (e.g. HSC; or lin- cells) are transduced in vitro with an oncogene, here MLL-AF9. These cells are then transplanted into a syngeneic animal, where the leukemic stem cells present in the bulk cells give rise to AML in the recipient mice, with a different latency time, depending on the number of LSC, and on the aggressiveness of the disease. Generally, prior to transplantation the recipient mice are irradiated to deplete the endogenous HSC and to create a more favorable environment for the engraftment of the infected cells [36]. The irradiation can be lethal or sublethal, depending on the competition in vivo potential of the transplanted cells. If the mouse is lethally irradiated and the transplanted cells are not able to repopulate and restore the hematopoiesis, some helper cells need to be injected with the target preleukemic cells. For research, usually sublethal irradiation is always performed.

The AML subtype used in this work, MLL-AF9+, is quite effective in engraftment, even without previous irradiation, and engrafts within 2-3 months from transplantation. To shorten the latency time up to AML onset, the mice were sublethally irradiated (6 Gy). To our surprise, the LSD1 inhibition that was initiated after AML onset (1-2 weeks), while showing effect on non-irradiated mice resulting in a longer overall survival, it did not show any response in the irradiated group. This led to the suspicion that irradiation alters the bone marrow in such a way, that a resistance is built up and LSD1 inhibition cannot take effect anymore (unpublished data).

MLL-AF9 rearranged AML cells respond to LSD1 inhibition treatment and differentiate into more mature forms. This is detectable in in vitro experiments where AML monocultures are observed, but also in vivo, where a complex microenvironment is present. In this work AML cells were treated with LSD1i in the presence of one-timepoint supernatant or were cocultured with MSC through a membrane (only passable for soluble factors). In terms of total cell count, AML cells were similarly sensitive to LSD1i in the

presence of medium and SN treated-AML cultures. However, AML cells co-cultured with indirect contact with OP9 or S17 were less sensitive to LSD1i treatment. This was apparent through the persistence of blast colony forming units.

Based on the previously stated hypothesis of an irradiation-related resistance phenotype this project was started, to reproduce in an in vitro controlled system, the effect observed in vivo. The microenvironment found in vivo was mimicked using MSC. Cell lines, as well as primary murine cells were used. The cells were cultured over a longer period of time. In this work stromal cells were characterized alone after irradiation, after treatment with LSD1i and the combination of both treatments. Under all conditions compared to the control (a normal cell culture) MSC differentiation induction could be reported. While irradiated MSC tended towards adipogenesis, LSD1i treated MSC rather leaned towards osteogenesis. Furthermore, after initial enhanced apoptosis a regeneration step could be observed after 2 weeks, as previously described in chapter 3.3.4.

In detail, LSD1i treatment at the therapeutic dosage of 0.5 µM slightly decreased the cell count of BM derived MSC, while there was no difference in CB derived MSC. Furthermore, the MSC cell number was inversely proportional to irradiation dosage; 6 Gy led to a strong decline of proliferation. Apoptosis was increased after irradiation independently of the LSD1i. After some days past the irradiation timepoint, a regeneration of the proliferation could be detected. This was accompanied by the RNAseq results, where two weeks after irradiation at 6 Gy the MSC, both the not treated and the treated group showed the Gene Set “GNF2_CCNA2” to be in the top 10 enriched results of the GSEA. Cyclin A2 regulates the cell cycle and the cell division in somatic cells.

The transcriptomic analysis of the LSD1i treated cells in comparison to the control, revealed that the inhibition changes the metabolism of the MSC. In particular, glycolysis and glucose metabolism were elevated as well as expression of genes involved in ion membrane gradient maintenance. In line with this, the RNA levels of for example ATPases were elevated and Gene Sets for glucose catabolism enriched. In parallel protein sysnthesis was reduced by regulating the cytosolic ribosomes.

Surface markers were also indicating a change in the immunophenotype of the treated cells. CD29, a receptor involved in migration, was slightly upregulated only in double treated cells. This could reflect the morphological changes observed (protrusions), in

line with the transcriptional changes involving structural proteins. CD44 can be found on surface of MSC from many different origins and is a very common surface marker, important in inflammatory processes because it is involved in the recruitment and activation of inflammatory cells[94]. In this work, proportion of cells positive for CD44 was increased upon irradiation and even more upon IRR+LSD1i, may be reflecting an increased inflammatory feature of the cells.

The differentiation potential of MSC can easily be manipulated, therefore their differentiation abilities were investigated. MSC can become adipocytes or osteocytes, among other cell types. For this, the differentiation marker FABP4 for the adipogenesis and osteocalcin and osteopontin as osteogenic markers were researched. After two weeks of culture, cells did not completely differentiate. While irradiation increased the adipogenesis-associated features, LSD1i without irradiation led to increase to osteogenesis markers. In the western blot results, the irradiated group showed the biggest FABP4 band out of all conditions. The RNAseq results showed no difference in FABP4 expression between the irradiated group and the control, but a downregulation of FABP4 in the LSD1i-treated groups. The transcription factor Runx2 is vital to the differentiation of MSC to osteoblasts and causes the upregulation of important bone matrix genes like SPP1 and BGLAP[120,121]. At the protein level, the LSD1i treated group showed the greatest osteocalcin amount. The RNAseq results reveal, that all conditions significantly induce the SPP1 upregulation, this applies especially to the combination of LSD1i and Irradiation. This was in line with previously published results, where the LSD1 inhibitor Pargyline has shown that BM-MSC under treatment and two weeks in culture have an increased osteogenesis potential, where RT-PCR analysis showed the significantly upregulated gene Runx2[71]

Irradiation can lead to imbalance in the differentiation process of MSC, in favor of adipogenesis according to a study on rat BM-MSC[75]. Irradiation is known to cause cell injury. The transcriptome analysis for irradiation vs. ctrl has shown that genes regulated by NF-κB in response to TNF are downregulated in irradiated MSC. Depending on the cell type, the TNF receptor and NF-κB molecules can induce, different reactions leading to cell death or survival, and inflammation response and/or control[122].

In this work, eight days after irradiation, MSC displayed an increased apoptosis and two weeks after irradiation the MSC started to proliferate again in an exponential way as sign of regeneration. Additionally, the inflammatory response and the TNF signaling

were downregulated. This could indicate that in the MSC two weeks after the irradiation, the inflammation caused by irradiation[123], is inhibited by downregulating key genes of inflammation. Similar to only irradiated MSCs, the combination of LSD1i and irradiation also upregulates mechanisms for proliferation. The top upregulated “Hallmark” result for LSD1i+IRR cells shows the upregulation of E2F targets. E2F is a group of transcription factors, which regulate the cell cycle. In parallel genes belonging to microtubules-associated signatures were enriched. This could reflect the morphological effects observed in line with the differentiation induction. Parallel the transcriptome analysis suggests that LSD1i+IRR cells lose their stem cell features, meaning they could begin to differentiate, in line with the immunological and differentiation-specific analyses.

These were the effects of irradiation and treatment with LSD1i on MSC alone in vitro. However, in vivo AML cells and the bone-marrow stromal cells represent a dynamic system as they influence each other. Cell interactions affect intracellular signaling and homeostasis, regulate inflammation processes, apoptosis and can even lead to the development of malignancies. A key player in these interactions are cytokines. They can act as autocrine, paracrine, and endocrine factors. Interleukins, colony stimulating factors, chemokines and tumor necrosis factors are some of the many different cytokine groups[100]. In this project, the leukemic cells were treated with LSD1i in the presence of supernatant, through a membrane, or in direct contact with stromal cells, which were previously irradiated.

In cultures, where AML cells and MSC undergo a direct contact (co-culture) the production of the cytokines CCL2 and CXCL1 was significantly reduced when the MSC were previously irradiated and the AML cells (as well as the co-cultured MSC) were simultaneously treated with LSD1i, in comparison to the untreated control and single treatments. The concentration of both cytokines was also in the same range as the MSC only cultures, suggesting that the production of CCL2 and CXCL1 is (almost) solely dependent on the MSC. Both cytokines are involved in inflammatory processes. Another cytokine CCL5, which enjoys high levels in cultures containing MSC, did seem to barely be produced by AML. When one-time-point filtered (cell free) supernatant from MSC was added to the AML culture, the AML possibly uptake the CCL5 and therefore lower the measurable concentration of the cytokine. However, when the MSC were irradiated CCL5 reduction in the AML culture was not visible. Increased CCL5 levels were previously reported in midostaurin-resistant cells (a tyrosine kinase

inhibitor, TKI) compared to TKI-sensitive cells. In the same work TKI-sensitive cells were treated with CCL5 and became resistant to midostaurin. Similarly, CCL5 has been reported to be a resistance mediator in different tumor types[124].

Supporting this, the proportion of more aggressive c-kit+/Mac-1+ known LSC subpopulation in this AML model was higher in the co-cultures where the OP9 were irradiated. This means that these cells survive the double treatment mediating the resistance phenotype that could be observed.

In conclusion, upon irradiation and LSD1i, MSC undergo unique transcriptome changes, show altered differentiation preferences and cytokine release changes. In this process they also lose their stem cell features. Immunophenotypical changes of surface proteins such as CD44 were observed, especially an increase of CD44 after LSD1i exposure (more so when previously irradiated). CD29 was slightly increased after the combination treatment of LSD1i and irradiation. Microenvironmental changes, such as irradiation of the MSC, affected the response of AML cells to the targeted epigenetic therapy with LSD1i. Further research is necessary to assess if CCL5 mediates the resistance phenotype and how this phenotype translates to the in vivo system. Similarly, the role of lymphocytes as mediators in the cell-interaction should be assessed in a triple co-culture system.

References

1. ZfKD. *Krebs in Deutschland für 2017/2018*. Vol. 13. Ausgabe. 2021:142-145.

2. Rölling. Akute Myeloische Leukämie (AML). Deutsche Gesellschaft für Hämato-Onkologie (DGHO). Accessed 12.10.2022, https://www.onkopedia.com/de/onkopedia/guidelines/akute-myeloische-leukaemie-aml/@@guideline/html/index.html#litID0EONAI

3. Bennett JM, Catovsky D, Daniel MT, et al. Proposals for the classification of the acute leukaemias. French-American-British (FAB) co-operative group. *Br J Haematol*. Aug 1976;33(4):451-8. doi:10.1111/j.1365-2141.1976.tb03563.x

4. Vardiman JW, Harris NL, Brunning RD. The World Health Organization (WHO) classification of the myeloid neoplasms. *Blood*. Oct 1 2002;100(7):2292-302. doi:10.1182/blood-2002-04-1199

5. Khoury JD, Solary E, Abla O, et al. The 5th edition of the World Health Organization Classification of Haematolymphoid Tumours: Myeloid and Histiocytic/Dendritic Neoplasms. *Leukemia*. Jul 2022;36(7):1703-1719. doi:10.1038/s41375-022-01613-1

6. Juliusson G, Antunovic P, Derolf A, et al. Age and acute myeloid leukemia: real world data on decision to treat and outcomes from the Swedish Acute Leukemia Registry. *Blood*. Apr 30 2009;113(18):4179-87. doi:10.1182/blood-2008-07-172007

7. Thein MS, Ershler WB, Jemal A, Yates JW, Baer MR. Outcome of older patients with acute myeloid leukemia: an analysis of SEER data over 3 decades. *Cancer*. Aug 1 2013;119(15):2720-7. doi:10.1002/cncr.28129

8. Fraumeni JF, Jr., Miller RW. Epidemiology of human leukemia: recent observations. *J Natl Cancer Inst*. Apr 1967;38(4):593-605.

9. Ichimaru M, Tomonaga M, Amenomori T, Matsuo T. Atomic bomb and leukemia. *J Radiat Res*. Dec 1991;32 Suppl 2:14-9. doi:10.1269/jrr.32.supplement2_14

10. Bueso-Ramos CE, Kanagal-Shamanna R, Routbort MJ, Hanson CA. Therapy-Related Myeloid Neoplasms. *Am J Clin Pathol*. Aug 2015;144(2):207-18. doi:10.1309/AJCPU1JO2LYTWUAV

11. Jin MW, Xu SM, An Q, Wang P. A review of risk factors for childhood leukemia. *Eur Rev Med Pharmacol Sci*. Sep 2016;20(18):3760-3764.

12. Menssen AJ, Walter MJ. Genetics of progression from MDS to secondary leukemia. *Blood*. Jul 2 2020;136(1):50-60. doi:10.1182/blood.2019000942

13. Bullinger L, Dohner K, Dohner H. Genomics of Acute Myeloid Leukemia Diagnosis and Pathways. *J Clin Oncol*. Mar 20 2017;35(9):934-946. doi:10.1200/JCO.2016.71.2208

14. Team TUoCHMCR. How I diagnose and manage individuals at risk for inherited myeloid malignancies. *Blood*. 2016;128(14):1800-1813. doi:10.1182/blood-2016-05-670240

15. Tomasetti C, Vogelstein B. Cancer etiology. Variation in cancer risk among tissues can be explained by the number of stem cell divisions. *Science*. Jan 2 2015;347(6217):78-81. doi:10.1126/science.1260825

16. Gilliland DG, Griffin JD. The roles of FLT3 in hematopoiesis and leukemia. *Blood*. Sep 1 2002;100(5):1532-42. doi:10.1182/blood-2002-02-0492

17. Myelodysplastische Neoplasien (Myelodysplastische Syndrome, MDS). 2024. 2024. https://www.onkopedia.com/de/onkopedia/guidelines/myelodysplastische-neoplasien-myelodysplastische-syndrome-mds/@@guideline/html/index.html

18. Khwaja A, Bjorkholm M, Gale RE, et al. Acute myeloid leukaemia. *Nature Reviews Disease Primers*. 2016/03/10 2016;2(1):16010. doi:10.1038/nrdp.2016.10

19. Meyer C, Burmeister T, Groger D, et al. The MLL recombinome of acute leukemias in 2017. *Leukemia*. Feb 2018;32(2):273-284. doi:10.1038/leu.2017.213

20. Muntean AG, Hess JL. The pathogenesis of mixed-lineage leukemia. *Annu Rev Pathol*. 2012;7:283-301. doi:10.1146/annurev-pathol-011811-132434

21. Marschalek R. MLL leukemia and future treatment strategies. *Arch Pharm (Weinheim)*. Apr 2015;348(4):221-8. doi:10.1002/ardp.201400449

22. GeneCards. 2022. https://www.genecards.org/

23. Olsen SN, Godfrey L, Healy JP, et al. MLL::AF9 degradation induces rapid changes in transcriptional elongation and subsequent loss of an active chromatin landscape. *Mol Cell*. Mar 17 2022;82(6):1140-1155 e11. doi:10.1016/j.molcel.2022.02.013

24. Dave M, Daga A, Rawal R. Structural and functional analysis of AF9-MLL oncogenic fusion protein using homology modeling and simulation based approach. *Int J pharm Pharm sci*. 2015;7(12):155-161.

25. Stavropoulou V, Kaspar S, Brault L, et al. MLL-AF9 Expression in Hematopoietic Stem Cells Drives a Highly Invasive AML Expressing EMT-Related Genes Linked to Poor Outcome. *Cancer Cell*. Jul 11 2016;30(1):43-58. doi:10.1016/j.ccell.2016.05.011

26. Southam CM, Craver LF, Dargeon HW, Burchenal JH. A study of the natural history of acute leukemia with special reference to the duration of the disease and the occurrence of remissions. *Cancer*. Jan 1951;4(1):39-59. doi:10.1002/1097-0142(195101)4:1<39::aid-cncr2820040105>3.0.co;2-g

27. Dohner H, Wei AH, Appelbaum FR, et al. Diagnosis and management of AML in adults: 2022 recommendations from an international expert panel on behalf of the ELN. *Blood*. Sep 22 2022;140(12):1345-1377. doi:10.1182/blood.2022016867

28. Hourigan CS, Gale RP, Gormley NJ, Ossenkoppele GJ, Walter RB. Measurable residual disease testing in acute myeloid leukaemia. *Leukemia*. Jul 2017;31(7):1482-1490. doi:10.1038/leu.2017.113

29. Forte D, Garcia-Fernandez M, Sanchez-Aguilera A, et al. Bone Marrow Mesenchymal Stem Cells Support Acute Myeloid Leukemia Bioenergetics and Enhance Antioxidant Defense and Escape from Chemotherapy. *Cell Metab*. Nov 3 2020;32(5):829-843 e9. doi:10.1016/j.cmet.2020.09.001

30. Papaemmanuil E, Gerstung M, Bullinger L, et al. Genomic Classification and Prognosis in Acute Myeloid Leukemia. *N Engl J Med*. Jun 9 2016;374(23):2209-2221. doi:10.1056/NEJMoa1516192

31. Liu H. Emerging agents and regimens for AML. *J Hematol Oncol*. Mar 23 2021;14(1):49. doi:10.1186/s13045-021-01062-w

32. Nicolaus Kröger AB, Dietger Niederwieser, Gerald Wulf. Konditionierung. onkopedia. Updated 11.2020. Accessed 10.10.2023, https://www.onkopedia.com/de/onkopedia/guidelines/konditionierung/@@guideline/html/index.html

33. team TACSmaec. Typical Treatment of Acute Myeloid Leukemia. Accessed 16.10.2022, https://www.cancer.org/cancer/acute-myeloid-leukemia/treating/typical-treatment-of-aml.html

34. team TACSmaec. Radiation Therapy for Acute Myeloid Leukemia Accessed 16.10.2022, https://www.cancer.org/cancer/acute-myeloid-leukemia/treating/radiation-therapy.html

35. Paix A, Antoni D, Waissi W, et al. Total body irradiation in allogeneic bone marrow transplantation conditioning regimens: A review. *Crit Rev Oncol Hematol*. Mar 2018;123:138-148. doi:10.1016/j.critrevonc.2018.01.011

36. Stevens SK, Moore SG, Kaplan ID. Early and late bone-marrow changes after irradiation: MR evaluation. *AJR Am J Roentgenol*. Apr 1990;154(4):745-50. doi:10.2214/ajr.154.4.2107669

37. Zuro D, Madabushi SS, Brooks J, et al. First Multimodal, Three-Dimensional, Image-Guided Total Marrow Irradiation Model for Preclinical Bone Marrow Transplantation Studies. *Int J Radiat Oncol Biol Phys*. Nov 1 2021;111(3):671-683. doi:10.1016/j.ijrobp.2021.06.001

38. Robak T, Wierzbowska A. Current and emerging therapies for acute myeloid leukemia. *Clin Ther*. 2009;31 Pt 2:2349-70. doi:10.1016/j.clinthera.2009.11.017

39. DiNardo CD, Tiong IS, Quaglieri A, et al. Molecular patterns of response and treatment failure after frontline venetoclax combinations in older patients with AML. *Blood*. Mar 12 2020;135(11):791-803. doi:10.1182/blood.2019003988

40. Yan B, Claxton D, Huang S, Qiu Y. AML chemoresistance: The role of mutant TP53 subclonal expansion and therapy strategy. *Exp Hematol*. Jul 2020;87:13-19. doi:10.1016/j.exphem.2020.06.003

41. Witkowski MT, Lasry A, Carroll WL, Aifantis I. Immune-Based Therapies in Acute Leukemia. *Trends Cancer*. Oct 2019;5(10):604-618. doi:10.1016/j.trecan.2019.07.009

42. Joshi SK, Nechiporuk T, Bottomly D, et al. The AML microenvironment catalyzes a stepwise evolution to gilteritinib resistance. *Cancer Cell*. Jul 12 2021;39(7):999-1014 e8. doi:10.1016/j.ccell.2021.06.003

43. Tonk CH, Witzler M, Schulze M, Tobiasch E. Mesenchymal Stem Cells. In: Brand-Saberi B, ed. *Essential Current Concepts in Stem Cell Biology*. Springer International Publishing; 2020:21-39.

44. Porcellini A. Medicina regenerativa: uma revisão. *Revista Brasileira de Hematologia e Hemoterapia*. 2009;v. 31(suppl 2):pp. 63-66.

45. Antwerpes F. Mesenchym. DocCheck Flexikon. Accessed 02.12.2022, https://flexikon.doccheck.com/de/Mesenchym

46. Galipeau J, Sensebe L. Mesenchymal Stromal Cells: Clinical Challenges and Therapeutic Opportunities. *Cell Stem Cell*. Jun 1 2018;22(6):824-833. doi:10.1016/j.stem.2018.05.004

47. Valero MC, Huntsman HD, Liu J, Zou K, Boppart MD. Eccentric exercise facilitates mesenchymal stem cell appearance in skeletal muscle. *PLoS One*. 2012;7(1):e29760. doi:10.1371/journal.pone.0029760

48. Dominici M, Le Blanc K, Mueller I, et al. Minimal criteria for defining multipotent mesenchymal stromal cells. The International Society for Cellular Therapy position statement. *Cytotherapy*. 2006;8(4):315-7. doi:10.1080/14653240600855905

49. Haasters F, Prall WC, Anz D, et al. Morphological and immunocytochemical characteristics indicate the yield of early progenitors and represent a quality control for human mesenchymal stem cell culturing. *J Anat*. May 2009;214(5):759-67. doi:10.1111/j.1469-7580.2009.01065.x

50. Docheva D, Popov C, Mutschler W, Schieker M. Human mesenchymal stem cells in contact with their environment: surface characteristics and the integrin system. *J Cell Mol Med*. Jan-Feb 2007;11(1):21-38. doi:10.1111/j.1582-4934.2007.00001.x

51. Almalki SG, Agrawal DK. Key transcription factors in the differentiation of mesenchymal stem cells. *Differentiation*. Jul-Aug 2016;92(1-2):41-51. doi:10.1016/j.diff.2016.02.005

52. Komori T. Regulation of osteoblast differentiation by transcription factors. *J Cell Biochem*. Dec 1 2006;99(5):1233-9. doi:10.1002/jcb.20958

53. Djouad F, Charbonnier LM, Bouffi C, et al. Mesenchymal stem cells inhibit the differentiation of dendritic cells through an interleukin-6-dependent mechanism. *Stem Cells*. Aug 2007;25(8):2025-32. doi:10.1634/stemcells.2006-0548

54. Hart DA. What Molecular Recognition Systems Do Mesenchymal Stem Cells/Medicinal Signaling Cells (MSC) Use to Facilitate Cell-Cell and Cell Matrix Interactions? A Review of Evidence and Options. *International Journal of Molecular Sciences*. 2021;22(16):8637.

55. Alberts B JA, Lewis J, et al. Molecular Biology of the Cell. Garland Science. Accessed 25.10.2022, https://www.ncbi.nlm.nih.gov/books/NBK26867/

56. Todd RF, 3rd. The continuing saga of complement receptor type 3 (CR3). *J Clin Invest*. Jul 1 1996;98(1):1-2. doi:10.1172/JCI118752

57. Mezu-Ndubuisi OJ, Maheshwari A. The role of integrins in inflammation and angiogenesis. *Pediatr Res*. May 2021;89(7):1619-1626. doi:10.1038/s41390-020-01177-9

58. Khalaf K, Hana D, Chou JT, Singh C, Mackiewicz A, Kaczmarek M. Aspects of the Tumor Microenvironment Involved in Immune Resistance and Drug Resistance. *Front Immunol*. 2021;12:656364. doi:10.3389/fimmu.2021.656364

59. Lo Sicco C, Reverberi D, Balbi C, et al. Mesenchymal Stem Cell-Derived Extracellular Vesicles as Mediators of Anti-Inflammatory Effects: Endorsement of Macrophage Polarization. *Stem Cells Transl Med*. Mar 2017;6(3):1018-1028. doi:10.1002/sctm.16-0363

60. Cancer Treatment. Accessed 27.10.2022, https://www.cancer.gov/about-cancer/treatment

61. Katzel JA, Fanucchi MP, Li Z. Recent advances of novel targeted therapy in non-small cell lung cancer. *J Hematol Oncol*. Jan 21 2009;2:2. doi:10.1186/1756-8722-2-2

62. Targeted Therapy to Treat Cancer. National Cancer Institute. Accessed 27.10.2022, https://www.cancer.gov/about-cancer/treatment/types/targeted-therapies#what-is-targeted-therapy

63. tumor board review. Accessed 28.10.2022, https://www.cancer.gov/publications/dictionaries/cancer-terms/def/tumor-board-review?redirect=true

64. team TACSmaec. History of Cancer Treatments: Targeted Therapy. 28.10.2022. https://www.cancer.org/treatment/understanding-your-diagnosis/history-of-cancer/cancer-treatment-targeted-therapy.html

65. Rudolph T, Beuch S, Reuter G. Lysine-specific histone demethylase LSD1 and the dynamic control of chromatin. *Biol Chem*. Aug 2013;394(8):1019-28. doi:10.1515/hsz-2013-0119

66. HGNC. Entrez Gene: Lysine (K)-specific demethylase 1A. Updated 20.11.2022. Accessed 02.12.2022, https://www.ncbi.nlm.nih.gov/gene?cmd=retrieve&list_uids=23028

67. Vinyard ME, Su C, Siegenfeld AP, et al. CRISPR-suppressor scanning reveals a nonenzymatic role of LSD1 in AML. *Nat Chem Biol*. May 2019;15(5):529-539. doi:10.1038/s41589-019-0263-0

68. Cusan M, Cai SF, Mohammad HP, et al. LSD1 inhibition exerts its antileukemic effect by recommissioning PU.1- and C/EBPalpha-dependent enhancers in AML. *Blood*. Apr 12 2018;131(15):1730-1742. doi:10.1182/blood-2017-09-807024

69. Fang Y, Liao G, Yu B. LSD1/KDM1A inhibitors in clinical trials: advances and prospects. *J Hematol Oncol*. Dec 4 2019;12(1):129. doi:10.1186/s13045-019-0811-9

70. Mardani F, Saad W, El-Hachem N, et al. LSD1 Inhibition Enhances the Immunogenicity of Mesenchymal Stromal Cells by Eliciting a dsRNA Stress Response. *Cells*. Jun 1 2022;11(11)doi:10.3390/cells11111816

71. Lv L, Ge W, Liu Y, et al. Lysine-specific demethylase 1 inhibitor rescues the osteogenic ability of mesenchymal stem cells under osteoporotic conditions by modulating H3K4 methylation. *Bone Research*. 2016/12/27 2016;4(1):16037. doi:10.1038/boneres.2016.37

72. Gao X, Xu C, Asada N, Frenette PS. The hematopoietic stem cell niche: from embryo to adult. *Development*. Jan 22 2018;145(2)doi:10.1242/dev.139691

73. Ruckert M, Flohr AS, Hecht M, Gaipl US. Radiotherapy and the immune system: More than just immune suppression. *Stem Cells*. Sep 2021;39(9):1155-1165. doi:10.1002/stem.3391

74. Wennerberg E, Lhuillier C, Vanpouille-Box C, et al. Barriers to Radiation-Induced In Situ Tumor Vaccination. *Front Immunol*. 2017;8:229. doi:10.3389/fimmu.2017.00229

75. Zuo R, Liu M, Wang Y, et al. BM-MSC-derived exosomes alleviate radiation-induced bone loss by restoring the function of recipient BM-MSCs and activating Wnt/beta-catenin signaling. *Stem Cell Res Ther*. Jan 15 2019;10(1):30. doi:10.1186/s13287-018-1121-9

76. Zhang S, Chuah SJ, Lai RC, Hui JHP, Lim SK, Toh WS. MSC exosomes mediate cartilage repair by enhancing proliferation, attenuating apoptosis and modulating immune reactivity. *Biomaterials*. Feb 2018;156:16-27. doi:10.1016/j.biomaterials.2017.11.028

77. OP9. Accessed 03.12.2022, https://www.atcc.org/products/crl-2749

78. Cellosaurus S17. Accessed 03.12.2022, https://www.cellosaurus.org/CVCL_E226

79. Culture and Analysis of Hematopoietic Progenitor Cells in CFU Assays Accessed 07.10.2023, https://www.stemcell.com/culture-and-analysis-of-hematopoietic-progenitor-cells-in-cfu-assays.html

80. "Mouse Colony-Forming Unit (CFU) Assays Using MethoCult". 2020. https://cdn.stemcell.com/media/files/manual/10000005597-Mouse_Colony_Forming_Unit_Assays_Using_MethoCult.pdf?_ga=2.145953527.23719384.1670270677-1718527331.1666732130

81. "ICC/IF of suspension cells using Cytospin". Abcam. 2020. http://docs.abcam.com/pdf/protocols/icc-if-of-suspension-cells-using-cytospin.pdf

82. "Immunocytochemistry and immunofluorescence protocol". Abcam. 2020. https://docs.abcam.com/pdf/protocols/immunocytochemistry.pdf

83. "Direct flow cytometry protocol". Abcam. 2020. https://docs.abcam.com/pdf/protocols/direct-flow%20cytometry.pdf

84. "Annexin V Staining Protocol". BD Biosciences. 2020. https://www.bdbiosciences.com/en-de/resources/protocols/annexin-v-staining-protocol

85. "General western blot protocol". Abcam. 2020. https://www.abcam.com/protocols/general-western-blot-protocol

86. "Bio-Plex Pro Cytokine, Chemokine, and Growth Factor Assays. Instruction Manual". www.bio-rad.com. 2020. https://www.bio-rad.com/webroot/web/pdf/lsr/literature/10014905.pdf

87. Chen Y, Lun AT, Smyth GK. From reads to genes to pathways: differential expression analysis of RNA-Seq experiments using Rsubread and the edgeR quasi-likelihood pipeline. *F1000Res*. 2016;5:1438. doi:10.12688/f1000research.8987.2

88. Ritchie ME, Phipson B, Wu D, et al. limma powers differential expression analyses for RNA-sequencing and microarray studies. *Nucleic Acids Res*. Apr 20 2015;43(7):e47. doi:10.1093/nar/gkv007

89. Liberzon A, Subramanian A, Pinchback R, Thorvaldsdottir H, Tamayo P, Mesirov JP. Molecular signatures database (MSigDB) 3.0. *Bioinformatics*. Jun 15 2011;27(12):1739-40. doi:10.1093/bioinformatics/btr260

90. Melzer C, Jacobs R, Dittmar T, et al. Reversible Growth-Arrest of a Spontaneously-Derived Human MSC-Like Cell Line. *Int J Mol Sci*. Jul 3 2020;21(13)doi:10.3390/ijms21134752

91. Ode A, Kopf J, Kurtz A, et al. CD73 and CD29 concurrently mediate the mechanically induced decrease of migratory capacity of mesenchymal stromal cells. *Eur Cell Mater*. Jul 6 2011;22:26-42. doi:10.22203/ecm.v022a03

92. Beeravolu N, McKee C, Alamri A, et al. Isolation and Characterization of Mesenchymal Stromal Cells from Human Umbilical Cord and Fetal Placenta. *J Vis Exp*. Apr 3 2017;(122)doi:10.3791/55224

93. L. Ramos T, Sánchez-Abarca LI, Muntión S, et al. MSC surface markers (CD44, CD73, and CD90) can identify human MSC-derived extracellular vesicles by conventional flow cytometry. *Cell Communication and Signaling*. 2016/01/12 2016;14(1):2. doi:10.1186/s12964-015-0124-8

94. Zhou L, Hao Q, Sugita S, et al. Role of CD44 in increasing the potency of mesenchymal stem cell extracellular vesicles by hyaluronic acid in severe pneumonia. *Stem Cell Res Ther*. May 20 2021;12(1):293. doi:10.1186/s13287-021-02329-2

95. Holmes C, Stanford WL. Concise review: stem cell antigen-1: expression, function, and enigma. *Stem Cells*. Jun 2007;25(6):1339-47. doi:10.1634/stemcells.2006-0644

96. Morcos MNF, Schoedel KB, Hoppe A, et al. SCA-1 Expression Level Identifies Quiescent Hematopoietic Stem and Progenitor Cells. *Stem Cell Reports*. Jun 6 2017;8(6):1472-1478. doi:10.1016/j.stemcr.2017.04.012

97. Valorani MG, Germani A, Otto WR, et al. Hypoxia increases Sca-1/CD44 co-expression in murine mesenchymal stem cells and enhances their adipogenic differentiation potential. *Cell Tissue Res*. Jul 2010;341(1):111-20. doi:10.1007/s00441-010-0982-8

98. Harting M, Jimenez F, Pati S, Baumgartner J, Cox C, Jr. Immunophenotype characterization of rat mesenchymal stromal cells. *Cytotherapy*. 2008;10(3):243-53. doi:10.1080/14653240801950000

99. "FABP4 Gene - Fatty Acid Binding Protein 4". GeneCards. Updated 10.01.2023. 2023. https://www.genecards.org/cgi-bin/carddisp.pl?gene=FABP4

100. Netzker R DR. *Duale Reihe Biochemie*. vol 5. Thieme; 2022.

101. Schenk T, Chen WC, Gollner S, et al. Inhibition of the LSD1 (KDM1A) demethylase reactivates the all-trans-retinoic acid differentiation pathway in acute myeloid leukemia. *Nat Med*. Mar 11 2012;18(4):605-11. doi:10.1038/nm.2661

102. Wass M, Gollner S, Besenbeck B, et al. A proof of concept phase I/II pilot trial of LSD1 inhibition by tranylcypromine combined with ATRA in refractory/relapsed AML patients not eligible for intensive therapy. *Leukemia*. Mar 2021;35(3):701-711. doi:10.1038/s41375-020-0892-z

103. Somervaille TC, Cleary ML. Identification and characterization of leukemia stem cells in murine MLL-AF9 acute myeloid leukemia. *Cancer Cell*. Oct 2006;10(4):257-68. doi:10.1016/j.ccr.2006.08.020

104. Krivtsov AV, Feng Z, Armstrong SA. Transformation from committed progenitor to leukemia stem cells. *Ann N Y Acad Sci*. Sep 2009;1176:144-9. doi:10.1111/j.1749-6632.2009.04966.x

105. Basova P, Pospisil V, Savvulidi F, et al. Aggressive acute myeloid leukemia in PU.1/p53 double-mutant mice. *Oncogene*. Sep 25 2014;33(39):4735-45. doi:10.1038/onc.2013.414

106. Lynch JT, Cockerill MJ, Hitchin JR, Wiseman DH, Somervaille TC. CD86 expression as a surrogate cellular biomarker for pharmacological inhibition of the histone demethylase lysine-specific demethylase 1. *Anal Biochem*. Nov 1 2013;442(1):104-6. doi:10.1016/j.ab.2013.07.032

107. Chandrasekar B, Deobagkar-Lele M, Victor ES, Nandi D. Regulation of chemokines, CCL3 and CCL4, by interferon gamma and nitric oxide synthase 2 in mouse macrophages and during Salmonella enterica serovar typhimurium infection. *J Infect Dis*. May 15 2013;207(10):1556-68. doi:10.1093/infdis/jit067

108. Liberzon A, Birger C, Thorvaldsdottir H, Ghandi M, Mesirov JP, Tamayo P. The Molecular Signatures Database (MSigDB) hallmark gene set collection. *Cell Syst*. Dec 23 2015;1(6):417-425. doi:10.1016/j.cels.2015.12.004

109. Young MD, Wakefield MJ, Smyth GK, Oshlack A. Gene ontology analysis for RNA-seq: accounting for selection bias. *Genome Biol*. 2010;11(2):R14. doi:10.1186/gb-2010-11-2-r14

110. Liu T, Zhang L, Joo D, Sun S-C. NF-κB signaling in inflammation. *Signal Transduction and Targeted Therapy*. 2017/07/14 2017;2(1):17023. doi:10.1038/sigtrans.2017.23

111. Ensembl. 2022. https://www.ensembl.org/

112. The Human Protein Atlas. 2022. https://www.proteinatlas.org/

113. SPINT2 serine peptidase inhibitor, Kunitz type 2 [Homo sapiens (human)]. 2024. 2024. https://www.ncbi.nlm.nih.gov/gene/10653

114. McTavish N, Copeland LA, Saville MK, Perkins ND, Spruce BA. Proenkephalin assists stress-activated apoptosis through transcriptional repression of NF-kappaB- and p53-regulated gene targets. *Cell Death Differ*. Sep 2007;14(9):1700-10. doi:10.1038/sj.cdd.4402172

115. "Human Gene Set: BOQUEST_STEM_CELL_UP". 2022. http://www.gsea-msigdb.org/gsea/msigdb/cards/BOQUEST_STEM_CELL_UP

116. 2022. https://bioinfogp.cnb.csic.es/tools/venny/

117. Wu K, Feng J, Lyu F, et al. Exosomal miR-19a and IBSP cooperate to induce osteolytic bone metastasis of estrogen receptor-positive breast cancer. *Nat Commun*. Aug 31 2021;12(1):5196. doi:10.1038/s41467-021-25473-y

118. Chen Y, Wang H, Yang Q, et al. Single-cell RNA landscape of the osteoimmunology microenvironment in periodontitis. *Theranostics*. 2022;12(3):1074-1096. doi:10.7150/thno.65694

119. MSigDB v3.0 Release Notes. 2022. https://software.broadinstitute.org/cancer/software/gsea/wiki/index.php/MSigDB_v3.0_Release_Notes

120. Komori T. Runx2, an inducer of osteoblast and chondrocyte differentiation. *Histochem Cell Biol*. Apr 2018;149(4):313-323. doi:10.1007/s00418-018-1640-6

121. Komori T. Regulation of Proliferation, Differentiation and Functions of Osteoblasts by Runx2. *Int J Mol Sci*. Apr 4 2019;20(7)doi:10.3390/ijms20071694

122. Hayden MS, Ghosh S. Regulation of NF-kappaB by TNF family cytokines. *Semin Immunol*. Jun 2014;26(3):253-66. doi:10.1016/j.smim.2014.05.004

123. Sprung CN, Ivashkevich A, Forrester HB, Redon CE, Georgakilas A, Martin OA. Oxidative DNA damage caused by inflammation may link to stress-induced non-targeted effects. *Cancer Lett*. Jan 1 2015;356(1):72-81. doi:10.1016/j.canlet.2013.09.008

124. Waldeck S, Rassner M, Keye P, et al. CCL5 mediates target-kinase independent resistance to FLT3 inhibitors in FLT3-ITD-positive AML. *Mol Oncol*. Apr 2020;14(4):779-794. doi:10.1002/1878-0261.12640

Acknowledgements

First and foremost, I would like to thank Dr. med. Monica Cusan and Prof. Dr. med. Philipp Greif for giving me the opportunity to contribute to their research group in this very interesting field. I appreciate their guidance and the numerous discussions at every step of the research project and for their insightful criticism, which pushed me to improve the ways I organise and execute scientific research.

I would also like to thank Prof. Dr. med. O. Weigert (ELLF, Med. Clinic III, LMU) and Prof. Dr. med. S. Eber for co-supervising and enabling my doctoral degree, as well as all my colleagues in the lab that I had the chance to work with for showing and teaching me new techniques and ways to setup experiments and analyse and interpret experimental data. Special thanks to A. Caroleo, P. Kerbs, V. Arfelli, C. Strobl.

Next, I would like to thank Prof. Dr. med. E. Nößner (Helmholtz Zentrum Munich) and Mrs. B. Mosetter for their advice and insightful discussions, as well as their expertise regarding the cytokine detection assay.

I also want to express my gratitude to Prof. Dr. rer. nat. K. Lauber and Mr. N. Brix (Department of Radiation Oncology, LMU) for their help in cell irradiation, to Dr. A. Moosmann (Helmholtz Zentrum Munich) and his research group for the access to the facilities and the irradiation device, to Mr. L. Wange (Department of Anthropology and Human Genomics, LMU) for his great help and advice on RNA sequencing and to Mrs. B. Ksienzyk (Med. Clinic III, LMU) for her assistance and guidance in cell sorting.

Lastly, I would like to thank all my friends and family who helped me and motivated me along the way.

Affidavit

Affidavit

_____

Mariggi, Maria Despoina

I hereby declare, that the submitted thesis entitled:

Irradiation of the microenvironment affects epigenetic therapy by LSD1 inhibition in murine AML model.

is my own work. I have only used the sources indicated and have not made unauthorised use of services of a third party. Where the work of others has been quoted or reproduced, the source is always given.

I further declare that the submitted thesis or parts thereof have not been presented as part of an examination degree to any other university.

München, 13.05.2025 Maria Despoina Mariggi

_____

Place, date

Signature doctoral candidate